2010

THE PROGNOSTIC POTENTIAL OF THE EPIDERMAL GROWTH FACTOR RECEPTOR AND NUCLEAR FACTOR KAPPA B PATHWAYS AND ASSOCIATED THERAPEUTIC STRATEGIES IN PATIENTS WITH SQUAMOUS CELL CARCINOMA OF THE HEAD AND NECK

Pamela Wirth
Virginia Commonwealth University

THE PROGNOSTIC POTENTIAL OF THE EPIDERMAL GROWTH FACTOR RECEPTOR AND NUCLEAR FACTOR KAPPA B PATHWAYS AND ASSOCIATED THERAPEUTIC STRATEGIES IN PATIENTS WITH SQUAMOUS CELL CARCINOMA OF THE HEAD AND NECK

A dissertation submitted in partial fulfillment of the requirements for the degree of Doctorate of Philosophy in Health Related Sciences at Virginia Commonwealth University.

by

PAMELA SUSAN WIRTH
Master of Science in Biology, Northeastern Illinois University, 1999
Bachelor of Science in Biology, Virginia Polytechnic Institute and State University, 1995

Director: Teresa S. Nadder, PhD
Chairman and Associate Professor, Clinical Laboratory Sciences

Virginia Commonwealth University
Richmond, Virginia
August 2010

ACKNOWLEDGMENTS

I could not have completed this project without the help of several people. I owe a great deal of gratitude to my committee members Dr. Linda Beck, Dr. Christine Chung, Dr. Jim Cotter, Dr. Cecil Drain, and Dr. Teresa Nadder. I would like to acknowledge my boss and mentor Dr. Christine Chung, who taught me what it means to be a better scientist and gave me the guidance and leadership to complete this dissertation. Special thanks go to Dr. Teresa Nadder and Dr. Linda Beck for providing the vision, encouragement and direction necessary for me to proceed through the doctoral process. My family has been extremely supportive throughout my PhD journey. I especially want to thank my parents, Wesley and Patricia Turner for their love and support and most of all, my husband David Wirth.

TABLE OF CONTENTS

Page

LIST OF TABLES

Table Page

LIST OF FIGURES

Figure Page

ABSTRACT

THE PROGNOSTIC POTENTIAL OF THE EPIDERMAL GROWTH FACTOR RECEPTOR AND NUCLEAR FACTOR KAPPA B PATHWAYS AND ASSOCIATED THERAPEUTIC STRATEGIES IN PATIENTS WITH SQUAMOUS CELL CARCINOMA OF THE HEAD AND NECK

By Pamela Susan Wirth, Ph.D.

A Dissertation submitted in partial fulfillment of the requirements for the degree of Doctor of Philosophy at Virginia Commonwealth University.

Virginia Commonwealth University, 2010

Major Director: Teresa S. Nadder, Ph.D.
Chairman and Associate Professor, Department of Clinical Laboratory Sciences

Little is known about the signaling pathways that contribute to treatment response in advanced stage head and neck tumors. Increased expression of epidermal growth factor receptor (EGFR) and downstream pathways such as nuclear factor kappa B (NFκB) are implicated in aggressive tumor phenotypes and limited response to therapy. This study explored the rationale for combining the proteasome inhibitor bortezomib with the EGFR inhibitor gefitinib in a subset of head and neck squamous cell carcinomas with high EGFR gene amplification. Drug responses of gefitinib and bortezomib as single agents and in combination within head and neck squamous cell carcinoma cell lines were analyzed using MTS assays. The effects of gefitinib on the activation of EGFR and itsthree major downstream pathways, Akt, STAT3 and MAPK were determined by

western blotting. The activation status of NFκB and the effects of bortezomib on the canonical pathway were assessed by DNA binding assays. Resistance to lower doses of gefitinib was associated with elevated EGFR and activated Akt expression. Gefitinib was able to effectively inhibit activation of STAT3, Akt and MAPK in HNSCC to varying degrees depending on EGFR expression status. Bortezomib treatment inhibited TNFα – induced nuclear NFκB/RelA expression but demonstrated variability in levels of baseline nuclear NFκB/RelA expression between sensitive and resistant cell lines. Bortezomib effectively suppresses NFκB/RelA nuclear activation but demonstrates additional modes of cellular toxicity beyond the NFκB pathway in sensitive cell lines. Further understanding of tumor response to the targeted inhibitors gefitinib and bortezomib may provide novel approaches in managing HNSCCs.

CHAPTER 1: INTRODUCTION

Background

Head and neck cancers comprise about five percent of all cancers in the United States. These malignant tumors can arise in the lip and oral cavity, nasal cavity, pharynx, larynx, thyroid, paranasal sinuses, salivary glands and cervical lymph nodes of the neck. The majority of head and neck cancers involve epithelial tissues and are classified as squamous cell carcinomas. Head and neck squamous cell carcinomas (HNSCCs) predominantly affect males over 40 years of age with major risk factors including tobacco and alcohol use (Sanderson & Ironside, 2002). Human papillomavirus is a significant risk factor for oropharynx carcinomas and has been found to be associated with approximately 20 to 25% of head and neck tumors (Chung & Gillison, 2009).

Many different treatments and therapies are used in the management of head and neck cancer. The type of treatment and therapy depends largely on the location of the tumor and the extent of metastasis at the time of diagnosis (Choong & Vokes, 2008). The lack of survival benefit from current therapies for advanced stage patients has prompted the search for markers that may provide therapeutic targets such as nuclear factor kappa B (NFκB) and epidermal growth factor receptor (EGFR) pathways. NFκB and EGFR are key players in the regulation of cell proliferation and survival and are known to be deregulated in head and neck tumors (Chung, Parker, Ely, Carter, Yi, Murphy, et al.,

2006). There is an urgent need to identify prognostic markers that may reliably predict a subset of patients responsive to these pathway-targeted therapies. Currently the preclinical evidence necessary to demonstrate the efficacy of combination therapies is lacking. The use of two agents, bortezomib, an NFκB pathway inhibitor, and gefitinib, an anti-EGFR tyrosine kinase inhibitor, were examined for their efficiency as combination agents in head and neck carcinomas.

Clinical Management of Head and Neck Cancer

Staging of the tumor remains the standard method of determining treatment modality and prognostic outcome for the patient, although reliability and effectiveness are questionable. Survival rates for head and neck cancer have not significantly improved over the past 25 years as advanced-stage patients experience only a five year relative survival rate at approximately 50% (Chin, Boyle, Porceddu, Theile, Parsons, & Coman, 2006). Treatment regimens involve surgical resection, radiotherapy and/or chemotherapy. The choice of treatment is unique to each patient depending upon cancer staging, the desire for organ preservation or previous response to treatment (Spencer, Ferguson, & Wiesenfeld, 2002). When achievable, organ preservation is the preferred goal for many patients. Issues reported with organ loss in head and neck patients involve difficulty with swallowing, speech, eating and respiration. Chemotherapy in combination with radiation without surgical intervention for the purpose of larynx preservation has shown success in improving the quality of life in patients with site specific cancers such as the larynx and hypopharynx. Chemoradiotherapy in conjunction with surgical resection has become the standard method of care for the majority of locally advanced HNSCCs, not only for the

benefit of potential organ preservation but also to improve treatment success over radiation alone. Altered combinations of chemotherapy and radiotherapy may include: induction chemotherapy (chemotherapy given before radiotherapy), adjuvant chemotherapy (chemotherapy given after radiotherapy), and concurrent or concomitant chemoradiotherapy (chemotherapy given at the same time as radiotherapy). Concurrent chemoradiotherapy has proven the most successful nonsurgical option (Choong & Vokes, 2008).

Common chemotherapy agents include the taxanes, 5-fluorouracil (5-FU) and platinum-derivatives. The taxanes are a group of drugs that target microtubules, intracellular proteins that assist in cellular support and movement. Paclitaxel (Taxol) and docetaxel (Taxotere) are commonly used anti-microtubule agents in the treatment of head and neck cancer which act to prevent the disassembling of these cellular proteins. Microtubules then accumulate in excess, preventing the cancer cells from growing and dividing. Two of the most common platinum chemotherapeutic agents used in combination therapy are cisplatin and 5-FU. These platinum agents bind and cross-link DNA preventing cell division ultimately resulting in apoptosis of cancer cells. 5-FU specifically blocks the synthesis of thymidine, a nucleotide required for DNA replication (Bernier & Bentzen, 2006).

Radiation therapy is measured in gray (Gy), the unit measurement to indicate the amount of dose applied to the patient. A standard radiation dose and schedule for head and neck patients involves daily fractions of 1.8 to 2 Gy for five days over five to seven weeks. Accelerated schedules may be employed with more frequent dosing during the

five day treatment schedule or include additional days of treatment during the week. Radiation can also be used to help sensitize tumors to chemotherapeutic agents and improve local tumor control. Common side effects caused by radiation and/or combination treatments specifically affecting the quality of life for many head and neck patients are pain, increased inflammation, accumulation of mucous in airways and weight loss. These place a particularly increased burden on older patients and/or those with comorbidities (Lalami, de Castro, Bernard-Marty, & Awada, 2009).

Targeted agents are specifically being investigated as a means of reducing toxicity and overcoming treatment resistance. Targeted agents are less likely to have toxic effects on surrounding normal tissues or cells that do not express a specific receptor or molecule. Recent clinical trials have investigated the impact of combining targeted therapies such as EGFR inhibitors gefitinib with cisplatin or 5-FU, demonstrating improved survival rates over single agent platinum-based chemotherapy regimens. These results indicate the addition of EGFR inhibitors to chemotherapy in patients with metastatic HNSCC is beneficial in terms of improved survival rates over the use of single agents. The addition of targeted agents with standard chemotherapy resulted in an improvement in median survival from 7.4 months to 10.1 months. Unfortunately, improving overall survival rates among all tumor sites and stages continues to present a challenge (Choong & Vokes, 2008).

Approximately 70% of HNSCC patients presenting without metastasis receive aggressive therapy due to the difficulty in determining patient response to treatment (Yarbrough, Slebos, & Liebler, 2006). With radiation treatment alone, survival rates

average a mere 12 months. Chemoradiotherapy can extend average overall survival rates (67% versus 37% with radiation alone) in site specific tumors such as the nasopharynx and oropharynx. Although overall survival rates remain unchanged in other sites such as the larynx and hypopharynx, organ preservation is still often possible preserving the voice and an intact airway (Marur & Forastiere, 2008).

Combination treatments with radiation and chemotherapy can be beneficial in terms of organ preservation but present additional obstacles in terms of increased toxicities. As much as one-third of patients are unable to maintain the full course regimen due to severe side effects. Toxicities such as permanent dry mouth and difficulty swallowing are comparable with both single agent and combination therapies. For those patients able to withstand the concurrent chemoradiotherapy treatments, some studies show significant improvement in overall survival and locoregional control rate when compared to radiotherapy alone. A large phase III study demonstrated an overall survival benefit (49% versus 24%) and 3-year locoregional control rate (35% versus 17%) with chemoradiotherapy treatment over radiation alone; however, this benefit was primarily confined to oropharynx tumors (Bernier & Schneider, 2007).

The EGFR Pathway in Head and Neck Cancers

EGFR exists on the cell surface and is activated by the binding of specific ligands, including epidermal growth factor (EGF) and transforming growth factor alpha (TGFα). The ErbB family consists of four family members, ErbB1, ErbB2, ErbB3 and ErbB4. EGFR is also known as ErbB1 or HER1. ErbB2, ErbB3 and ErbB4 are also known as HER2, HER3 and HER4, respectively. The ErbB receptor group belongs to a family of

numerous growth signals including EGF and TGFα. Receptor tyrosine kinases are transmembrane glycoproteins with a cysteine rich ligand-binding extracellular domain, a transmembrane domain, and an intracellular tyrosine kinase domain with a tyrosine rich C-terminal tail. Activation of the ligand-binding domain by the binding of an extracellular ligand leads to homodimerization or heterodimerization among the members of the ErbB family. Upon activation by its growth factor ligands, EGFR may form a homodimer by binding with another ErbB1 receptor or form a heterodimer by binding with other members of the family (Bianco, 2004). The joining of receptors induces the activation of the tyrosine kinase domain of the EGFR, recruitment of a number of adaptor proteins, followed by initiation of downstream signaling cascades (Arteaga, 2002).

Several investigators determined that HER2 does not appear to have relevance as a prognostic marker in head and neck cancer as gene mutations are low to absent in head and neck tumors (Ali, Gunduz, Gunduz, Tamamura, Beder, Katase, et al., 2009; Tse, Yu, Chan, King, Chen, Wong, et al., 2009; Low, Ch'ng, Ng, Sullivan, Brasch, Davis, et al., 2009). Eckberg et al studied 19 cases of metastatic HNSCCs by immunohistochemistry (IHC) and did not find protein expression differences in either HER3 or HER4 between tumor and matched normal tissues (Eckberg, Nestor, Engstrom, Nordgren, Webster, Carlsson, et al., 2005). Wheeler et al demonstrated HNSCC cells show low baseline HER3 and HER4 levels but upon acquired resistance to the extracellular EGFR inhibitor cetuximab, demonstrate significant activation of HER2 and HER3 (Wheeler, Huang, Kruser, Nechrebecki, Armstrong, Benavente, et al., 2008). Upregulation of the receptor as a mechanism of acquired EGFR inhibitor resistance may result in increased

heterodimerization with other ErbB family members, potentially activating downstream signaling pathways (Arteaga, 2002).

EGFR expression is highly elevated in head and neck cancers; and upon EGFR activation, sets off downstream signaling proteins to initiate cell proliferation and survival, principally the mitogen activated protein kinase (MAPK), Akt and STAT (Signal Transducers and Activators of Transcription) pathways. Tumors with a high risk of poor clinical outcome cluster separately based on gene expression analysis from other intermediate or low risk tumors with an expression profile reflective of EGFR activation (Chung, Levy, &Yarbrough, 2005). Akt contributes to cell survival pathways by inhibiting programmed cell death or apoptosis. Since it can block apoptosis, and thereby promote cell survival, Akt has been implicated as a major factor in many types of cancer. Akt's normal functions are to regulate the cell cycle, survival and support metabolism by binding and regulating many downstream factors such as NFκB (Marmor, Skaria, & Yarden, 2004). Akt can activate NFκB through the alternative pathway by binding to IKKα, an NFκB activator. IKKα is then able to phosphorylate the NFκB inhibitor IκB that normally serves to sequester NFκB/RelB in an inactive state within the cytoplasm. Once released from its inhibitor, NFκB is able to translocate to the nucleus activating several proinflammatory and anti-apoptotic signals (Nakayama, Ikebe, Beppu, & Shirasuna, 2001).

The three main signaling pathways induced by ligand stimulation of the EGFR include Ras/MAPK, STAT and PI3K/Akt. EGFR exists on the cell surface and is activated by binding of its specific ligands. Two structurally similar subunits of the

EGFR called monomers join together or dimerize when bound to an activating ligand like EGF or TGFα. EGFR dimerization initiates phosphorylation of the receptor and stimulates its intracellular protein-tyrosine domain. This elicits downstream activation and signaling of proteins, principally the MAPK, Akt, and STAT pathways involved in DNA synthesis, cell proliferation, and cell migration (Figure 1).

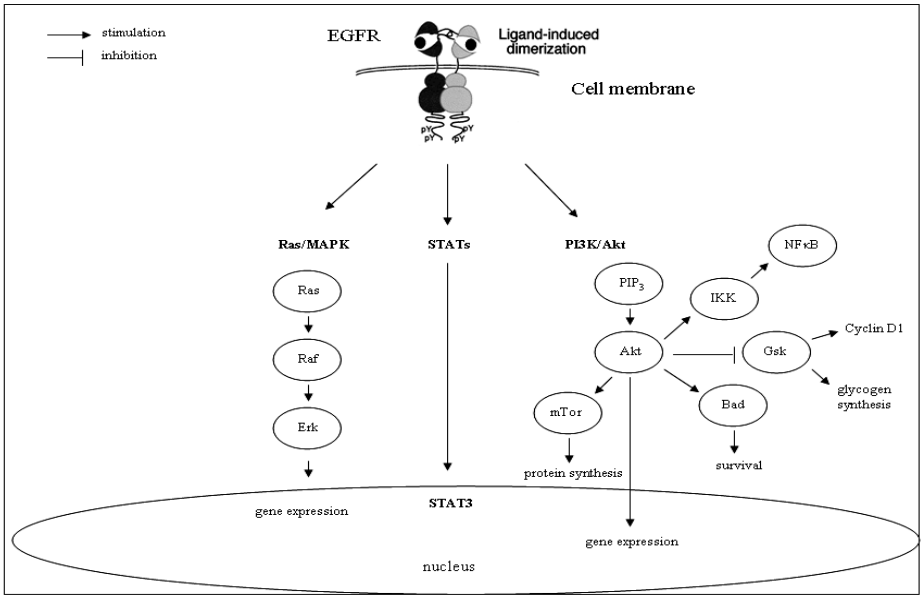

Figure 1. The Three Main Signaling Pathways Induced by EGFR Stimulation Including MAPK, STAT and PI3K/Akt.

Of the seven known ligands that bind to the EGFR, EGF and transforming growth factor alpha (TGFα) are the most well-known. Other factors outside of ligands can cause activation of the receptor, including radiation and chemotherapy. EGFR can be phosphorylated and translocated to the nucleus upon irradiation and cellular stress as shown in DNA precipitation assays and confocal microscopy (Dittman, Mayer, Fehrenhacher, Schaller, Raju, Milas, et al., 2005). Mutations in the tyrosine kinase

domain of EGFR can act as activating mutations in a ligand-independent manner, leading to tumor-cell dependence on EGFR signaling (Sharma, Bell, Settleman, & Haber, 2007). The phosphorylation of the growth factor receptor stimulates the downstream activation of several proteins that influence cell division, migration and survival (Scaltriti & Baselga, 2006).

The Ras/MAPK/ERK pathway plays a vital role in regulating cell responses through EGFR. Multiple downstream effectors are phosphorylated, then translocated to the nucleus, promoting tumor cell invasion, increased vessel growth and altered gene expression. Upon activation of the EGFR, the Ras/Raf/MAPK pathway initiates translocation of MAPK into the nucleus. Once in the nucleus, MAPK activates specific transcription factors which regulate cell proliferation and growth. Akt is a central mediator in a number of pathways as a promoter of cell survival and migration through the inactivation of glycogen synthase kinase 3 (GSK-3). GSK-3 inactivation leads to increased glycogen and protein synthesis. GSK-3 inactivation also prevents the degradation of β-catenin, allowing it to build up in the cytoplasm with subsequent translocation into the nucleus. β-catenin can function as an oncogene leading to increased cell proliferation. Akt's anti-apoptotic activities are also carried out through NFκB and Bad, a member of the Bcl-2 family member that governs a cell's overall homeostatic balance between growth and death (Scaltriti & Baselga, 2006).

STAT, signal transducer and activator of transcription, is a family of proteins involved in normal and oncogenic pathways. Of the seven members of the STAT family of proteins, STAT3 and STAT5 are the most highly studied. They are activated by a wide

range of hormones, cytokines and growth factors including EGF. Only STAT3 has been shown to be critical for early development. Other growth-promoting functions of this protein include wound healing, cell division and liver regeneration (Lim & Cao, 2006). The overexpression of STAT3 is associated with several tumor types including leukemia, prostate, breast and head and neck. Elevation in STAT3 expression is possible through growth factor pathways like EGFR as well as inflammatory pathways in an autostimulatory manner. Once activated, STAT proteins are able to initiate cellular proliferation through gene transcription (Marmor et al., 2004). Blockage of the EGFR and NFκB pathways decreases STAT3 activity in head and neck squamous carcinoma cells (Squarize, Castilho, Sriuranpong, Pinto, & Gutkind, 2006).

Akt (also known as protein kinase B, PKB) is activated as a result of PI3-kinase (PI3K) activity and through its downstream effectors, coordinates cell growth, invasion, metastasis and cell survival. The first evidence pointing to a role of Akt in oncogenesis was provided by early studies of the retrovirus AKT8 isolated from the AKR mouse. AKR mice have a tendency to contract spontaneous T cell lymphomas as a result of low tolerance to viruses. AKT8 was later shown to transform epithelial cells to a more malignant phenotype. In 1981, the human homologue of the AKT8 retrovirus was discovered. The nonviral, oncogenic counterpart was designated v-Akt (Staal, 1987). There are three forms of Akt: Akt1, Akt 2, and Akt 3. Although all three forms are similar in size and composition, Akt 1 and 2 play a more important role in pathological signaling. Akt 3 is less relevant to the cancer phenotype as it has a more restricted expression pattern in the brain and testes. Binding of growth factors such as EGF or

TGFα to their receptors leads to stimulation of Akt, blocking the activation of a number of targets including the pro-apoptotic protein BAD, GSK-3 (anti-apoptotic functions) as well as activating cell growth proteins like mTOR (promotes hypertrophy), Raf (a member of the MAPK pathway) and NFκB/p65 (Song, Ouyang, & Bao, 2005).

The activation of EGFR and its downstream signal transduction kinases is known to modulate tumor development, progression and therapeutic resistance. The activation of these intermediaries has been implicated in the upregulation of NFκB, which has been described in many cancer cell types as a supporter of tumor invasion, metastasis and proliferation (Bancroft, Chen, Yeh, Sunwoo, Yeh, Jackson et al., 2002).

Role of NFκB Pathway in HNSCCs

NFκB, a *f*actor in the *n*ucleus of *B* cells that binds to the enhancer of the *k*appa light chain of immunoglobulin was first discovered in the lab of David Baltimore in 1986. It was originally believed to be required only for B cell maturation and development but is now known to be expressed ubiquitously (Sun & Andersson, 2002). A pro-inflammatory transcription factor, NFκB is part of a large family of transcription factors that regulate normal cellular processes such as immune responses, cellular growth, and apoptosis (Aggarwal, 2004). NFκB can be activated by a number of factors including bacteria, viruses, stress factors, mitogens, growth factors and hormones. EGFR is also able to activate NFκB through Akt (Nakano, Shindo, Sakon, Nishinaka, Mihara, & Yagita, 1998). Finally, treatment related stresses such as chemotherapy and radiation can suppress apoptosis through induction of NFκB (Sun & Andersson, 2002).

NFκB family members consist of five Rel (reticuloendotheliosis) domain-

containing proteins: RelA (p65), RelB, c-Rel, p50/p105 (NFκB1) and p52/p100 (NFκB2). Reticuloendotheliosis designates a group of pathologic syndromes in several avian species caused by a retrovirus resulting in B and T lymphomas. Later the human genomic sequence homologous to the avian strain was isolated and is used to describe a large family of transcriptional regulators all of which contain a DNA binding domain, a nuclear localization signal, dimerization domains and the IκB binding domain (Brownell, O'Brien, Nash, & Rice, 1985; Shehata, 2005).

Two pathways predominate in NFκB activation, the classical or canonical pathway and the noncanonical or alternative pathway. The common regulatory step in both of these pathways is activation of the IκB kinase (IKK) complex consisting of the catalytic kinase subunits (IKKα and/or IKKβ) and the regulatory protein NEMO (NFκB essential modulator also known as IKKγ) (Tergaonkar, 2006). The IκB family consists of seven nuclear proteins, three of which regulate transcription by interacting with NFκB family members in the nucleus. The remaining IκB family members interact with NFκB in the cytoplasm preventing its translocation to the nucleus. NFκB family members are sequestered in the cytoplasm in their inactive state by IκB, NFκB1 p105 and NFκB p100. NFκB/p65 consists of a heterotrimer of p50, p65 and IκB in the cytoplasm. The degradation of IκB releases the heterodimer p50-p65 to travel to the nucleus and affect gene transcription. This form is the most highly studied of the NFκB family members in relation to carcinogenesis (Sun & Andersson, 2002). Cleavage of p100 produces p52; whereas p105 is cleaved to form p50, thereby allowing NFκB activation through nuclear translocation (Graham & Gibson, 2005).

The IKK complex degrades IκB via the 26S proteasome. The 26S proteasome is a multifunctional complex present in the cytoplasm of most eukaryotic cells that serves to recognize degradation signals on certain proteins. Unneeded or damaged proteins are marked for destruction by the cell and disassembled by the proteasome. The proteasome also acts to control gene transcription by removing inhibitory molecules like IκB from active forms of NFκB. Inhibitors of the proteasome, such as the drug bortezomib, can prevent the activation of proteins like NFκB without causing undue harm to normal cells (Schwartz & Davidson, 2004).

One of bortezomib's mechanisms of action is attributed to its ability to downregulate the PI3K/Akt pathway through increased proteasomal inhibition. Although total protein expression levels of Akt remained unchanged after bortezomib treatment, the activated phosphorylated form is significantly decreased after treatment in colon, lung and squamous cell carcinoma cell lines (Cascone, Morelli, Morgillo, Kim, Rodolico, Pepe et al., 2008). Despite bortezomib's ability to decrease activated Akt, recent studies demonstrate high levels of basal, phosphorylated Akt can overwhelm bortezomib's actions supporting a rationale for combination therapy using EGFR targeted agents in conjunction with proteasome inhibitors to accomplish synergistic inhibition (McConkey & Zhu, 2008).

IKKβ is the primary activator of IκB in the classical or canonical pathway whereas IKKα activates RelB through the alternative or noncanonical pathway (Bonizzi & Karin, 2004). RelB was once believed to be important only in B lymphocyte development but has recently shown relevance in carcinogenesis through the inhibition of

apoptosis (Allen, Saigal, Nottingham, Arun, Chen, & Van Waes, 2008). c-Rel as an oncogenic driver is less well studied but may target other transcription factors related to the inflammatory process. Constitutive activation of NFκB family members is common in tumors as a mechanism of apoptotic evasion and increased cellular proliferation, making it an attractive target for therapy (Pacifico & Leonardi, 2006).

Activation of the NFκB pathway through the ligand, tumor necrosis factor alpha (TNFα) leads to activation of proteins that control cell survival, proliferation, migration and resistance to chemotherapeutic agents (Jackson-Bernitsas, Ichikawa, Takada, Myers, Lin, Darnay, et al., 2006). The TNF family of cytokines is produced by a wide variety of cells within the immune system and is known for producing both antitumor and tumor promoting activities. In mouse tumor models, TNFα demonstrates anti-tumor activity by inducing a hemorrhagic necrosis and is believed to stimulate the lytic function of the host's inflammatory response. Lysis occurs through proteins known as complement, causing the destruction of the cell membrane and subsequent release of its contents. Although the liver is the primary site for complement synthesis, macrophages are induced by cytokines such as TNFα to release components of the complement cascade during infections (Carroll, 2004).

Tumor promoting activities of TNFα involve signaling that directly regulates the expression of anti-apoptotic genes, stimulation of angiogenesis, tumor adherence and cellular migration (von Biberstein, Spiro, Lindquist, & Kreutzer, 1995). TNFα is the most potent activator of NFκB and is the primary ligand for the classical or canonical pathway of NFκB (Hacker & Karin, 2006). The canonical pathway is stimulated by various

immune receptors that lead to the activation of the IKK complex which in turn phosphorylates and activates NFκB. The alternative pathway, although triggered by immune receptors and TNF members as well, are affected by a more limited number of ligands (Sun & Ley, 2008).

In addition to the roles that NFκB plays in inflammatory diseases, constitutive activation of the NFκB pathway is involved in several cancers including head and neck. Mostly it is thought that changes in the upstream pathways that lead to NFκB activation become deregulated in cancer. Most of the activities mediated by TNFα are carried out by tumor necrosis factor receptor 1 (TNFR1). TNFR1 can have opposing effects by stimulating apoptotic and anti-apoptotic pathways. NFκB is a central factor in initiating the transcription of proliferative proteins and anti-apoptotic signaling (Wang, Mayo, & Baldwin, 1996). Cell survival pathways via TNFR1 involve the activation of transcription factors via MAPK and cJun N-terminal kinase (JNK). TNFα can initiate opposing effects through binding of its receptor TNFR1 and the recruitment of caspase-8, leading to apoptosis. The noncanonical pathway is responsible for the activation of RelB and occurs during the development of lymphoid organs. Only a small number of stimuli are known to activate NFκB via this pathway including lymphotoxin, CD40 and receptor activator of NFκB (RANK). This pathway also uses the IKK complex that comprises two IKKα subunits, but not NEMO. In the noncanonical pathway, ligand- induced activation results in the activation of NFκB-inducing kinase (NIK), which phosphorylates and activates the IKKα complex (Bonizzi & Karin, 2005). For a summarized comparison of differences between classical NFκB signaling versus alternative signaling see Table 1.

Table 1. Summary of Classical (Canonical) NFκB Pathway Versus Alternative (Noncanonical) Pathway.

	Classical NFκB pathway	**Alternative NFκB pathway**
Stimulators	Toll-like receptors Interleukin-1 receptor TNFR1 via TNFα B-cell receptor	B-cell activating factor receptor Lymphotoxin CD40 RANK
Activated proteins	IκB kinase complex (IKK) composed of IKKα, IKKβ and NEMO but mostly dependent on IKKβ NFκB (RelA/p65), c-Rel, NFκB1 is activated to travel to nucleus	NIK and IKKα IKKα activates NFκB2/p100 to produce p52 to travel to nucleus (complexed with RelB)
Targeted Actions	Cell survival Part of normal development and function of immune system	Cell survival, activation and proliferation Regulation of lymphoid organogenesis and development of B and T lymphocytes

Normal cells rarely show constitutive NFκB activation except proliferating T and B cells, thymocytes, monocytes and astrocytes (Aggarwal, 2004). NFκB is deregulated in many cancers including head and neck, breast, non-small cell lung, thyroid, T and B-cell lymphocyte leukemia and several virally-induced tumors (Chen, Castranova, Shi, & Demers, 1999). NFκB further supports tumor- promoting activities through stimulation of cell proliferation, inhibition of apoptosis and promotion of angiogenesis by encoding cyclin-dependent kinases such as cyclin D1 (Aggarwal, 2004).

Aberrant Cell Cycle Machinery in HNSCCs

Individuals chronically exposed to carcinogens such as those found in tobacco and ethanol are predisposed to genetic modifications leading to loss of cell cycle control. Among the most common genetic abnormalities involve those in a family of cell cycle regulators called cyclins. Cyclins regulate a cell's progression from the G_1 growth phase into the S (synthesis) phase, contributing to proliferation and growth (Karin, Cao, Greten,

& Li, 2002). These proteins were appropriately named because their concentration varies in a recurrent fashion during the cell cycle. During the cell cycle, non-dividing cells exist in a maintenance phase called G_0 (resting phase). Once they have received the instructions for division, they enter the G_1 (gap) phase, the period when the cell grows and prepares for division. In order to proceed to the actual division of cellular contents, the cell must pass a restriction point in the G_1 phase. Cells that do not pass this point may re-enter G_0, leave the cell cycle and cease dividing or die by the apoptotic pathway. During G_1 cellular contents are duplicated and cyclin D1 dominates. Before the cell can proceed to synthesis, cellular damage is assessed at the DNA damage checkpoint where p53 may arrest the cell cycle for repair or send the cell into apoptosis. During the S phase chromosomes are duplicated and cyclins E and A predominate. During G_2 the cell prepares for division in the M phase of mitosis controlled by B cyclins. During G_0 the cell may leave the cell cycle and quit dividing or die through the apoptotic pathway (Figure 2).

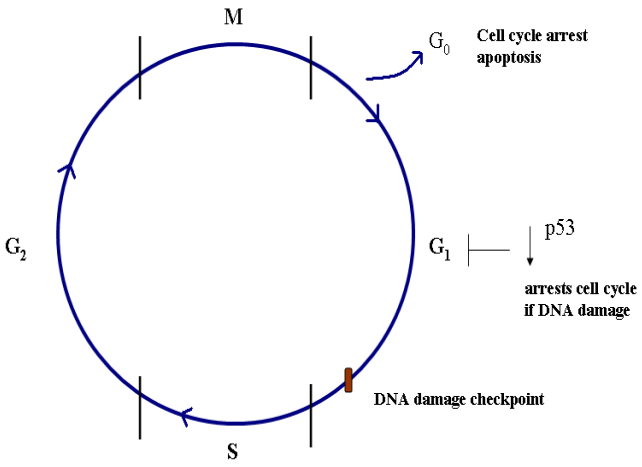

Figure 2. Cell Cycle Phases (perpendicular lines indicate inhibition).

Apoptosis is induced by events such as growth factor withdrawal, toxins or DNA damage. Survival functions are supported by preventing the release of pro-apoptotic proteins from the mitochondria. If a cell is damaged beyond repair, apoptosis is initiated through pro-apoptotic genes like B-cell lymphoma 2 (Bcl-2) associated X protein (Bax) and downregulation of pro-survival genes like Bcl-2 (Partridge, Costea, & Huang, 2007). The majority of Bax is found in the cytoplasm but when activated inserts itself into the membrane of the mitochondria releasing the pro-apoptotic signaling molecules of the caspase family. Within the mitochondria are cell death factors capable of initiating apoptosis through the caspases. Caspases, or **c**ysteine-**asp**artic prote**ases**, play essential roles in programmed cell death. The activation of the caspase cascade leads to characteristic morphological changes in the cell including shrinkage, chromatin condensation, DNA fragmentation and plasma membrane blebbing. Cells undergoing apoptosis are eventually removed by phagocytosis. This process is in contrast to necrosis, a form of cell death marked by swelling of the cell and eventual rupture (Pop & Salvesen, 2009).

Once past the restriction point, normal dividing cells enter S (synthesis) phase, a period of DNA replication and chromosome duplication. During the M (mitotic) phase the cell divides. G_2 (gap) follows S phase allowing the cell to prepare for another round of cell division by expanding cellular material and organelles. Cell cycle progression is controlled by individual cyclins, D, E, A and B. Cyclins E and A control a cell's progression into synthesis while cyclin B controls the process of mitosis. Cyclin D family members regulate the entry of cells into G_1 from G_0. The aberrant expression of cyclin

D1 has been documented in several human cancers including head and neck and is upregulated by growth factors (Kim & Diehl, 2009). Many cancers have determined ways to hijack the cell cycle machinery by progressing through the DNA damage checkpoint unimpeded (Collins, Jacks, & Pavletich, 1997).

Role of p53 in Cell Cycle Control

The p53 tumor suppressor gene is commonly involved in many human cancers including head and neck. It plays an important role in arresting the cell cycle to allow damaged DNA to be repaired or initiate apoptosis if repair is not possible. Stress signals stimulate p53 to translocate to the nucleus and induce apoptosis, preventing damaged cells from moving through the cell cycle and proliferating. Once in the nucleus, p53 binds DNA and activates expression of several genes involved in the cell cycle such as p21(WAF1). P21 binds to and inhibits the activity of cyclin dependent kinase 2 (CDK2) to regulate cell cycle progression, preventing the cell's entry into the synthesis phase. CDK2 is a subunit of the cyclin-dependent kinase complex and a known initiator of the cell cycle. The expression of p21 is tightly controlled by p53 to prevent cell growth (Junttila & Evan, 2009).

Inactivating mutations in p53 are found in many cancers, including head and neck, with an overall prevalence of 50 percent. The overexpression of p53 is usually indicative of the presence of mutant p53. The absence of p53 staining is typically considered synonymous with a wild-type phenotype, although such a staining pattern could also be explained by deletion of the gene. Overexpression of mutant p53 is capable of downregulating the normal, tumor-suppressing activities of wild-type p53 (Theoret,

Cohen, Nahvi, Ngo, Suri, Powell, et al., 2008). Without functional p53 actions, tumor growth is allowed to progress unchecked and may contribute to upregulated NFκB activity (Levine, 1997).

The proteasome inhibitor bortezomib has been shown to stabilize cell cycle regulatory proteins like p53 in tumor cells. The resulting increased levels of activated p53 inhibits uncontrolled cell cycle progression and/or promotes apoptosis attributing additional anti-tumor actions to bortezomib beyond just inhibition of NFκB (Schwartz & Davidson, 2004).

Targeted Therapies in HNSCCs

Background

Targeted therapy refers to anticancer treatments which specifically target key molecules or pathways of cancer cells aiming to stop the processes of cell growth and metastasis. EGFR was the first receptor to be investigated for targeted cancer therapy, known to be commonly overexpressed in a wide range of solid tumors including head and neck. Targeted agents have been developed against EGFR and used clinically as monotherapies, but their successful applications have been limited to a small population of patients. Due to the complexity of signaling between multiple pathways, drug combinations targeting several pathways are proposed to optimize treatment results (Scaltriti & Baselga, 2006).

Gefitinib was one of the first tyrosine kinase inhibitors developed to block the downstream pathways activated by EGFR through its primary ligands, EGF and TGFα, resulting in increased cellular proliferation and survival. Gefitinib is proposed to block

several downstream molecules that may potentially crosstalk with other pathways (Cooper & Cohen, 2009). Although initially developed as a hematological cancer agent, bortezomib is currently being investigated as a potential solid tumor agent. Bortezomib seems to have a wide range of anti-cancer effects including stabilization of the cell cycle regulator p53, upregulation of pro-apoptotic genes such as Bax and downregulation of anti-apoptotic genes like Bcl-2 (Schwartz & Davidson, 2004). More selective targeted agents such as bay 11-7082 are used in the laboratory to specifically target NFκB but appear to be less effective than the broad-spectrum drug bortezomib (Gasparian, Guryanova, Chebotaeve, Shiskin, Yemelyanov, & Budunova, 2009). The use of combination agents aims to enhance current therapies as well as prevent the development of treatment resistance.

Bortezomib and Bay 11-7082

Determining specific pathways of activation in the HNSCC patient population are critical for designing combination therapies as each treatment agent has specific modes of action. Bortezomib inhibits NFκB by preventing the proteasome from degrading IκBα and the inhibitory domain of p100. The United States Food and Drug Administration (FDA) approved bortezomib for use in multiple and mantle cell myeloma patients who have received at least one prior therapy. PS-341 or bortezomib is the only proteasome inhibitor in clinical development (Nencioni, Grunebach, Patrone, Ballestrero, & Brossart, 2007). Bortezomib's toxicity is well tolerated and superior to high-dose glucocorticoids in the areas of median time to progression, response rate, and survival in patients with relapsed myeloma (Schwartz & Davidson, 2004). Glucocorticoids are steroid-based

agents used clinically to suppress an overactive immune system. Because of their broad-spectrum effects, they may impair a patient's ability to overcome DNA damage and stress produced by cancer progression and their associated treatments (Keith, 2008). Proteasome inhibitors like bortezomib target proliferating cells which appear to be more sensitive to the drug than non-dividing cells. This greater sensitivity is attributed to cell cycle arrest caused by the proteasome which leads to eventual apoptosis of tumor cells. Bortezomib not only induces apoptosis in cancer cells but sensitizes tumors to chemotoxic and radiation therapies (Olivier, Robe, & Bours, 2006). Inhibition of the proteasome is also postulated to initiate accumulation of the tumor suppressor p53 as will as apoptotic proteins while decreasing NFκB expression (Schwartz & Davidson, 2004). Bortezomib's actions are multi-factorial as it can cause apoptosis in cell lines lacking p53 as well. The accumulation of misfolded proteins due to the inhibition of the proteasome leads to cell death, attributing additional factors to bortezomib's cytotoxic actions (Kisselev & Goldberg, 2001).

NFκB is a well-characterized molecule involved in treatment resistance and is believed to be the main target of bortezomib, although data suggests proteasome inhibitors have additional cytotoxic targets. When cell cycle progression is inhibited in cells treated with bortezomib, the levels of caspase increase contributing to higher levels of apoptosis (Allen et al., 2008). In order to further define on target and off-target effects of bortezomib, targeted inhibitors have been employed to assess the efficacy of specifically inhibiting NFκB. Bay 11-7082 is a specific NFκB inhibitor that primarily targets the activating IKK complex, in particular IKKβ (Figure 3).

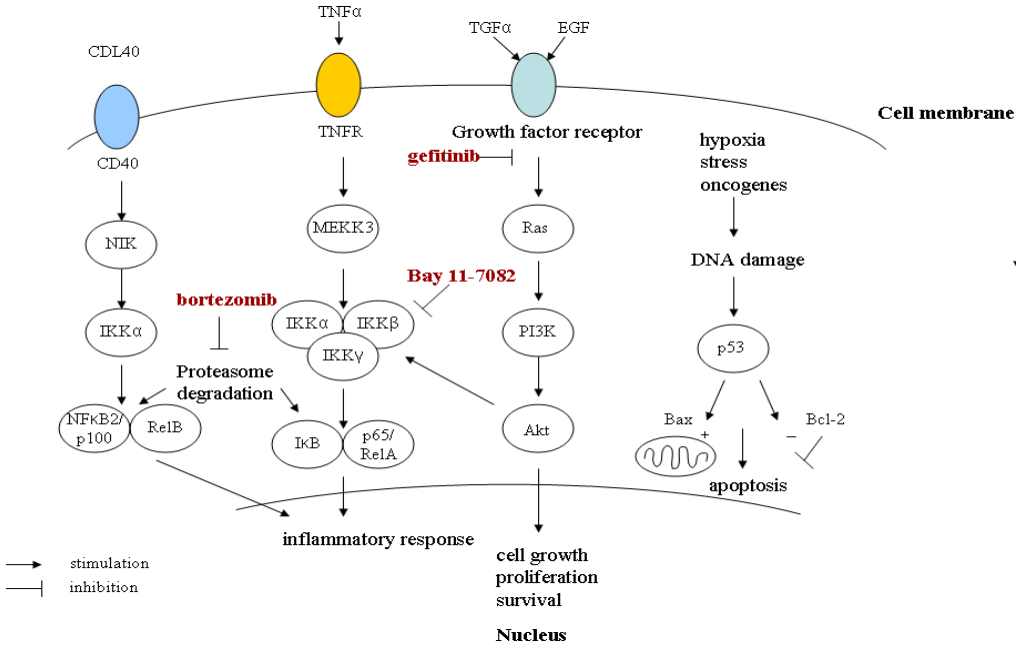

Figure 3. Targeted Agents in the NFκB and EGFR pathways.

Agents targeting several pathways in tumor growth are potentially effective against treatment resistance. Cross-talk between pathways like NFκB and EGFR requires modulation of multiple downstream markers with broad scope inhibitors such as gefitinib and more specific targeted agents like bortezomib. Bay 11-7082 and bortezomib act to block pathways of resistance such as the canonical and noncanonical pathways of NFκB. Bortezomib further helps to stabilize tumor suppressors like p53 and increase pro-apoptotic proteins like Bax and decrease anti-apoptotic proteins such as Bcl-2. To date, IKK inhibitors remain in the preclinical stage of testing to determine their efficacy as therapeutic agents. Recent studies in cell lines have demonstrated a broader and more potent cell killing effect from proteasome inhibitors over IKKβ specific inhibitors (Gasparian, et al., 2009).

Bortezomib acts in a specific and reversible manner to target the proteasome and

promote tumor cells to become apoptotic (Adams, Palombella, Sausville, Johnson, Destree, Lazarus, et al., 1999). Several clinical studies are currently underway to determine if combinations of bortezomib with conventional chemotherapy and/or radiation will benefit HNSCC patients. Further understanding of bortezomib's effects in HNSCC tumor tissues is necessary and at this point has only been effectively addressed in hematological malignancies (Montagut, Rovira, & Albanell, 2006; Nencioni et al., 2007).

Gefitinib

EGFR targeted treatments like gefitinib inhibit cell proliferation through intracellular competitive binding of the tyrosine kinase domain of the receptor (Mandic, Rodgarkia-Dara, Zhu, Folz, Bette, Weihe et al., 2006). Gefitinib (Iressa® ZD1839) is a small, oral EGFR tyrosine kinase inhibitor that prevents the activation of EGFR and any downstream signals triggered by its phosphorylation (see Figure 3). Tyrosine kinase inhibitors have the potential benefit of cross reactivity between EGFR and other receptors of the same family such as the HER receptors due to their nonspecific reactivity towards the ATP site of tyrosine kinases (Dassonville, Bozec, Fischel, & Milano, 2007). Gefitinib was approved by the FDA in 2004 as a monotherapy for patients with locally advanced or metastatic non-small cell lung cancer after failure of both platinum-based and docetaxel chemotherapeutic regimens. In phase I-II studies, gefitinib showed low toxicity and efficient anti-tumor activity in solid malignant tumors including HNSCCs (Erjala, Raitanen, Kulmala, & Grenman, 2007). Since June 2005, gefitinib was withheld from United States markets for use in patients with non-small cell lung cancer refractory to

previous platinum-based chemotherapy as the result of negative phase III trial results. These results were unable to show the drug's efficacy in improving survival rates for these patients. Gefitinib continues to be tested as a monotherapy and combination regimen for HNSCC patients, although clinically relevant responses are limited in the majority of head and neck tumors (Cooper & Cohen, 2009). It appears to be well tolerated with a number of current therapies such as cisplatin, carboplatin, paclitaxel, taxanes, doxorubicin and radiotherapy. In a single agent trial, an overall response rate of 10.6% was achieved with gefitinib in 47 assessable HNSCC patients (Cohen, 2006). A recent study combining gefitinib with chemoradiotherapy in advanced stage HNSCC patients saw a negligible increase of 3% in survival rates over chemoradiotherapy alone (Hainsworth, Spigel, Burris, Markus, Shipley, Kuzur, et al., 2009). Efficient combinations and drug schedules continue to be explored using tyrosine kinase inhibitors in advanced stage head and neck patients.

Targeted agents designed to block only one pathway in most HNSCCs will result in decreased treatment efficiencies or the development of drug resistance, suggesting that effective therapy will require a combination of agents. By combining agents such as bortezomib and gefitinib aimed at multiple pathways, greater response rates are expected in patients presenting with limited treatment options.

Summary

Although advanced treatments have improved a head and neck patient's quality of life, the survival rate has not improved over the past several decades. The ability to classify a patient into specific treatment responsive categories continues to be a

challenge. Advances in genomics have improved the understanding of the processes governing head and neck cancer and have indentified major pathways of deregulation. Two of these deregulated pathways, NFκB and EGFR are predicted to provide downstream molecular markers relevant to determining treatment response in these patients. Further characterization of these pathways is required to define those patients most likely to respond to targeted therapies.

Statement of Problem

Despite the overexpression of EGFR and NFκB in head and neck cancers, the use of targeted inhibitors as single agents has shown minimal success. A combined treatment regimen using an EGFR pathway inhibitor, gefitinib, and an NFκB pathway inhibitor, bortezomib, is expected to demonstrate improved cellular toxicity over single agent treatment in HNSCC cell lines. The use of EGFR inhibitors with other targeted therapies show promise for extending patient survival and reducing toxicities but further data is needed to establish the correct drug combinations as well as a potentially responsive patient population. This study characterized the deregulated pathways of EGFR and NFκB in a subset of HNSCC patients with EGFR gene amplification in order to assist the clinician in determining the best course of treatment.

CHAPTER 2: LITERATURE REVIEW

Only a small number of patients with HNSCC respond to EGFR-directed therapies due to the lack of predictive markers for selecting the right patients and applying the correct combination of pathway-directed treatments. EGFR expression status alone may not be predictive of anti-EGFR inhibitor response in head and neck patients. While elevated EGFR protein expression correlates with poorer survival in many cancers including head and neck, the underlying molecular mechanisms associated with EGFR gene copy number in advanced stage head and neck patients remains unexplored. The deregulation of multiple pathways such as EGFR and NFκB present a challenging obstacle to overcoming treatment resistance. Bortezomib has so far demonstrated efficiency as an NFκB inhibitor in hematological cancers and may potentially hold promise in solid tumors. The use of EGFR inhibitors like gefitinib with bortezomib show promise for combating resistance, but further data is needed to establish appropriate patient selection and treatment combinations.

Background

EGFR is commonly expressed at high levels in epithelial tumors, including head and neck carcinomas. This increased activity results in enhanced cellular proliferation and survival (Arteaga, 2002). Excessive activation of EGFR can occur from several mechanisms including increased synthesis of the receptor, receptor-activating mutations,

decreased degradation of EGFR protein, and amplification of the EGFR gene (Franovic, Gunaratnam, Smith, Robert, Patten & Lee, 2007). The rationale for targeting this receptor is substantial and has lead to the development of agents blocking activation of EGFR like gefitinib. Unfortunately, EGFR inhibitors as a monotherapy have produced lower response rates than expected in advanced stage tumors (Dassonville et al., 2007). In a subset of head and neck tumors, EGFR is activated by gene amplification; and multivariate analysis has shown amplification is a significant and unfavorable predictor for overall survival in head and neck patients (Temam, Kawaguchi, El-Naggar, Jelinek, Tang, Liu et al., 2007).

Existing data suggests that amplification and overexpression of the EGFR gene may be a useful diagnostic and prognostic marker in advanced stage HNSCCs. The underlying molecular mechanisms contributing to the deregulation of EGFR require further investigation in order to focus targeted treatments towards a responsive patient population as current therapies remain largely ineffective. Although poorer patient prognosis is known to be associated with EGFR gene amplification in HNSCC patients, what this means for optimal treatment regimens remains to be determined. Gefitinib has been determined to be effective against EGFR amplified tumors in vitro but is showing limited success in patient centered clinical trials (Cooper & Cohen, 2009). Unimpressive in vivo results are leading the search for combination agents to augment the cytotoxic effects of anti-EGFR therapies like gefitinib. Bortezomib is a potential combination agent that may complement gefitinib's cytotoxic actions without adding significant overlapping toxicities. Bortezomib is still being explored as a viable treatment agent in solid tumors

as both a monotherapy as well as in combination with current targeted therapies. A multi-faceted drug, bortezomib continues to demonstrate a wide-range of cytotoxic abilities that may enhance the already more characterized tyrosine kinase inhibitor gefitinib (Weber, Cerniglia, Maity, & Gupta, et al., 2007). Targeted patient selection with combination treatments focused on multiple pathways of deregulation are proposed to overcome treatment resistance and achieve better patient outcomes (McCarty & Block, 2006).

Common Laboratory Assays for DNA, RNA and Protein Measurement

Gene amplification is a cellular process in which multiple copies of a gene are produced. The result is an amplification of the phenotype or expressed trait associated with the gene, for example the epidermal growth factor receptor which can be measured by the polymerase chain reaction (PCR) or fluorescent in situ hybridization (FISH). There may also be an increase in the protein made from that gene which can be measured by immunohistochemistry (IHC) in tissue specimens or by western blot analysis in cellular extracts (Killeen, 2003).

Gene amplification is common in cancer cells, and some amplified genes may cause cancer cells to grow or become resistant to anticancer drugs (Wells, 2007). Quantitative polymerase chain reaction or qPCR is a method that allows the estimation of the amount of a given DNA sequence present in a sample. Real-time PCR is an established tool for DNA quantification that measures the accumulation of DNA product after each round of PCR amplification in "real time." Real-time PCR is based on the detection of fluorescence produced by a reporter molecule which increases, as the reaction proceeds. This occurs due to the accumulation of the PCR product with each

cycle of amplification. These fluorescent reporter molecules include dyes such as SYBR®Green that bind to the double-stranded DNA of the target which is monitored as the reaction is occurring in real time. Real-time PCR can be used to compare (control) samples like HaCaT cells, skin keratinocytes that express normal levels of EGFR to experimental cell samples, giving an idea as to expression changes in the EGFR gene. qPCR is considered the gold standard in gene amplification techniques, often applied to quantitatively determine levels of gene expression in tissue samples, cell culture or fluids (Derveaux, Vandesompele, Hellemans, 2010; Sisti, Guescini, Rocchi, Tibollo, D'Atri, Stocchi, 2010, Wells, 2007).

In tissue biopsies, gene amplification is effectively measured by fluorescence in situ hybridization (FISH). Tissue samples recovered during surgical removal are fixed in formaldehyde and processed into paraffin blocks for storage in the clinical pathology laboratory. This provides a convenient medium for analysis in the laboratory as biopsies are commonly stored as paraffin blocks and fluorescent EGFR probes are commercially available. The use of fluorescently labeled probes in the FISH assay allow for precise identification of gene amplification within the tumor in relation to the surrounding tissue morphology (Martin, Mazzucchelli, & Frattini, 2009).

Protein expression is commonly measured in tissue biopsy specimens in the laboratory by an immunohistochemistry (IHC) assay using antibodies against a known antigen expressed in the tissue. As in the FISH assay, the advantage of assessing protein expression in tissue specimens allows for assessment of tissue morphology as a whole (Eastmond, Schuler, & Rupa, 1995). Expression levels of EGFR downstream pathways

are commonly measured by IHC. For instance, the phosphorylation status of Akt, STAT and MAPK can be effectively measured in tissue biopsy specimens using this technique (Agulnik, Santos, Hedley, Nicklee, dos Reis, et al., 2007; Pernas, Allen, Winters, Yan, Friedman, Dabir, et al., 2009).

For determining protein expression levels in cell culture, western blotting methods are used. Cells are lysed to release their contents then the corresponding protein samples are run on a gel which separates the proteins on the basis of size. These gel proteins are transferred onto a membrane using electricity. This membrane is then probed for proteins of interest using antibodies (Gallagher & Chakavarti, 2008). Quantitative comparisons can be made between samples after normalization to a loading control. β-actin or glyceraldehyde 3-phosphate dehydrogenase (GAPDH) are highly conserved proteins present in all eukaryotic cells commonly used to confirm protein integrity and equal loading of protein samples in a western blot gel (Killeen, 2003).

Gene Amplification in HNSCCs

Several studies suggest response to the targeted agent gefitinib may depend on the level of expression of EGFR in the tumor. Although EGFR protein expression is commonly found in head and neck tumors, EGFR protein levels have failed to predict gefitinib sensitivity in head and neck tumors by IHC analysis or immunoblotting (Pernas et al., 2009). On the other hand, the prognostic significance of EGFR gene overexpression in head and neck tumors is linked to a poor prognosis and may be correlated with gefitinib response in head and neck tumors. Chung et al showed decreased survival in HNSCC patients with EGFR gene amplification as compared to

tumors classified as normal in EGFR gene expression. EGFR amplified groups experienced worse progression free survival at 18 months compared with 25 months for the control group. Overall survival was 20 months for EGFR gene amplified patients versus 29 months for negative patients. Fifty of the 86 specimens were surveyed for EGFR protein expression by IHC, although no correlation was found between protein expression and gene expression of the receptor (Chung, Ely, McGavran, Varella-Garcia, Parker, Parker, et al., 2006).

EGFR gene amplification generally results in increased protein expression, although differences in the prevalence of EGFR overexpression reported by different studies may be due to variations in techniques and type of antibodies used in IHC, criteria for determining overexpression and interobserver variability (Kersting, Packeisen, Leidinger, Brandt, von Wasielewski, Winkelmann, et al., 2005). Braut et al found 16% (8 of 50 total samples) of biopsied laryngeal tumors to contain amplification of the EGFR gene by FISH. Immunohistochemical analysis indicated a signficantly higher protein expression of EGFR in all 8 biopsies as compared to control samples without EGFR gene amplification (Braut, Krstulja, Kujundzic, Manestar, Hadzisejdic, Jonjic, et al., 2009). Sheu et al also demonstrated a high correlation between EGFR amplification and EGFR protein expression in oral squamous cell carcinomas. Using PCR and FISH analysis, multiple DNA copies of the EGFR gene were noted in 90% of tumors (18 of 20). Each of these EGFR amplified tumors displayed strong positive IHC staining indicating a high level of corresponding protein expression by the receptor (Sheu, Hua, Wan, Lin, Lai, Tseng, et al., 2009).

Temam et al reviewed 134 HNSCC specimens graded as well, moderately or poorly differentiated for EGFR gene expression by fluorescent in situ hybridization (FISH) and EGFR protein expression by IHC and found 24% of tumors with an atypical EGFR gene copy number. Twenty-two tumors had an increased gene copy number while 10 tumors had a decreased copy number. Tumors with abnormal gene copy numbers correlated significantly with increased lymph node metastasis and advanced pathologic stage. Patients with abnormal gene copy number also exhibited significantly worse overall, cancer-specific and disease-free survival times compared to patients with normal EGFR gene copy numbers. However, IHC results did not show a significant correlation between EGFR protein expression and gene copy number. This could be the result of a limited amount of data, as only 12% of tumors were used to assess protein expression by IHC (Temam et al., 2007). The correlation between EGFR gene copy number, protein expression and patient prognosis in advanced stage head and neck carcinomas require further study in order to assist in patient selection for EGFR directed therapy.

EGFR Targeted Therapeutics

Introduction

EGFR overexpression is found in approximately 90% of head and neck tumors, although this prevalence has not been definitively correlated with EGFR inhibitor sensitivity (Cooper & Cohen, 2009). Current therapeutic trends focus on the development of novel agents specifically targeting those growth factor pathways that are deregulated in tumor cells and using them in conjunction with traditional palliative regimens. As single agents, EGFR inhibitors have shown success in 4 to 17% of patients but these

percentages increase when used in combination with radiation to 10 to 26% (Chung, Ely, et al., 2006). Combination strategies using traditional therapies such as radiation and chemotherapy with gefitinib demonstrate some clinical value but negative results from large scale phase III clinical trials in both lung and head and neck cancers have caused investigators to continue the search for optimal treatments (Huang, Armstrong, Benavente, Chinnaiyan, & Harari, 2004; Siu, Soulieres, Chen, Pond, Chin, Francis et al., 2007). The selection of head and neck patients for combination therapies is especially important to maximize response rates and significantly increase survival times.

Determining anti-EGFR treatment efficiency or resistance in advanced stage tumors may depend on the exact pathway of activation; therefore, identifying and characterizing these abnormal downstream signaling molecules will be critical. The optimal administration and treatment schedule of EGFR inhibitors may also require optimization for this subset of patients. The most clinically advanced anti-EGFR therapies, monoclonal antibodies and tyrosine kinase inhibitors, target the EGFR extracellularly and intracellularly, resulting in different routes of EGFR pathway blockade. Cetuximab blocks ligand binding of the EGFR extracellularly, triggering receptor internalization and breakdown, ultimately resulting in downregulation in the number of EGFRs on the cell surface. All tyrosine kinase inhibitors act intracellularly to prevent downstream signaling by EGFR without causing the receptor's internalization or degradation. Together the combination of the two modes of therapy can inhibit cell proliferation and enhance tumor cell toxicity to improve long term survival (Rocha-Lima, Soares, Raez, & Singal, 2007).

Matar et al studied the in vitro effects of the tyrosine kinase inhibitor gefitinib and the monoclonal antibody cetuximab in a panel of carcinoma cell lines with varying levels of EGFR from medium to high. The possibility of additive effects between gefitinib and cetuximab were determined by combining both EGFR inhibitors on each cell line. Cetuximab was found to exhibit a plateau effect at the maximum dose of 10nmol/L. A synergistic effect was found with the addition of gefitinib at 0.1, 1 and 10μmol/L doses to 0.01μM of cetuximab in high-EGFR expressing A431 cells. Gefitinib was not found to have a plateau effect possibly due to its nonspecific kinase inhibitory effects. These authors further investigated the effects of combining inhibitors on the phosphorylation of EGFR, MAPK and Akt by western blot analysis. A431 cells, a human epithelial carcinoma line expressing high levels of EGFR, were exposed to different concentrations of cetuximab and gefitinib for two hours either alone or in combination demonstrating a decrease for each signal transduction marker. A greater decrease was evident for the combined treatment of both agents using 1 μmol/L gefitinib and 0.005 μmol/L cetuximab over either agent alone (Matar, Rojo, Cassia, Moreno-Bueno, Di Cosimo, Tabernero, et al., 2004). The data presented suggest that combining a diverse set of inhibitors may lead to a more significant clinical response.

Data regarding tyrosine kinase inhibitors in head and neck tumors is more limited in comparison to lung carcinomas for which gefitinib is currently approved for third line treatment. Striking differences exist between non-small lung cancer studies and head and neck tumors as studies reveal that lung cancer patients with EGFR gene amplification respond significantly to EGFR tyrosine kinase inhibitors. Variable sensitivities to

tyrosine kinase inhibitors such as gefitinib and erlotinib are noted in head and neck cancers. Due to the similar etiologies between lung and HNSCCs, treatment options for these two EGFR overexpressing carcinomas often follow a similar course in the literature, although variable results are reported owing to the genetic complexity between these epithelial tumor types. Mutations in the tyrosine kinase domain of the EGFR are indicative of gefitinib sensitivity and are more prevalent in non-smoking, Asian females with pulmonary adenocarcinomas. Similar tyrosine kinase domain mutations are rarely found in head and neck patients, thereby limiting a potentially gefitinib-responsive patient population (Varella-Garcia, 2006). Despite the disparities in tumor phenotypes, head and neck tumors are under investigation to determine if biomarkers of gefitinib sensitivity can be determined and correlated with EGFR gene copy status and prognosis.

Response to Tyrosine Kinase Inhibitors

Agulnik et al conducted a biomarker study of patients with recurrent or metastatic head and neck cancer showing better response rates to the tyrosine kinase inhibitor erlotinib in patients with high gene copy number versus low EGFR gene copy number. Erlotinib is similar in action to gefitinib, blocking the ATP binding site of the tyrosine kinase domain of EGFR. Agulnik et al used FISH to assess EGFR gene copy number in 32 head and neck tumor samples. Patients were designated FISH positive based on gene amplification and high polysomy (multiple chromosomes) or negative in all other categories. IHC analysis was used to assess protein expression of total and phosphorylated EGFR, -ERK, -AKT and STAT3 for evaluation of changes in EGFR pathway activation before and after a seven day erlotinib treatment. Ki67 was also

evaluated as a marker of proliferation, phosphorylated p27 to assess cell cycle inhibition, and phosphorylated NFκB for evaluation of NFκB pathway activation. Patients whose tumors showed decreases in phosphorylated EGFR and phosphorylated NFκB after erlotinib treatment were significantly associated with improved time to disease progression and overall survival. A decrease in p27 (a cell cycle inhibitor) protein after treatment was associated with an increase in time to disease progression and decreased overall survival. The decrease in p27 was an unexpected finding as cell cycle arrest is a typical response to tyrosine kinase inhibitors. A benefit of combined inhibition may result from targeting those cells that continue to proliferate by using additional cytotoxic agents rather than the use of monotherapies. Although FISH values were not statistically significant, this study was the first to suggest a possible association between increased gene copy number in head and neck cancers and response to the tyrosine kinase inhibitor erlotinib (Agulnik et al., 2007).

Gefitinib

Gefitinib inhibits the EGFR tyrosine kinase domain and is presently used in the treatment of locally advanced or metastatic non-small cell lung cancer. There is currently no reliable predictive factor for response to therapy with EGFR inhibitors like gefitinib in head and neck cancer. Lung cancer patients responsive to EGFR tyrosine kinase inhibitors are those with mutant tyrosine kinase domains and/or those with tumors dependent on EGFR phosphorylation for proliferation and metastasis as opposed to just receptor amplification or mutation (Rogers, Box, Chambers, Barbachano, Nutting, Rhys-Evans, et al., 2009). Other predictive factors are being considered for head and neck

tumors as similar mutations are rare and EGFR activation levels demonstrate variable results.

Sebastian et al studied gefitinib effectiveness in a panel of 14 head and neck cell lines from various locations including the larynx, oral cavity, tonsil and hypopharynx. A three day dose schedule of gefitinib was not able to modulate total EGFR expression in these cell lines as expected for an intracellular receptor inhibitor but a slight blockage of the cell cycle was demonstrated after treatment with a resulting variable reduction in phosphorylated Akt expression. Those cell lines with apparent signaling through phosphorylated Akt tended to respond to gefitinib. Gefitinib was able to affect downstream signaling with a 30 to 100% decrease in activated Akt. Six of 13 head and neck cell lines with measurable phosphorylated Akt at baseline showed complete loss of activity after gefitinib treatment of 1.9 – 5.4μM over 72 hours. Gefitinib's effect on MAPK was markedly less as five of 11 cell lines with detectable baseline expression maintained at least 80% of the protein's expression after treatment. The two highest EGFR expressing cell lines, HNC-211 and HNC-199 demonstrated variable sensitivity with IC_{50} values of 0.064μM and one of the highest IC_{50} values of 9.3μM, respectively, after 72 hours of treatment, indicating receptor expression status is not predictive of gefitinib response. Genomic analysis was not able to identify any activating mutations in the kinase domain of these cell lines (Sebastian, Azzariti, Accardi, Conti, Pilato, LaCalamita, et al., 2008). Heterogeneity in anti-EGFR inhibitor responses among cell lines and patients is attributed to the current lack of consistent markers able to identify a responsive population. Various clinical trials using gefitinib alone or in combination with

standard therapies continue to demonstrate variable responses to treatment (Modjtahedi & Essapen, 2009).

Pernas et al further defined gefinitib's actions in a panel of four head and neck cell lines consistent with the results of Sebastian et al showing that EGFR expression status alone is not predictive of gefitinib response. Pernas et al compared two cell lines, UMSCC-11A and UMSCC-11B, with high constitutive levels of EGFR to UMSCC-6 and UMSCC-9, two cell lines with intermediate to low levels of receptor expression. As expected, gefitinib was unable to affect total EGFR protein expression in any of the cell lines tested after a 5 day treatment. The UMSCC-11B cell line, a high EGFR expressing cell line, was most resistant to gefitinib treatment, almost 10-fold that of the remaining cell lines with an IC_{50} of 17μM.UMSCC-11B also demonstrated the highest levels of basal pSTAT3 activity, although gefitinib was able to reduce these levels in a dose dependent fashion. While NFκB p65 was inducible in UMSCC-6, UMSCC-11A and -11B through EGF ligand stimulation, gefitinib was not able to significantly decrease NFκB expression in the UMSCC-11B cell line. Similar to the findings presented by Sebastian et al, this study was unable to determine gefitinib sensitivity by EGFR expression status alone, although the activated, phosphorylation status of the receptor proved to be informative. UMSCC-9 exhibited the greatest response to gefitinib and the highest level of EGFR phophorylation at the Tyr1068 site of the receptor. Tyr1068 mediates Akt signaling, a consistent finding with Sebastian et al who found activated Akt levels to be indicative of a gefitinib response (Pernas et al., 2009).

Bortezomib

Bortezomib has been approved by the FDA in the treatment of multiple myeloma. Bortezomib's efficiency as a monotherapy in various solid tumors is being investigated. Noted toxicities from bortezomib treatment include diarrhea, vomiting and peripheral neuropathy that significantly increase with rising dosages. Bortezomib acts in a specific and reversible manner to target the proteasome and promote tumor cells to become apoptotic. One of bortezomib's mechanisms of actions is attributed to its ability to downregulate the PI3K/Akt pathway and NFκB. NFκB's activation is regulated by a family of inhibitory proteins called IκBs. When phosphorylated, IκBs become targeted for degradation by the proteasome, a multifunctional protein involved in removing damaged or misfolded proteins, governing regulatory tasks of the cell cycle, transcription factor activation, apoptosis and cell trafficking (Adams et al., 1999).

Allen et al. used DNA binding assays to assess bortezomib's ability to inhibit RelA in the head and neck cell lines UMSCC-9, UMSCC-11A and UMSCC-11B. Bortezomib was able to suppress TNFα-induced RelA in the three cell lines, although baseline constitutive activation of RelA was not affected by either 0.01μM or 0.1μM dosages over 12 or 24 hours. Interestingly, bortezomib had a decreased effect on other Rel subunits, including RelB, c-Rel and p52. All Rel subunits except c-Rel in both head and neck tumor specimens and cell lines demonstrated increased nuclear expression by IHC and DNA binding respectively. Bortezomib was not as effective at inhibiting nuclear expression of Rel subunits in the three cell lines through the noncanonical pathway as measured by DNA binding assay. Variable sensitivity to bortezomib was determined for

the three cell lines using the (3-(4,5-Dimethylthiazol-2-yl)-2,5-diphenyltetrazolium bromide, a tetrazole) MTT assay. Only UMSCC-11B showed sensitivity to bortezomib in the range of 0.01-1μM over a 5 day drug exposure (Allen et al., 2009). Sensitivity ranges in Allen et al.'s study were based on concentrations achieved in patient serum from previous studies conducted by Papandreou et al. Phase III trials established the efficacy of bortezomib at 1.3mg/m^2 administered by intravenous injection on days 1, 4, 8, and 11 of a 21-day cycle for a maximum of eight cycles in patients with relapsed/refractory multiple myeloma (Papandreou, Daliani, Nix, Yang, Madden, & Wang, 2004). Based on these findings by Allen et al, potential signaling through the noncanonical pathway in head and neck cancers supports the use of combination agents like gefitinib that may target Akt and downstream RelB activation.

To evaluate bortezomib's ability to downregulate the PI3K/Akt signaling pathway, Weber et al used the head and neck cell line SQ20B which has constitutively active expression levels of EGFR that results in upregulation of Akt. The cells were treated with 0.0005, 0.001, 0.01, 0.1 and 1μM bortezomib. Protein was harvested 2, 4, 8 and 24 hours after treatment and analyzed by western blotting. Downregulation of Akt was evident at 0.001μM, but 0.01μM was sufficient for almost complete down regulation of phosphorylated Akt protein expression after 24 hours. Although bortezomib has been a standard single agent treatment in hematological cancers, its efficiency as a dual agent in solid tumors awaits further investigation (Weber, Cerniglia, Maity, & Gupta, 2007).

Ooi attempted to characterize bortezomib's broad cytotoxic actions in the context of p53 stabilization using multiple myeloma and epithelial tumor cells. By comparing the

response of bortezomib-sensitive multiple myeloma cells to bortezomib-resistant solid tumors such as breast, prostate, colon, and thyroid, these authors sought to characterize how bortezomib increases protein levels of p53. The ubiquitin ligase human double minute 2 (Hdm2) promotes the degradation of p53 by tagging the protein and marking it for degradation by the proteasome. Once ubiquinated, p53 remains in the cytoplasm and becomes transcriptionally inactive. Although p53 levels may increase as a result of bortezomib's inhibition of the proteasome, the ability of the tumor suppressor p53 to affect the cell cycle becomes impaired. These authors were able to sensitize previously bortezomib-resistant tumors with the addition of an Hdm2-inhibitor nutlin-3 (Ooi, Hayden, Kotoula, McMillin, Charalambous, Daskalcki, et al., 2009). These results also provided evidence for bortezomib's cytotoxic actions being independent of p53 status. Combaret et al studied a panel of twelve neuroblastoma cell lines and found p53 mutational status to be independent of bortezomib response. After a 72 hour treatment with 0.01μM bortezomib, the accumulation of p53 protein was observed in all cell lines by western blot irrespective of sensitivity or resistance to the drug. An exploration for the involvement of other proteins involved in bortezomib resistance demonstrated high pre-treatment and post-treatment expression of phosphorylated HSP27 (heat shock protein), a group of proteins frequently upregulated as part of the stress response, in the two resistant cell lines, CLB-Sedp and SHEP (Combaret, Boyault, Iacono, Brejon, Rousseau, & Puisieux, 2008). In sensitive cell lines, bortezomib has been shown to stimulate p53 translocation to the nucleus in a time and concentration dependent manner as measured by DNA binding assays (Williams & McConkey, 2003).

Dual Blockage of EGFR and NFκB Pathways

The activation of EGFR and its downstream signal transduction kinases is known to modulate tumor development, progression and therapeutic resistance, suggesting that targeting common pathways may be essential for optimal inhibition. The activation of these intermediaries has been implicated in the upregulation of NFκB, which has been described in many cancer cell types as a supporter of tumor invasion, metastasis and proliferation. Bancroft et al examined the effects of the EGFR inhibitor PD153035, the anti-EGFR antibody C225, MEK (EGFR downstream effector) inhibitor U0126 and Akt inhibitor LY-294002 in human head and neck cell lines on NFκB and AP-1 activation. AP-1 or activator protein, is elevated in response to injury, cytokines and growth factors. Using luciferase reporter gene constructs, UMSCC-9 and UMSCC-11B HNSCC cell lines, were used to demonstrate basal NFκB and AP-1 activity. Upon pre-incubation with the EGFR inhibitor PD153035, greater than 50% of NFκB and Ap-1 basal activity was blocked. The anti-EGFR antibody C225, similar in action to cetuximab, significantly inhibited EGF inducible Ap-1 reporter activity by 50%. NFκB inhibition was not significant. Most notably the combination of the PI3K inhibitor and MEK inhibitor resulted in greater inhibition of constitutive and EGF-inducible NFκB activity than either agent alone. These authors found the MEK pathway, member of the MAPK pathway, was an important contributor to the activation of AP-1, whereas the PI3K/Akt pathway predominantly led to the activation of NFκB (Bancroft et al., 2002). As phosphorylation of PI3K leads to Akt activation, the Akt pathway as supporter of apoptotic resistance through NFκB provides a key mechanism in oncogenic EGFR signaling.

Piperdi et al studied the effects of combining bortezomib and erlotinib in a panel of NSCLC cell lines as these two agents have shown clinical activity with no overlapping toxicities. Seven NSCLC cell lines (H322, H358, H661, H460, H522, H1299, and A549) were used to evaluate the growth inhibitory activity by (MTT)-tetrazolium dye assay. Cells were treated with either erlotinib or bortezomib, alone or in combination, given either together or successively 24 hours apart. Cells were harvested at 48 hours from first drug exposure. Only two of the seven cell lines tested had IC_{50} levels indicating sensitivity to erlotinib at $\leq 1.46\mu M$ doses. Bortezomib had a narrower range of activity with IC_{50} levels of $0.01\mu M$ to $0.066\mu M$. For further study, two erlotinib sensitive cell lines, H322 and H358, were chosen and two resistant, A549 and H1299. In two of the four cell lines tested, H322 and A549, the cytotoxic effect from combining erlotinib and bortezomib was neither synergistic nor additive. Cell survival was measured by colony count and expressed as a fraction compared with baseline. The percentage of apoptosis was measured by flow cytometry. Although cellular toxicity and cell death was not significantly affected by combination treatment in 50% of the cell lines tested, increased cytotoxicity and apoptosis were discovered after 72 hours in the H358 cell line. H358 cells were exposed to $0.05\mu M$ bortezomib in combination with $2\mu M$ erlotinib. The schedule of drug dosage produced varying effects in the H358 cell line with the pre-exposure of elotinib abrogating the effect of bortezomib and synergistic effects with concomitant dosing or bortezomib pre-exposure (Piperdi, Ling, & Perez-Soler, 2007). Due to the selective action of erlotinib, additional studies are necessary to determine the efficiency of combination treatments using different cell lines and tissue types.

Summary

EGFR is highly expressed in most human head and neck cancer tumors. Despite the prevalence of the receptor, single agent EGFR inhibitors continue to demonstrate variable responses in HNSCCs. In order to further classify those patients that may respond to EGFR inhibitors versus nonresponders, markers of treatment resistance are continually being investigated. Studies have not been able to correlate EGFR protein expression status to anti-EGFR inhibitor sensitivity. EGFR gene amplified tumors are a subset of HNSCCs that demonstrate highly aggressive characteristics leading to decreased progression-free and overall survival rates and may harbor certain deregulated pathways that contribute to the resistance of currently employed treatments. Growth factor receptors such as EGFR have the potential to increase NFκB expression through Akt, contributing to the inefficiency of targeted treatments.

Differences in downstream pathways exist between head and neck tumors, although the defining phenotype that determines the optimal treatment regimen is not yet available. Downstream signal molecules may hold the key as cell lines that use Akt signaling have been shown to be gefitinib sensitive, although its overexpression may be an indicator of resistance. Bortezomib's primary target is NFκB, although the drug's ability to effectively downregulate all NFκB family members remains in question. NFκB overexpression has been proposed as a marker of treatment resistance through both classical and alternative pathways. Combination drug schedules using bortezomib with anti-EGFR inhibitors demonstrate promise in suppressing multiple deregulated pathways, although the optimum dose schedule requires further examination.

Significance of Study

HNSCCs represent a diverse population of cells guided by various oncogenic events and pathways. In order to improve the success of targeted therapies, patients must be categorized into responsive populations. Preliminary data has suggested advanced stage patients exhibit activation of EGFR and NFκB signaling pathways. High gene copy number of EGFR is frequent in HNSCCs and may be a sign of overly aggressive tumors. A better understanding of the EGFR and NFκB pathways could improve the use of targeted and combination therapies. The proposed studies are designed to provide preclinical data in support of bortezomib or gefitinib as targeted agents in head and neck squamous cell carcinomas. Effective combination therapies for patients with high EGFR gene copy number require continued exploration.

CHAPTER 3: METHODOLOGY

Background

The frequent overexpression of EGFR in HNSCC and the demonstration of its prognostic value have led to the evaluation of specific anti-EGFR agents as adjuncts to conventional therapeutic regimens. The EGFR signaling pathway and its downstream effectors play a key role in the growth of HNSCC and therefore represent attractive targets for therapy. As these agents are introduced in clinical practice, the identification of predictive markers for efficacy and toxicity becomes a crucial issue. The ultimate aim is to be able to deliver a treatment tailored to each individual patient based on their specific tumor profile. The objective of this study was to determine the potential chemosensitivity of HNSCCs with EGFR amplification to combination treatments using bortezomib, a proteasome inhibitor and gefitinib, an intracellular tyrosine kinase EGFR inhibitor. See Table 2 for a summary of experimental procedures.

Specific Aims

The primary goal of this study was to investigate the effects of the combined inhibition of bortezomib with gefitinib on human head and neck carcinoma cell lines with EGFR amplification. Specific aims of this study can be summarized as follows:

1) To test the hypothesis that **bortezomib could enhance the cytotoxic effects of gefitinib in HNSCC cell lines,** MTS assays were performed as a measure of cellular

Table 2. Summary of Experimental Procedures.

Aim	Hypothesis	Methods
Determine the effects of bortezomib and gefitinib in cell lines with normal and increased EGFR gene copy number.	Increased synergistic effects will result from the administration of bortezomib with gefitinib in cell lines with increased EGFR gene copy number.	PCR and Western blot to determine EGFR gene amplification and increased protein expression in cell lines. Cell proliferation measured by MTS assay to establish baseline responses to single drug dosing and effects of bortezomib and gefitinib in combination.
Determine the differences in the activation of EGFR downstream proteins between normal and increased EGFR gene copy number after gefitinib dosing.	Mechanisms of gefitinib response will be determined by expression levels of downstream effectors of the EGFR pathway.	Western blots of downstream EGFR pathways markers: EGFR, Akt, STAT3, & MAPK to determine protein expression levels before and after gefitinib treatment.
Determine the differences in the signaling pattern of NFκB in cell lines with normal and increased EGFR gene copy number.	Mechanisms of bortezomib response will be determined by the expression of target proteins in the canonical NFκB pathway.	DNA binding assay measuring NFκB/RelA nuclear activation levels to determine target presence for bortezomib.

proliferation after agent treatment with each drug alone then again after the use of bortezomib and gefitinib in combination. Three head and neck cell lines with EGFR gene amplification (SQ20B, HN5, HSC-3) as confirmed by real-time quantitative polymerase chain reaction (qPCR) were chosen for comparison to three EGFR wild-type (SCC25, SCC1, 1CC8) head and neck cell lines. 1CC8 is a cetuximab resistant clone developed from the SCC1 cell line and was used to assess anti-EGFR inhibitor resistance as an

additional factor in drug sensitivity. Single agent IC_{50} levels, a measure of drug concentration required for 50% inhibition of cellular growth, for both gefitinib and bortezomib were established for each cell line. 1CC8, an EGFR wild-type cell line proved equally resistant to lower doses of gefitinib and responsive to bortezomib on equivalent levels to EGFR amplified cell lines, eliminating EGFR resistance as an additional factor for study. To maintain equal comparisons between EGFR amplified groups and wild-type cell lines, four of the original six cell lines were chosen (the two most bortezomib responsive EGFR amplified cell lines, SQ20B and HN5 and the two most gefitinib responsive EGFR wild type cell lines, SCC25 and SCC1) for further drug combination studies by MTS assay using gefitinib, bortezomib and a specific NFκB inhibitor, bay 11-7082. Bay 11-7082 served to further isolate the importance of specificially inhibiting the NFκB pathway in these four cell lines.

2) To test the hypothesis that **gefitinib response in head and neck cell lines is associated with a tumor's dependence on the EGFR pathway**, western blot assays were performed to measure changes in protein expression levels of the three major downstream pathways of EGFR. To stimulate the EGFR pathway in the four cell lines (SQ20B, HN5, SCC25 and SCC1), TGFα, a primary ligand for EGFR was applied to serum starved cells for 30 minutes. Serum starvation involves the application of cell culture media minus fetal bovine serum (FBS) for 24 hours in order to isolate the effects of TGFα and activation of the EGFR pathway without interference from other growth factors normally present in FBS that could stimulate additional pathways (Mather & Roberts, 1998). Three cell culture plates were established for each cell line: baseline

protein levels without TGFα or drug stimulation, TGFα stimulation only, and 0.1μM gefitinib for 24 hours followed by TGFα stimulation for 30 minutes to measure the drug's ability to inhibit downstream pathways upon ligand stimulation. This dose of gefitinib was chosen based on previous studies by Sebastian et al indicating doses as low as 0.064μM were recorded in cell lines responsive to gefitinib (Sebastian, et al., 2008). Protein was then extracted for each cell line, run on a gel and probed for the three major EGFR downstream pathway markers: phosporylated Akt, total Akt, phosphorylated STAT3, total STAT, phoshorylated MAPK, and total MAPK by western blot analysis.

3) To test the hypothesis that **bortezomib response in head and neck cell lines is dependent on the presence of NFκB activity through the canonical pathway**, DNA binding assays were used to measure the nuclear protein expression levels of RelA in SQ20B, HN5, SCC25, SCC1, Hep2, and HSC-3 after TNFα stimulation. SQ20B, Hep2 and SCC25 were shown to be most responsive to bortezomib by MTS assay. HN5 was intermediate in response to bortezomib while SCC1 and HSC-3 were the two most resistant cell lines as measured by MTS assay. In preparation for DNA binding assays, three culture plates were established for each cell line and serum starved for 24 hours to isolate the effects of the ligand TNFα, the primary ligand for the canonical pathway of NFκB. The three culture plates consisted of: baseline nuclear protein levels without TNFα or drug stimulation, TNFα stimulation only, and 0.1μM bortezomib for 24 hours followed by TNFα stimulation for 30 minutes to measure the drug's ability to inhibit RelA upon ligand stimulation. The concentration of 0.1μM bortezomib for 24 hours was chosen based on previous studies by Allen et al. showing bortezomib was able to

suppress TNFα-induced RelA in head and neck cell lines using the same concentration over 24 hours (Allen et al., 2009).

Because DNA binding results indicated off-target effects (targets of cytotoxicity other than NFκB) for bortezomib in SQ20B and SCC25, Ingenuity Pathway Analysis (IPA) was employed comparing the gene sets of the two most bortezomib sensitive cell lines SQ20B and Hep2 versus the two most resistant cell lines tested, HSC-3 and SCC1. IPA determines which pathways are significantly linked to the microarray gene set previously compiled by the Chung laboratory and compared to the whole Ingenuity knowledge base. The analysis revealed p53 as the top significant pathway to be associated with the gene set. Western blot analysis was used to assess the p53 protein expression level differences in SQ20B, HN5, SCC25, SCC1, Hep2 and HSC-3 cell lines before and after bortezomib treatment.

Specific Aim 1

Cell Culture

Six cell lines were chosen from the Chung laboratory inventory for establishing gefitinib and bortezomib sensitivity by MTS assay. These six cell lines were taken from the original inventory of thirty-two HNSCC cell lines and were chosen based on the perimeters of likely EGFR gene amplification (SQ20B, HN5 & HSC-3) in addition to a negative status for human papilloma virus as previously determined by PCR in the Chung laboratory. Matching EGFR wild-type cells (SCC25 and SCC1) were chosen for comparison to SQ20B, HN5 & HSC-3. 1CC8 was the only cell line with intrinsic anti-EGFR inhibitor resistance. EGFR gene amplification was verified by real- time PCR.

HaCat cells were established for use as control cells for quantitative comparison in real-time qPCR assays. HaCaT cells are human keratinocyte cells with normal EGFR expression commonly used as control cells (Chung, Parker, Levy, Slebos, Dicker, & Rodeck, 2007; Patel, Ramesh, Traicoff, Baibakov, Emmert-Buck, Gutkind, et al., 2005). SQ20B was contributed by Ralph Weichselbaum at University of Chicago. SCC25 was purchased through American Type Culture Collection (Manassas, VA). SQ20B and SCC25 were maintained in 10% Fetal Bovine Serum (FBS), 1% Penicillin/Streptomycin, 0.4µg/mL hydrocortisone in Dulbecco's Modified Eagle Medium: Nutrient Mixture F-12 (Invitrogen, Carlsbad, CA). SCC1 was contributed by Thomas Carey, University of Michican. 1CC8 is a cetuximab-resistant clone of SCC1 established in the laboratory of Dr. Carey by continuous exposure to increasing concentrations of cetuximab over 6 months (Wheeler et al., 2008). 1CC8 and SCC1 were maintained in 10% FBS, 1% Penicillin/Streptomycin, 0.4µg/mL hydrocortisone in Dulbecco's Modified Eagle's Medium (Cellgro, Manassas, VA). HSC-3 was provided by the Japanese Collection of Research Bioresources (Shinjuku, Japan). HSC-3 was maintained in 10% FBS, 1% Penicillin/Streptomycin in Minimum Essential Medium (Invitrogen). HN5 was contributed by Ludwig Institute for Cancer Research (New York, NY). HN5 was maintained in 10% FBS, 1% Penicillin/Streptomycin, and 0.8µg/mL hydrocortisone in Dulbecco's Modified Eagle's Medium with 4.5 g/L Glucose, L-glutamine, & sodium pyruvate (Cellgro, Manassas, VA). HaCaT cells were purchased from Cell Lines Service (Eppelheim, Germany). HaCaT cells were maintained in MCDB-153 media (Mediatech, Manassas, VA) supplemented with 2% FBS and 1% penicillin/streptomycin.

Cell Line Verification

The integrity of each cell line, SQ20B, HN5, HSC-3, SCC1, 1CC8, HaCaT and Hep2 (described in Specific Aim 3) was verified by STR (single-locus short tandem repeats) typing using the AmpFLSTR Identifiler PCR Amplification Kit from Applied Biosystems (Carlsbad, CA). STR are located at specific loci in the genome of each cell line. The DNA typing process of cell lines involves simultaneously amplifying 15 STR loci by polymerase chain reaction. Due to the highly polymorphic nature of each STR loci, every cell line will have a unique molecular pattern that can distinguish it from other sources. Analysis was conducted by the Fragment Analysis Facility at John Hopkins University (Baltimore, Maryland) in March 2010. Each cell line, SQ20B, HN5, HSC-3, SCC1, 1CC8, HaCaT and Hep2 proved unique in typing results.

Real-Time Polymerase Chain Reaction

To determine the specific amplification status of EGFR in SQ20B, HN5, HSC-3, 1CC8, SCC1, SCC25, and HaCaT cell lines, real time PCR was performed using the DNA MasterMix SYBR Green (BioRad, Hercules, CA) and a iCycler IQ (Bio-Rad, Hercules, CA). DNA was isolated from seven HNSCC cell lines using Ambion RecoverAll Total Nucleic Acid Isolation kit (Ambion Inc., Austin, TX) according to the manufacturer's protocol. Cell line DNA was tested for the expression of EGFR using a specific primer for exon 18 (forward: 5'-AGCATGGTGAGGGCTGAGGTGAC-3'; reverse: 5' ATATACAGCTTGCAAGGACTCTGG-3') producing a 262 base pair amplifying product. Exons 18–21 of the EGFR gene are standard for analysis of mutations, as this is where EGFR mutations are clustered (Sharma, Bell, & Settleman,

2007). Primers for GAPDH (forward: 5'-GTTCGACAGTCAGCCGCATC-3'; reverse: 5'-GGAATTTGCCATGGGTGGA -3') were used as a positive internal control for amplification. PCR was performed as follows: an initial incubation step at 95°C, 40 amplification cycles of 95°C for 10 seconds, 60°C for 45 seconds, and a final extension cycle of 72°. Relative changes in EGFR gene expression were determined by the $2^{-\Delta\Delta CT}$ method (Livak & Schmittgen, 2001) normalized to GAPDH and relative to normal human keratinocyte cell line, HaCaT. Results were completed in triplicate and averaged. Normalized EGFR gene expression values are presented as means ± standard deviation (SD).

MTS Assay

The [3-(4,5-dimethylthiazol-2-yl)-5-(3-carboxymethoxyphenyl)-2-(4-sulfophenyl)-2H-tetrazolium, inner salt] (MTS) assay is a colorimetric method for determining the number of viable cells in proliferation or cytotoxicity assays. Growth inhibition was measured using the CellTiter 96 Aqueous One Solution Assay (Promega, Madison, WI) as recommended by the manufacturer. The CellTiter 96 Aqueous One Solution contains MTS [3-(4,5-dimethylthiazol-2-yl)-5-(3-carboxymethoxyphenyl)-2-(4-sulfophenyl)-2H-tetrazolium, inner salt] compound and an electron coupling reagent PES [phenazine ethosulfate]. The MTS compound is bioreduced by mitochondrial enzymes of cells into a colored formazan product that is soluble in tissue culture medium. The quantity of formazan product as measured by the amount of 490nm absorbance is directly proportional to the number of living cells in culture. After 2 hours of incubation under standard conditions of 5% CO_2 and 37°C, the purple formazan product (indicative of

reduction of MTS) was visible. Three head and neck cell lines verified for EGFR gene amplification (SQ20B, HN5, HSC-3) were compared to three EGFR wild-type cell lines (SCC25, SCC1 and 1CC8) and used for drug sensitivity assays.

Bortezomib (Millennium Pharmaceuticals, Cambridge, MA) was purchased from the Vanderbilt Pharmacy. Bortezomib was diluted in 0.9% sodium chloride at 1mM concentrations before being further diluted in culture medium prior to each experiment. Gefitinib was purchased from Tocris Bioscience (Ellisville, Missouri). Gefitinib was diluted in dimethyl sulfoxide (DMSO) at 1mM before being further diluted in culture medium prior to each experiment. Cells were seeded in flat-bottom 96-well culture plates with $2x10^3$ cells per well in quadruplicate at each dose level on day 0. The drugs were added on day 1: bortezomib or gefitinib at 0.01μM, 0.1μM, and 1μM, and kept in the media for 48 or 72 hours.

The absorbance was read at 48 and 72 hours using the BioTek Synergy HT microplate automated reader (Biotek Instruments, Winooski, VT) at 490 nm. The signal generated (color intensity) is directly proportional to the number of viable (metabolically active) cells in the wells. Relative cell numbers can therefore be determined based on the optical absorbance (optical density, OD) of the sample. The blank values (media only) were subtracted from each well of the treated cells and controls (saline only, the carrier solution for bortezomib or DMSO only, the carrier solution for gefitinib); and the mean and standard error for each treatment (single dose experiments and combination drug experiments) were calculated relative to the control. Background readings from untreated, control cells using the CellTiter 96 AQueous Systems are typically 0.1-0.3 absorbance

units. Culture media without cells (blank values) for each cell type was used in each experiment to provide a background absorbance value which was subtracted from all wells. Each data point represents the mean of four wells from three separate experiments.

Data Analysis

Single Agent Drug Studies

Statistical analysis was performed using unpaired Student's t test (two-tailed distribution) using SPSS version 15 comparing untreated control cells with treated cells when measurable IC_{50} levels were achieved at either the 48 or 72 hour time points for single agent drug studies.

In each cell culture plate, the first row (row A) contained medium only without cells, providing a base value of absorption when conducting the MTS Assay. Since each cell line experiment was done in triplicate, the results from each row were averaged to find the mean absorption for a certain concentration. The mean background absorbance value was subtracted from each row of averaged drug concentration value to achieve the normalized value. Table 3A represents the average of three separate experiments. For example, in the SCC25 cell line data above, the normalized value for gefitinib 0.01μM is calculated by subtracting the average medium only value (0.152) from the average concentration value for 0.01μM (1.2032) to reach the final normalized value 1.0509. The control value column is then calculated by taking the normalized value and dividing it by the control value, i.e. 1.0509/1.1589= 0.9068, to find the control rate for each drug concentration. These values are then plotted onto the graphs seen in Chapter IV: Results. These graphs show the decreasing viability of cells with increasing drug concentrations.

Table 3A. Example Data Analysis for Determining Single Agent Gefitinib Response in SCC25 Cells.

SCC25							
Gefitinib	1st	2nd	3rd	4th	Ave	Normalized	Control Rate
Medium (Row A)	0.139	0.152	0.166	.151	0.152		
Control (DMSO)	1.387	1.183	1.327	1.348	1.3112	1.1589	1
Gefitinib 0.01μM	1.162	1.361	1.161	1.129	1.2032	1.0509	0.9068
Gefitinib 0.1μM	1.026	1.011	1.092	0.915	1.011	0.8586	0.7409
Gefitinib 1μM	0.448	0.466	0.587	0.593	0.5235	0.3711	0.3202

The 100% viability mark is found at the point where no drug is being used to treat the cells (control value of 1). The point where 50% cell viability is achieved is where the IC_{50}, will be noted except in cases of drug resistance. In the case of the SCC25 data the IC_{50} value was found between the concentrations of 0.1 μM and 1 μM doses of gefitinib calculated as shown in Table 3B.

Table 3B. Example Data Analysis for Determining Gefitinib IC_{50} Level in SCC25 Cells.

Gefitinib 72 hours	
IC_{50}	SCC25
A:concentration of more than 50%	.1
B:concentration of less than 50%	1
C:inhibition rate of B	68
D:inhibition rate of A	26
IC_{50}	.373

Using the control rates found in Table 3A, the inhibition rate at 0.1μM concentration is 26% and the inhibition rate at 1μM concentration is 68% resulting in an IC_{50} of 0.373 for SCC25 at 48 hours of gefitinib exposure. Data was calculated using Microsoft Excel.

Drug Combination Studies

Bay 11-7082 was diluted in dimethyl sulfoxide (DMSO) at 1mM before being further diluted in culture medium prior to each experiment (Sigma, St. Louis, MO).

Single agent IC_{50} levels were determined for bay 11-7082 over 48 hours in triplicate before combination studies were continued. For the evaluation of antiproliferative effects of bortezomib in combination with gefitinib or bay 11-7082, three schedules were performed: (1) bortezomib for 24 hours followed by gefitinib for 24 hours or gefitinib for 24 hours followed by bortezomib for 24 hours, (2) bortezomib or bay 11-7082 for 24 hours followed by gefitinib for 24 hours, gefitinib for 24 hours followed by bortezomib or bay 11-7082, (3) simultaneous incubation of gefitinib with bortezomib or bay 11-7082 over 48 hours. HNSCC cell viability was then determined by MTS assay (Promega, Madison, WI). Dosage levels were determined for each inhibitor based on IC_{50} levels established in single agent experiments. Gefitinib did not reach an IC_{50} level in SQ20B, HN5, SCC25, and SCC1 at 48 hours, therefore for combination experiments gefitinib was dosed at 0.5μM concentrations, half the maximal dosage used in single agent studies to determine if synergistic combinations would be possible with these drugs in combination. Experiments were performed in triplicate.

The ANOVA or Kruskal-Wallis statistical tests were performed for drug combination studies involving bortezomib/gefitinib and gefitinib/bay 11-7082. The independent variable was the effect of combining gefitinib and bortezomib (or bay 11-7082) in combination or sequentially. The dependent variable was the percent cell viability resulting from these drug combinations. Cell viability results were normalized to the mean of the control and analyzed using the Student's t-test for single agents and ANOVA or Kruskal-Wallis for drug combination analysis. The statistical analysis was performed with SPSS for Windows, version 15.0 (SPSS, Inc., Chicago, IL). The

significance of differences among multiple groups was assessed using ANOVA. When the data sets failed the normality test, the Kruskal-Wallis one-way ANOVA was used. The distribution of cell viability data was assessed using boxplots generated by SPSS.

Levene's and Welch's test for equality of variance was computed and analyzed for violations of normality. Non-significant results indicated assumption of homogeneity was met. When the assumption of homeogeneity was not met as indicated by significant Levene's and Welch's tests, the Kruskal-Wallis nonparametric test was employed. This test is comparative to ANOVA and is used when the assumption of normality is violated (Gravetter & Wallnau, 2006). In the ANOVA, an F ratio was calculated which represents the variance between the drug combination groups divided by the variance within the groups. A large F ratio indicates more variability between groups (caused by the independent variable) than within groups. A significant ($P < 0.05$) F test rejects the null hypothesis that the population means are equal.

Specific Aim 2

Cell Culture

SQ20B, HN5, SCC1 and SCC25 were established as previously described (p. 54) and used to demonstrate the response of head and neck cell lines to gefitinib after stimulation of the EGFR pathway using the ligand TGFα (10ng/µl) after serum starvation. Serum starvation for 24 hours allowed for isolation of the effects of the EGFR pathway through TGFα ligand stimulation. Differences in downstream pathway response between EGFR amplified cell lines SQ20B and HN5 versus SCC25 and SCC1 was measured by protein expression levels before and after gefitinib drug dosage (0.1µM)

after 24 hours. This dose of gefitinib was chosen based on previous studies by Sebastian et al indicating doses as low as 0.064μM were sufficient for cell inhibition in HNSCC cell lines (Sebastian, et al., 2008).

Western Blotting

Cellular protein extracts were analyzed for EGFR downstream pathway expression differences via Western blotting analysis. SQ20B, HN5, SCC1 and SCC25 were lysed with RIPA lysis buffer (1mM NaVO3,1mM DTT, 1mM PMSF, phosphatase inhibitor cocktail and protease inhibitor cocktail mini tablet; Roche, Indianapolis, IN), then sonicated. Protein concentration was quantified with a standard Bradford absorbance assay using a microplate luminometer. Thirty micrograms of whole cell lysate from SQ20B, HN5, SCC25 and SCC1 was mixed with Laemmli loading buffer (containing β-mercaptoethanol) and heated at 95°C for 10 min. Samples were loaded onto 7.5% Tris-glycine precast gels and electrophoresed for 1.5 hours at 115V on a Biorad Mini-PROTEAN Tetra cell (Bio-rad, Hercules, CA). Proteins were transferred to a polyvinylidene fluoride (PVDF) membrane at 30V overnight at 4°C using a Biorad Tetra Blotting Module and incubated with rabbit anti-EGFR antibody and its activated form phosphoryated EGFR Tyr1068. To measure the activated status of EGFR, an antibody targeting the tyrosine phosphorylation site Tyr1068 was chosen for analysis as studies indicate it mediates signaling to Akt and MAPK pathways (Pernas, et al., 2009). The three major downstream pathways were assessed using antibodies targeting phosphorylated p44/42 MAPK, total MAPK, phosphorylated Akt, total Akt, and phosphorylated STAT3, total STAT3, (Cell Signaling Technology, Boston, MA) at the

dilution of 1:1000, followed by secondary antibody at 1:3000 dilution for anti-rabbit or 1:5000 dilution for anti-mouse. Anti-rabbit β-actin or anti-GAPDH antibody was used as a loading control (Cell Signaling Technology, Boston, MA). All antibodies were diluted in Odyssey Blocking Buffer (Li-cor Bioscience, Lincoln, NE, USA). Each blot was incubated with Amersham ECL plus Western Blotting Detection Reagents for the detection of EGFR, and its downstream proteins, β-actin or GAPDH and exposed to HyBlot CL Autoradiography Film (Denville Scientific, Metuchem, NJ). Experimental band intensity for each sample was determined relative to the corresponding loading control band using National Institutes of Health Image J, a public domain Java image analysis and processing program http://rsbweb.nih.gov/ij/. Image J allows for comparing the intensity of bands on a Western blot to standard proteins (β-actin or GAPDH) which are converted into pixels that represent quantitative values. This allows for relative intensity comparisons. The absolute intensity of each sample band (SQ20B, HN5, SCC25 or SCC1 for instance) is divided by the absolute intensity of the standard to come up with a unitless value for the relative intensity of each sample band. Some bands will have a relative intensity lower than 1 (they have less protein than the standard), and some bands might have a relative intensity larger than 1 (they have more protein than the standard).

Specific Aim 3

Cell Culture

Head and neck cell lines were established for subsequent analysis by DNA binding assay for measurement of NFκB nuclear binding activity after bortezomib dosing. SQ20B, HN5, HSC-3, SCC1, and SCC25 were analyzed for bortezomib

sensitivity by MTS assay as previously described (p. 54-56). Hep2, obtained from Nobuhiko Oridate from Hokkaido University, was added as an additional bortezomib sensitive cell line and maintained in DMEM with 5% FBS and 1% Penicillin/Streptomycin. All cell lines were serum starved for 24 hours. Serum starvation for 24 hours allowed for isolation of single pathway response to TNFα and the resulting canonical pathway of NFκB stimulation. Differences in nuclear expression levels of NFκB/RelA between the six cell lines was measured by DNA binding assays before and after 0.1μM bortezomib drug dosage for 24 hours.

MTS Assay

Hep2, an EGFR wild-type cell line, was previously established as a bortezomib-sensitive cell line in the laboratory and was reassessed for bortezomib sensitivity by MTS assay over 48 and 72 hours using previously established methods (p.54). HSC-3 was previously verified as bortezomib resistant by MTS Assay and added as an additional resistant cell line for analysis; see Results, Figure 13 (p. 75).

Nuclear Extraction and DNA Binding Assays

Having established by MTS Assay that SQ20B, Hep2 and SCC25 were significantly sensitive to bortezomib, the DNA binding assay was employed to determine the nuclear localization and activation of NFκB/RelA before and after TNFα stimulation. Nuclear cell extracts were prepared from serum starved cell lines SQ20B, HN5, SCC25, SCC1, Hep2 and HSC-3 by employing a kit from Active Motif (Carlsbad, CA). At the end of the incubations with bortezomib at 0.1μM for 24 hours with or without TNFα stimulation for 30 minutes, the cells were washed, collected in ice-cold PBS in

The presence of phosphatase inhibitors and centrifuged at 500 rpm for 5 min. This time and concentration of bortezomib (0.1μM) was chosen based on studies by Allen et al., demonstrating TNFα-induced RelA sensitivity to bortezomib in head and neck cell lines (Allen et al., 2009). The pellets were then resuspended in a hypotonic buffer, treated with detergent and centrifuged at 14,000 g for 30 sec. After collection of cytoplasmic fraction, the nuclei were lysed and nuclear proteins solubilized in the lysis buffer in the presence of protease inhibitor cocktail. The concentration of the nuclear extract was determined using a standard Bradford Assay using a microplate luminometer.

The binding of NFκB to DNA was measured in nuclear extracts with a specific TransAM NFκB p65 assay kit from Active Motif, according to manufacturers' instructions. This assay is based on the use of multi-well plates coated with an oligonucleotide containing the consensus binding site for NFκB. Nuclear proteins (5ug) were added to each well and incubated for 1 h to allow the binding of NFκB to this oligonucleotide. The presence of the DNA-bound transcription factor was then detected by the primary antibody that recognizes an epitope on p65 only when NFκB is activated and bound to its target DNA. After addition of an anti-rabbit secondary antibody the results were quantified by spectrophotometry. The absorbance was determined on a spectrophotometer (Microplate reader model 550, Bio-Rad) at 450 nm with a reference wavelength of 655 nm. The absorbance is proportional to the amount of NFκB p65 RelA bound to DNA. NFκB-binding activity of testing samples, controls, and blanks were measured in duplicate and averaged for statistical analysis. The statistical analysis of the data was performed by using ANOVA. P values <0.05 were considered significant.

Ingenuity Pathway Analysis

The Ingenuity Pathway knowledge base is the world's largest database of biological networks created from millions of individually modelled relationships between proteins, genes, complexes, cells, tissues, drugs, and diseases. Ingenuity Pathway Analysis (IPA) is a web-based software application that enables the researcher to identify pathways most relevant to their experimental datasets of interest. Relationships are modeled among genes identified in RNA screens performed by the researcher (http://www.ingenuity.com/). A microarray is a tool for analyzing gene expression that consists of a small membrane, chip or glass slide containing samples of many genes arranged in a regular pattern. The DNA is printed, spotted, or actually synthesized directly onto the support. A researcher uses the location of each spot in the array to identify a particular gene sequence. The spots themselves can be cDNA or oligonucleotides. mRNA is isolated from each cell type and used as templates to generate cDNA with a "fluorescent tag" attached. Different tags (red and green) are used so that the samples can be differentiated in subsequent steps. The two labeled samples are then mixed and incubated with a microarray containing the immobilized genes. The labeled molecules bind to the sites on the array corresponding to the genes expressed in each cell. The microarray is then placed in a scanner that consists of lasers, a special microscope, and a camera. The fluorescent tags are excited by the laser, and the microscope and camera work together to create a digital image of the array. These data are then stored in a computer, and a special program is used to calculate the red-to-green fluorescence ratio for each microarray spot by analyzing the digital image of the array. The program

thencreates a table that contains the ratios of the intensity of red-to-green fluorescence for every spot on the array. By isolating mRNA from the head and neck cell lines, SQ20B, Hep2, HSC-3 and SCC1, comparisons were able to be made in terms of gene expression through this microarray technique (Burguete, S., & McLachlan, G., 2009). Using the microarray data generated for SQ20B, Hep2, HSC-3 and SCC1, gene expression results were imported into the Ingenuity Pathway Analysis database, comparing bortezomib resistance and sensitivity profiles between SQ20B and Hep2 to SCC1 and HSC-3. Statistical analysis was done using Linear Model for Microarray Data (LIMMA). LIMMA is a well-known bioinformatics package for differential expression analysis of data arising from microarray experiments. The LIMMA package analyzes data from comparisons between two or more groups of samples simultaneously. The analysis is accomplished by fitting a linear model to the expression data for each gene. The main advantage of LIMMA over the regular t-test is that LIMMA uses Empirical Bayes and other shrinkage methods to borrow information across genes, whereas the t-test treats each gene as an independent observation. Thus LIMMA is more representative of the real gene regulation within the biological model (Smyth, 2004). The gene expression profile of bortezomib sensitive cell lines SQ20B and Hep2 was compared to bortezomib-resistant cell lines HSC-3 and SCC1. Examination of these genes on the context of biologic pathways using IPA revealed p53 as a key signaling pathway.

Western Blot Analysis

To explore the off-target effects of bortezomib in SCC25 and SQ20B, Western blot analysis was performed to assess p53 protein stabilization after drug treatment

in SQ20B, HN5, SCC25, HN5, HSC-3 and Hep2. Using previously described methods for western blot analysis (p.60), protein was extracted from serum starved cell lines SQ20B, HN5, SCC25, SCC1, Hep2 and HSC-3 before and after 24 hour bortezomib treatment at a concentration of 0.1μM. Protein extracts were quantified using a standard Bradford Assay and subjected to Western blotting assay using an anti-p53 antibody at 1:1000 dilution followed by anti-rabbit secondary at 1:3000 (Santa Cruz Biotechnology, Santa Cruz, CA). Bands were quantified using Image J analysis as previously described (p.61).

CHAPTER IV: RESULTS

Specific Aim 1

In this study, HNSCC cell lines SQ20B, HN5, HSC-3, 1CC8, SCC25, and SCC1 which express differing amounts of the EGFR gene were used to assess the efficacy of bortezomib and gefitinib. The cell lines were analyzed by qPCR in triplicate using primers spanning the exon 18 sequence of the receptor. An upregulated level of EGFR gene expression was noted in SQ20B (6 fold), HN5 (4 fold) and HSC-3 (3 fold) compared to the baseline receptor expression in SCC25, SCC1 and 1CC8 (Figure 4).

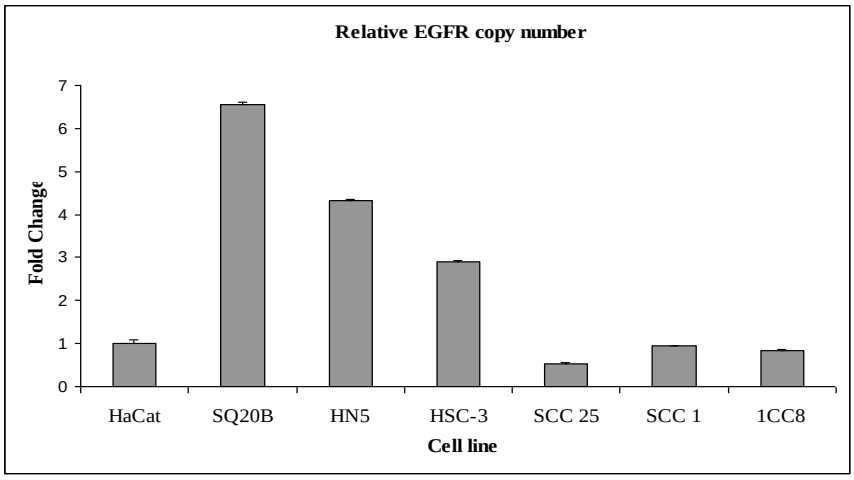

Figure 4. EGFR Amplification Status in HNSCC Cell Lines.

EGFR DNA expression was presented as the fold change in EGFR gene expression normalized to GAPDH and relative to human keratinocyte cell line, HaCaT. Results are reported in triplicate with error bars representing standard deviation.

Single Agent Drug Studies

Three EGFR amplified cell lines, SQ20B, HN5 and HSC-3, as assessed by PCR were chosen to assess drug sensitivity to gefitinib in order to establish baseline levels for subsequent combination studies. Three wild-type cell lines with normal EGFR receptor levels, SCC25, SCC1 and 1CC8, as assessed by PCR were chosen for drug sensitivity assessment in comparison. 1CC8 was derived from the parental SCC1 cell line by chronic, repeated exposure to cetuximab. Although 1CC8 is an EGFR wild-type line, the EGFR inhibitor resistance phenotype allowed for assessment of targeted agent treatment resistance using a drug with a similar mode of action. This provided an additional factor for analysis in drug sensitivity. Cetuximab is an antibody that binds to the extracellular domain of EGFR, preventing its activation and tumor-promoting effects.

In response to gefitinib treatment, all three EGFR amplified cell lines, SQ20B, HN5 and HSC-3 demonstrated resistance to doses of 1μM and less over 48 and 72 hour time points of exposure. Each cell line (2 $x10^3$ cells/well) was cultured in 96-well plates for 24 hr to allow 70-80% confluence then treated with varying concentrations (0.01μM, 0.1μM & 1μM) of gefitinib for 48 & 72 hours. Data points represent means of three independent experiments performed in triplicate with error bars representing standard error of the mean. The percent survival is plotted relative to control cells. Cells were assessed for post-treatment viability using the MTS assay. IC_{50} levels were not reached at either 48 hour or 72 hour time points for either SQ20B or HN5 (Figures 5 and 6). Although cell proliferation was downregulated slighlty by gefitinib at the 0.01μM concentration in HSC-3 cells, recovery of growth occurred at the 0.1μM drug dosage and

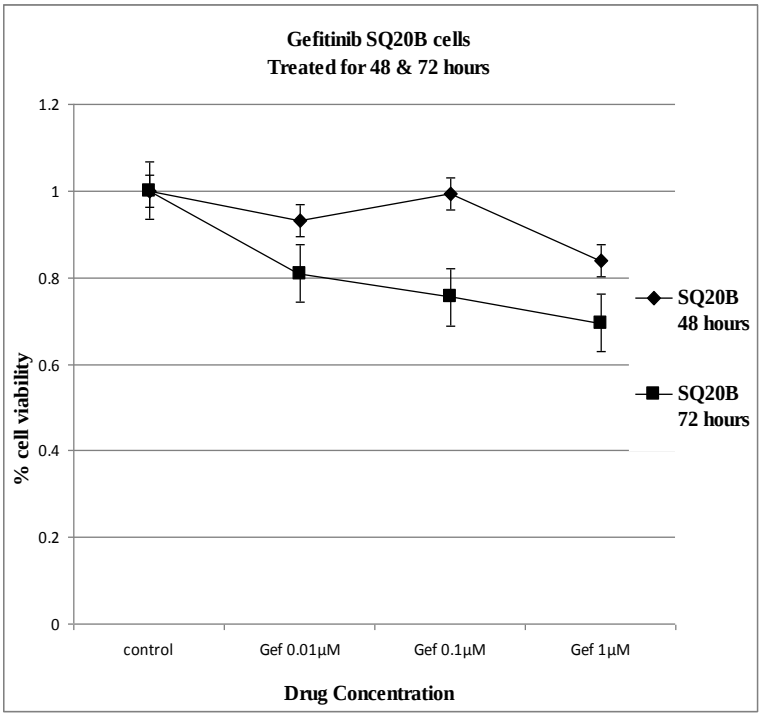

Figure 5. Gefitinib Treatment in EGFR Amplified Cell Line SQ20B.

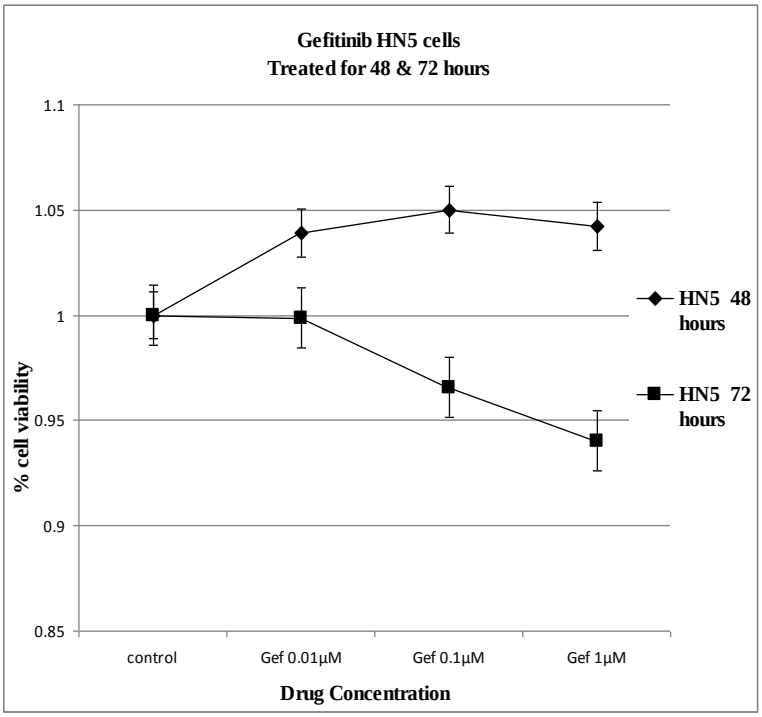

Figure 6. Gefitinib Treatment in EGFR Amplified Cell Line HN5.

remained resistant up to the 1μM dose (Figure 7). Compensatory signaling mechanisms

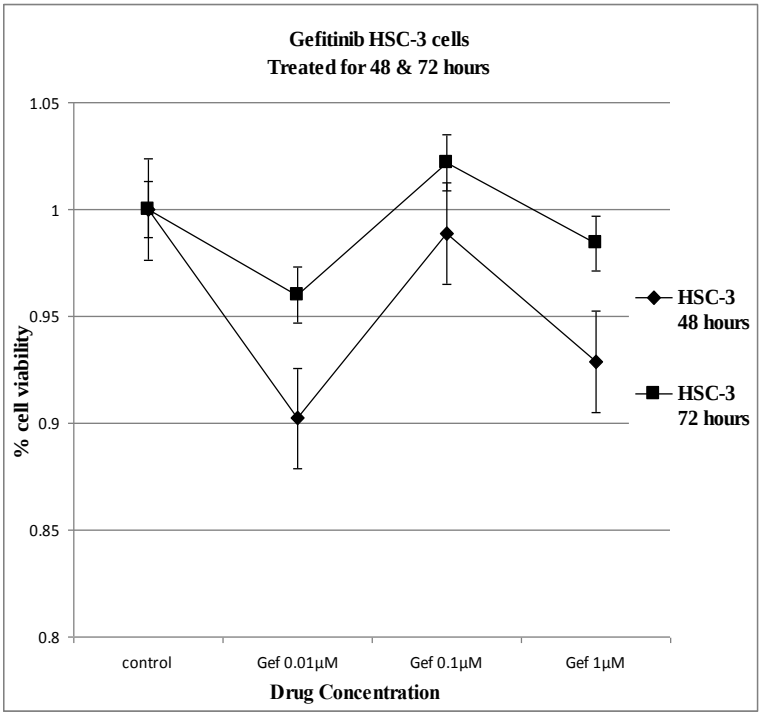

Figure 7. Gefitinib Treatment in EGFR Amplified Cell Line HSC-3.

may contribute to this cell lines' ability to recover survival pathways through activation of alternative receptors. pAkt is known to be upregulated in EGFR amplified cells lines, necessitating higher concentrations of gefitinib to suppress resistant cell populations. Sergina et al demonstrated that increased expression of additional ErbB receptors in addition to upregulated Akt contributes to escape mechanisms in cancer cell signaling (Sergina, Rausch, Wang, Blair, Hann, Hann, et al., 2007).

1CC8 also demonstrated resistance to gefitinib at doses of 1μM and less at both time points (Figure 8). SCC1 showed a trend towards sensitivity at the 48 hour time point but did not reach an IC_{50} level until the 72 hour time point with a significant concentration of 0.274μM by Student's t test (P=0.031) (Figure 9).

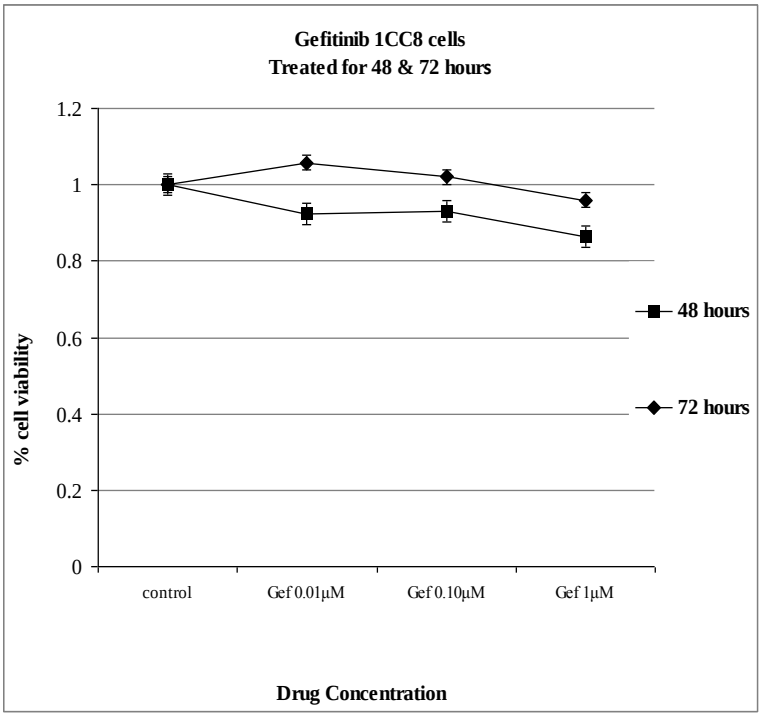

Figure 8. Gefitinib Treatment in EGFR Wild-Type Cell Line 1CC8.

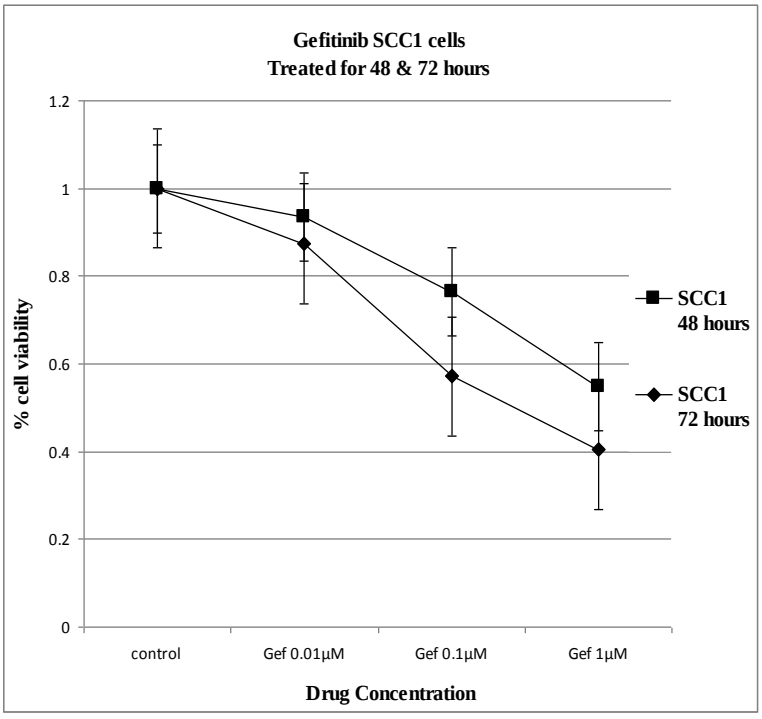

Figure 9. Gefitinib Treatment in EGFR Wild-Type Cell Line SCC1.

SCC25 showed significant sensitivity to gefitinib (P=0.023) with an IC_{50} of 0.475μM at the 48 hour time point and 0.373μM at the 72 hour time point with the use of the Student's t test (Figure 10). Graphical representation of MTS results for gefitinib in each cell line are shown below followed by summarized results (Table 4).

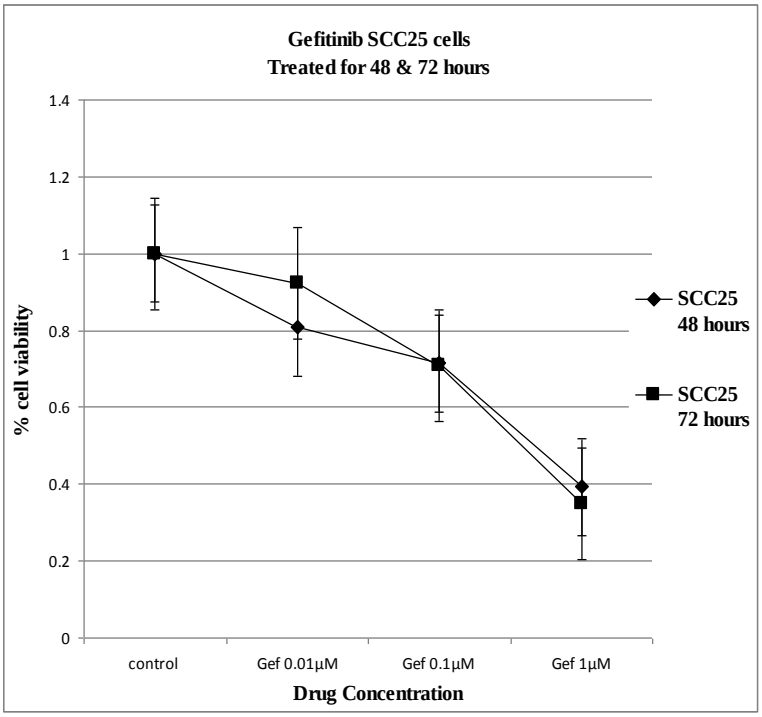

Figure 10. Gefitinib Treatment in EGFR Wild-Type Cell Line SCC25.

Table 4. Summary of Single Dose Gefitinib Results in HNSCC Cell Lines.

Cell Line	EGFR status	Gefitinib IC_{50}	
		48 hours	72 hours
SQ20B	Amplified	IC_{50}>1μM	IC_{50}>1μM
HN5	Amplified	IC_{50}>1μM	IC_{50}>1μM
HSC-3	Amplified	IC_{50}>1μM	IC_{50}>1μM
1CC8	Wild-type	IC_{50}>1μM	IC_{50}>1μM
SCC1	Wild-type	IC_{50}>1μM	0.274μM (P=0.031)*
SCC25	Wild-type	0.475μM (P=0.023)*	0.373μM (P=0.069)

Note: * indicates significance using Student's t test at P<0.05.

In this study, SQ20B, HN5, HSC-3, 1CC8, SCC25 and SCC1 were evaluated for sensitivity to bortezomib as a single agent using the MTS cell proliferation assay to establish baseline levels for subsequent combination studies. Three cell lines with EGFR amplification as determined by PCR analysis, SQ20B, HN5 and HSC-3 were chosen to assess drug sensitivity. Three wild-type cells lines with normal EGFR receptor levels as determined by PCR analysis, SCC25, SCC1 and 1CC8, were chosen for drug sensitivity assessment in comparison. 1CC8 is a cetuximab resistant clone derived from the SCC1 cell line with normal EGFR receptor levels. The addition of 1CC8 allowed for the assessment of EGFR inhibitor resistance as an additional factor in targeted agent sensitivity. 1CC8 proved resistant to single agent gefitinib as expected but this particular resistance phenotype has not been assessed in squamous cell carcinomas of the head and neck. Each cell line was analyzed for single agent bortezomib sensitivity using MTS assays. Each assay was performed in triplicate and shown in graphical format with error bars representing standard error of the mean.

In response to bortezomib treatment, cell line SQ20B showed greatest sensitivity to the drug, with an IC_{50} value of 0.328μM at 48 hours and 0.038 μM at 72 hours which proved significantly different from control cells by Student's t test (P=0.008) (Figure 11). HN5 also demonstrated sensitivity to bortezomib at the 48 hour and 72 hour time points with 0.473μM and 0.407μM doses, respectively (Figure 12). Although not as sensitive as SQ20B, HN5 showed an intermediate level of response to bortezomib. This cell line's response to bortezomib did not prove significantly different from control cells by Student's t test.

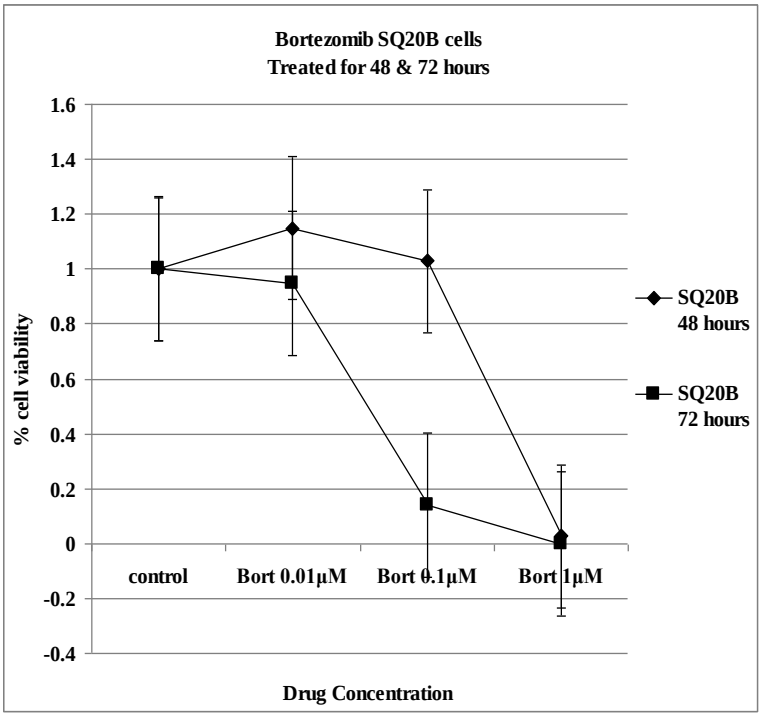

Figure 11. Bortezomib Treatment in EGFR Amplified Cell Line SQ20B.

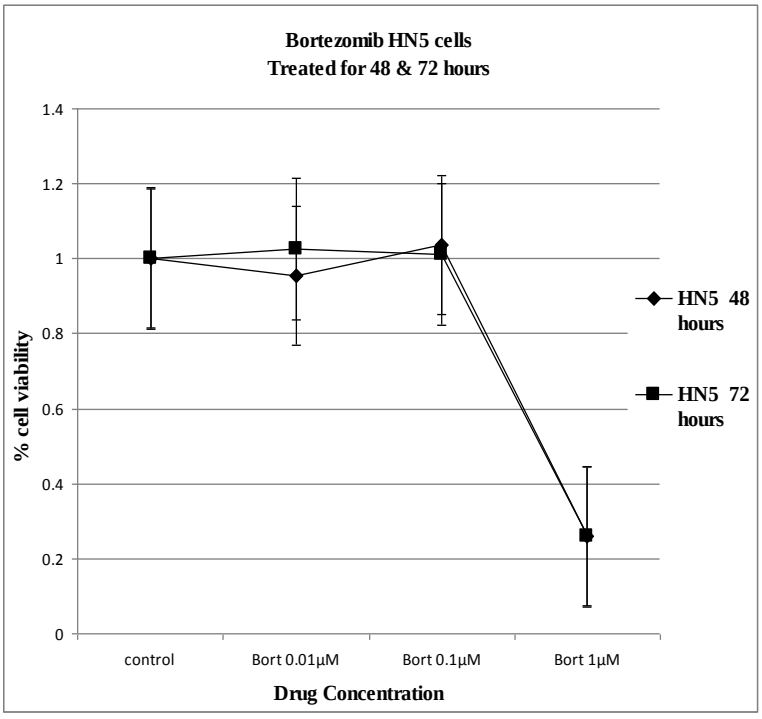

Figure 12. Bortezomib Treatment in EGFR Amplified Cell Line HN5.

HSC-3 proved resistant without a measurable IC_{50} at either the 48 or 72 hour time points (Figure 13). The resistance profile of HSC-3 at both 48 and 72 hours remains to be explored. Additional analyses were necessary to further define a bortezomib responsive profile in both EGFR amplified and wild-type cell lines. In general, the EGFR amplified cell lines SQ20B and HN5 demonstrated sensitivity to bortezomib after three days of exposure to the drug. 1CC8 showed sensitivity to bortezomib with an IC_{50} of 0.338μM

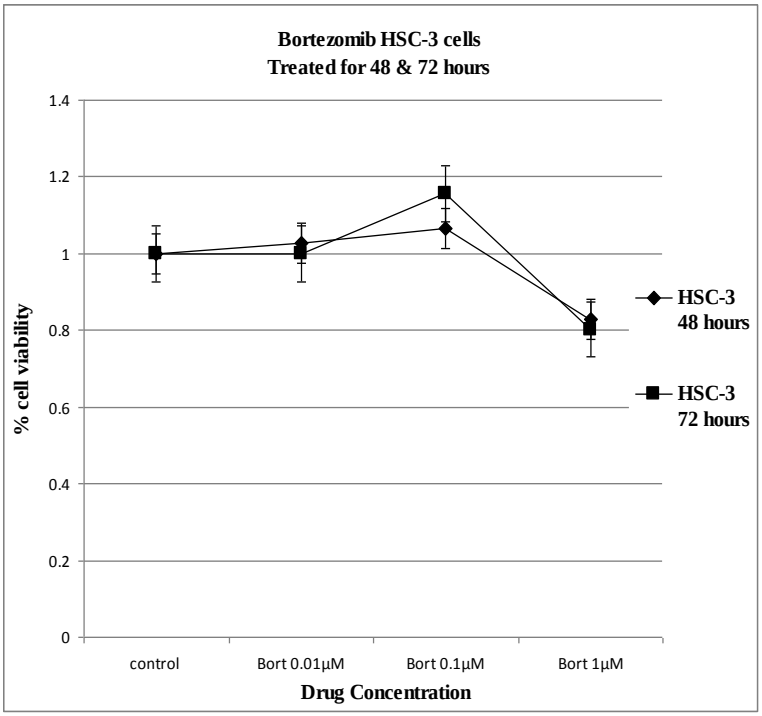

Figure 13. Bortezomib Treatment in EGFR Wild-Type Cell Line HSC-3

at the 72 hour time point, although this did not prove significant by Student's t test (Figure 14). SCC25 was significantly inhibited by bortezomib at 0.422μM over 72 hours (Figure 15). SCC1 required higher levels of the drug to elicit a response after 72 hours of exposure compared to its EGFR resistant clone 1CC8. Both cell lines were resistant to bortezomib at 48 hours of exposure. SCC1 had an IC_{50} level of 0.728μM at the 72 hour

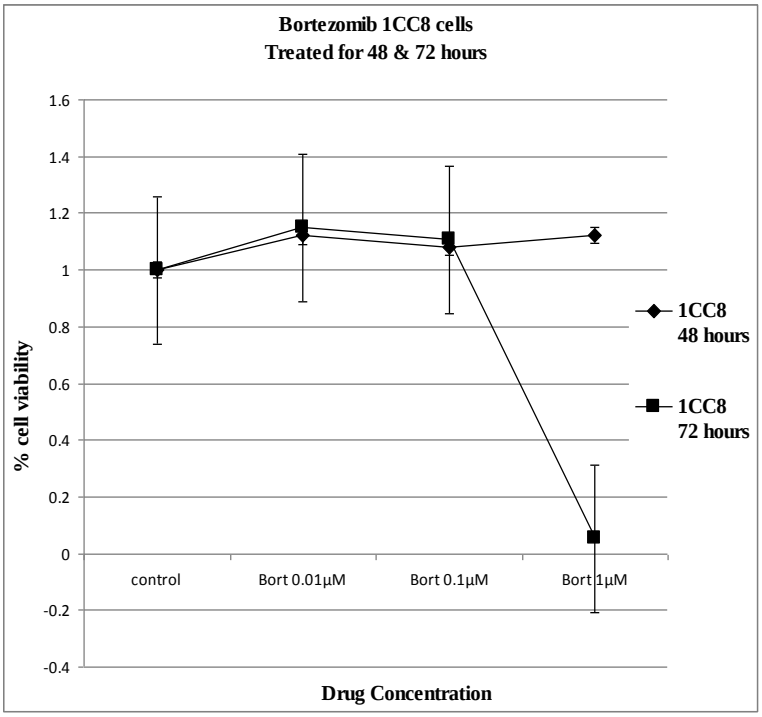

Figure 14. Bortezomib Treatment in EGFR Wild-Type Cell Line 1CC8.

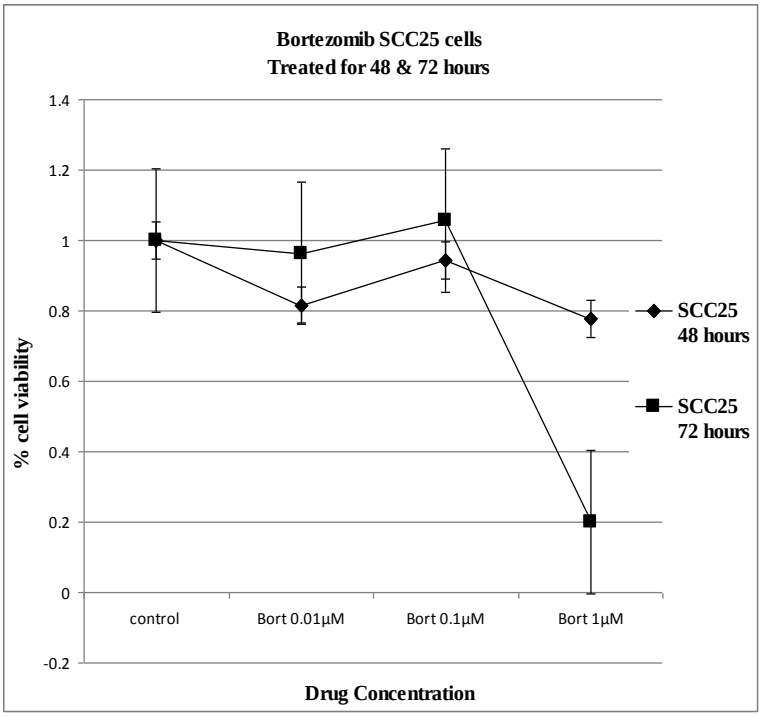

Figure 15. Bortezomib Treatment in EGFR Wild-Type Cell Line SCC25.

time point (Figure 16). Graphical representation of MTS results for bortezomib in each cell line are shown below followed by summarized results (Table 5).

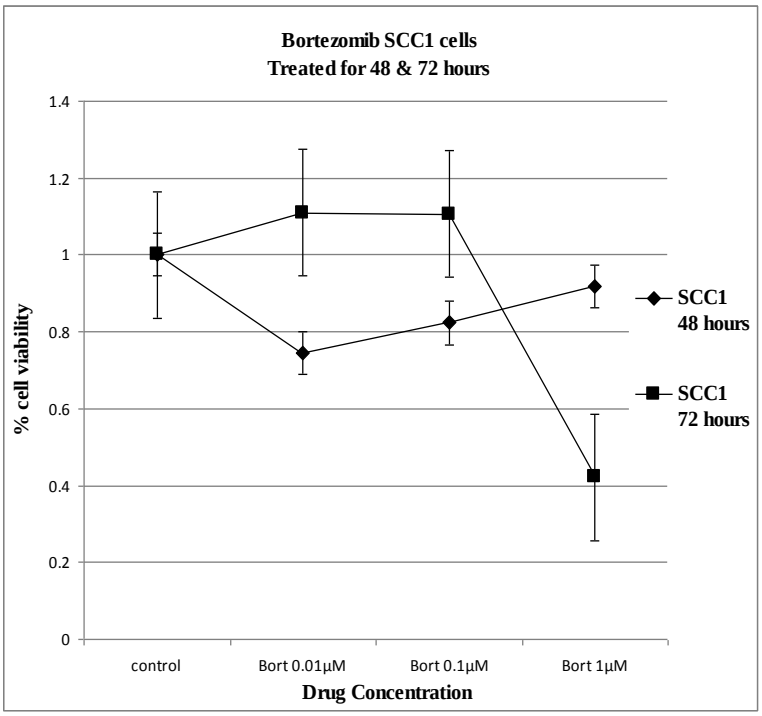

Figure 16. Bortezomib Treatment in EGFR Wild-Type Cell Line SCC1.

Table 5. Summary of Single Dose Bortezomib Results in EGFR Amplified and Unamplified Cell Lines.

Cell Line	EGFR status	Bortezomib IC_{50}	
		48 hours	72 hours
SQ20B	Amplified	0.328μM (P=0.104)	0.038 μM (P=0.008)*
HN5	Amplified	0.473 μM (P=0.299)	0.407 μM (P=0.08)
HSC-3	Amplified	IC_{50}>1μM	IC_{50}>1μM
1CC8	Wild-type	IC_{50}>1μM	0.338 μM (P=0.947)
SCC1	Wild-type	IC_{50}>1μM	0.728 μM (P=0.563)
SCC25	Wild-type	IC_{50}>1μM	0.422 μM (P=0.031)*

Note: * indicates significance using Student's t test at P<0.05.

Drug Combination Studies

Single agent sensitivity profiles were previously established for gefitinib and bortezomib in SQ20B, HN5, SCC25 and SCC1 using drug dosages up to 1μM (see Figures 5-16). To assess sensitivity to gefitinib and bortezomib in resistant cell lines, MTS assays were performed using higher doses of bortezomib and gefitinib until IC_{50} levels were reached in each cell line that previously demonstrated resistance to lower doses of inhibitors (i.e. when IC_{50} levels were not reached at doses of 1μM or less at 48 hours). Higher dose single agent results are demonstrated in combination graphs. Bay 11-7082 was added as an additional inhibitor to assess the specific inhibition of the NFκB pathway. 1CC8 was eliminated for further study based on consistent results with EGFR amplified cell lines, indicating EGFR inhibitor resistance was not a defining factor in targeted agent resistance.

The most bortezomib sensitive EGFR amplified cell lines, SQ20B and HN5 were chosen for further combination studies. SCC25 and SCC1 were chosen as comparison EGFR wild-type cell lines due to their gefitinib responsive profiles (see Figure 6). SQ20B, HN5, SCC25 and SCC1 were treated with bortezomib, gefitinib or bay 11-7082 alone or in combination for 48 hours. Bay 11-7082 as a monotherapy in each cell line was established for baseline levels for combination studies. SCC25 proved most responsive to bay 11-7082 over 48 hours at an IC_{50} of 3.9 μM, although this was not significant. SQ20B had an IC_{50} level of 32μM, HN5 an IC_{50} level of 26μM and SCC1 an IC_{50} level of 24μM, none of which proved significantly different from control cells as assessed by Student's t test.

Cells were seeded at $2x10^3$ in 96-well plates, grown overnight, then treated for 48 hours with the indicated concentrations of bortezomib, gefitinib or bay alone or in combination. Data were plotted as the percent of cell viability relative to untreated control wells and displayed in graphical form. Error bars represent standard deviation in all combination experiments.

Table 6. IC_{50} levels of Gefitinib and Bortezomib as Single Agents in HNSCC Cell Lines.

Cell Line	48 hours (μM)	72 hours (μM)	48 hours (μM)	72 hours (μM)
	Bortezomib		Gefitinib	
SQ20B	0.328	0.038	>1	>1
HN5	0.473	0.407	>1	>1
SCC25	>1	0.422	0.475	0.373
SCC1	>1	0.728	>1	0.274

Note: Previously established drug sensitivity levels as seen in Figures 5-16.

EGFR overexpressing cell lines SQ20B and HN5 were sensitive to bortezomib alone after 48 hours as demonstrated previously. Only SQ20B proved significantly inhibited by single agent bortezomib. In the EGFR overexpressing cell lines, the combination of both bortezomib and gefitinib and pre-exposure with bortezomib demonstrated increased sensitivity compared to pre-exposure with gefitinib, although no combination demonstrated significantly increased sensitivity over bortezomib as a single agent. Bortezomib did demonstrate a sensitizing effect for gefitinib by decreasing cell viability at smaller drug concentrations for SQ20B (Figure 17). The addition of bay 11-7082 also provided a sensitizing effect for gefitinib in SQ20B (Figure 18). As in SQ20B, bortezomib demonstrated a sensitizing effect for gefitinib by decreasing cell viability at smaller drug concentrations for HN5. The benefit of bortezomib pre-exposure in the cell

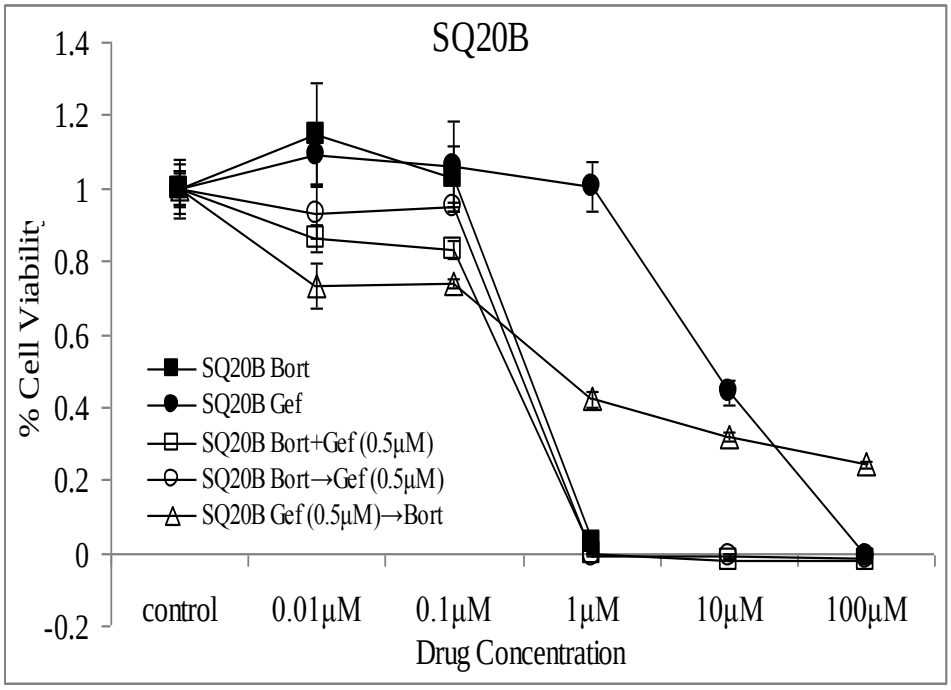

Figure 17. SQ20B Combination Experiments with Bortezomib (Bort) and Gefitinib (Gef).

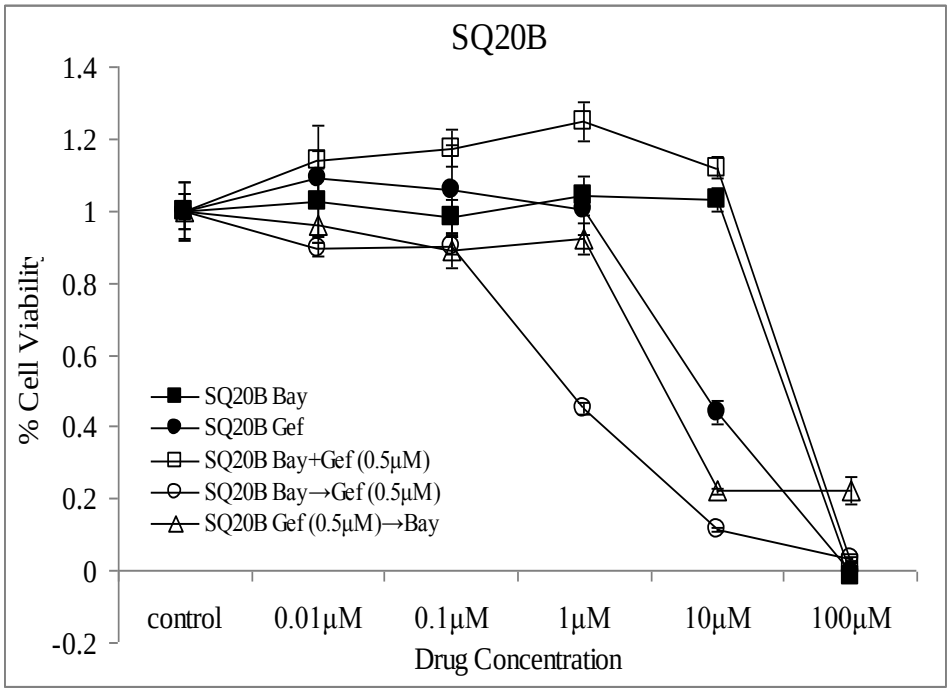

Figure 18. SQ20B Combination Experiments with Bay 11-7082 (Bay) and Gefitinib (Gef)

line HN5 did not appear to be as notable as that in SQ20B (Figure 19). Bay 11-7082 was

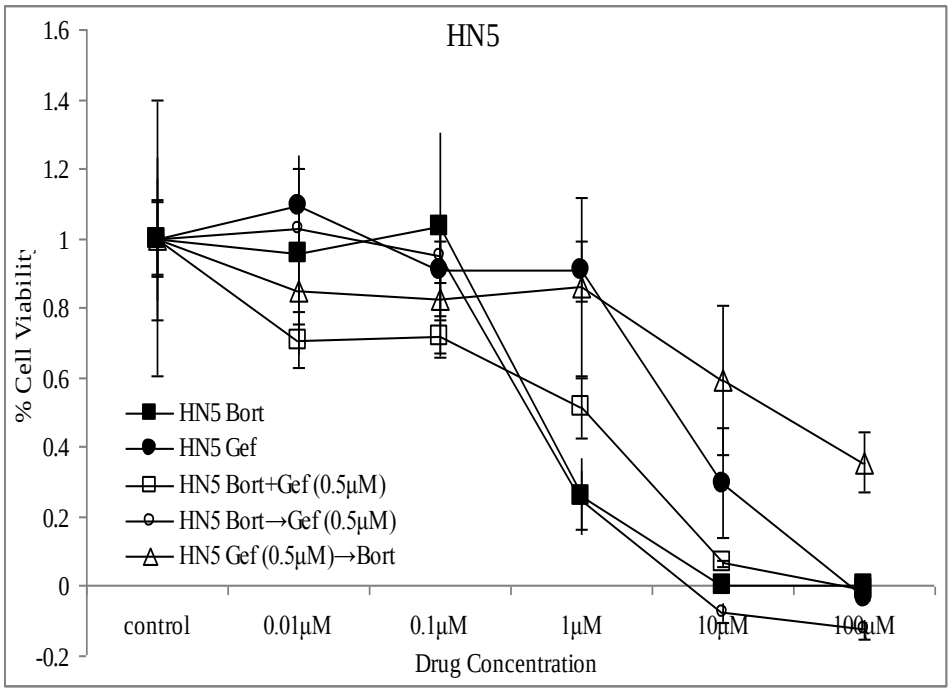

Figure 19. HN5 Combination Experiments with Bortezomib (Bort) and Gefitinib (Gef).

not able to demonstrate a sensitizing effect for gefitinib in the HN5 cell line. The addition of bay 11-7082 did not provide any additional cytotoxic effects in HN5 as a monotherapy or in combination with gefitinib (Figure 20). EGFR wild-type cell lines SCC25 and SCC1 demonstrated similar responsive profiles as SQ20B and HN5 when bortezomib was applied before gefitinib. SCC25 and SCC1 were sensitive to gefitinib alone but were insensitive to bortezomib after 48 hours of drug exposure as shown previously. Higher doses of bortezomib were required to achieve cellular proliferation using single agent bortezomib for SCC25 over 48 hours. Cellular proliferation increased at the 0.01μM and 0.1μM dosages until inhibition was achieved at the 1μM-10μM dosage range using bortezomib as a monotherapy (Figure 21).

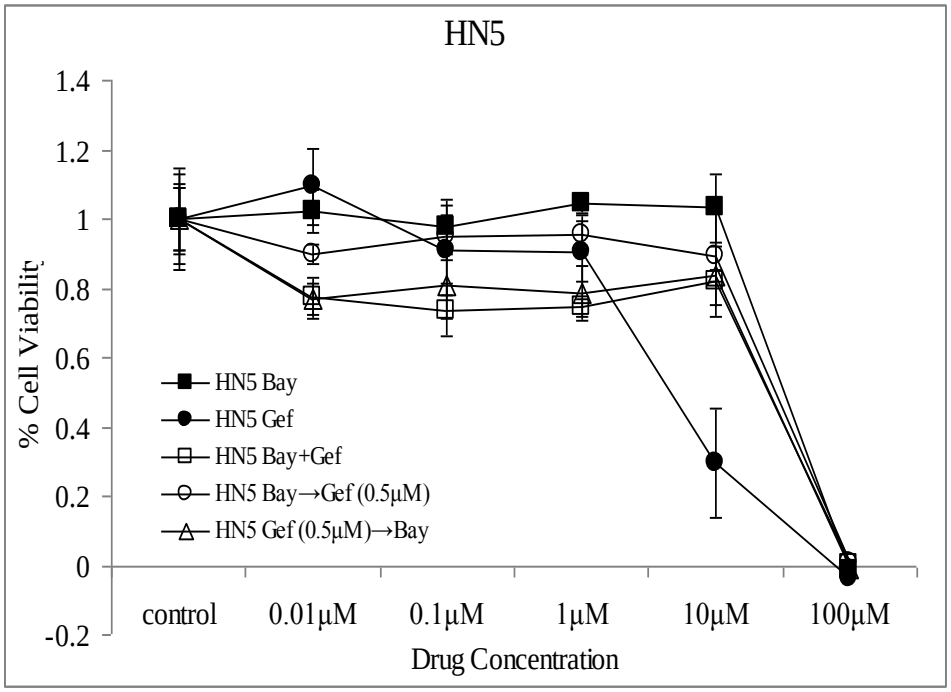

Figure 20. HN5 Combination Experiments with Bay 11-7082 (Bay) and Gefitinib (Gef).

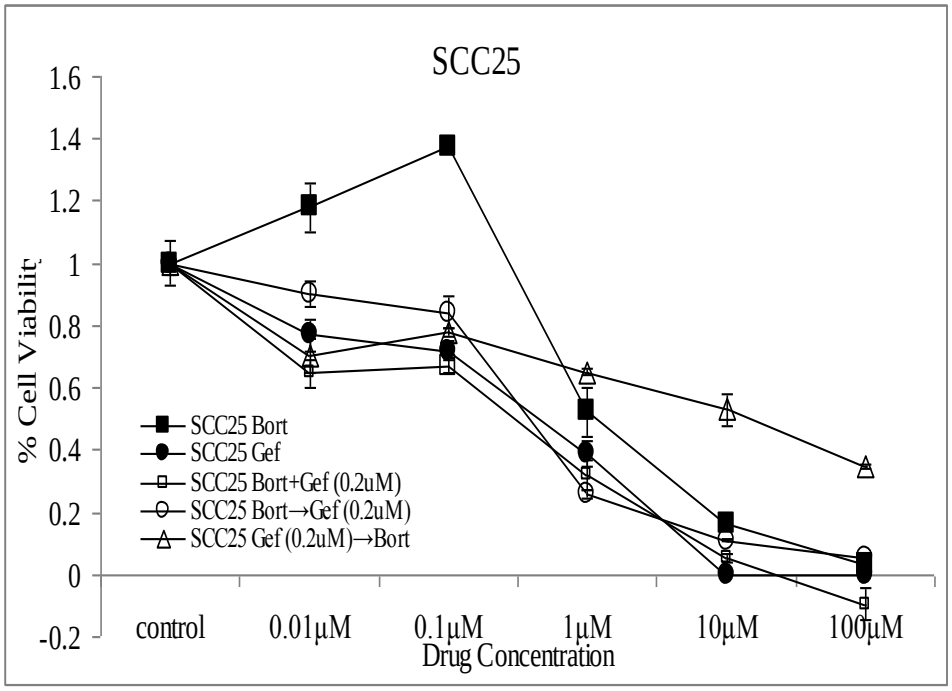

Figure 21. SCC25 Combination Experiments with Bortezomib (Bort) and Gefitinib (Gef).

Similar results were noted using the MTS Assay to analyze single agent bortezomib response in SCC25 over 48 hours. Longer exposure times were required (72 hours) to achieve IC_{50} levels in this cell line (see Figure 16). Bortezomib's ability to suppress cell proliferation through off-target effects may require increased drug concentrations as well as longer exposure times. Previous studies suggest NFκB may not be the only determinant of bortezomib activity in HNSCCs (Allen et al, 2008, Kisselev & Goldberg, 2001, Williams & McConkey, 2003). Bortezomib also downregulates or disrupts other resistance pathways or mechanisms, such as the p44/42 MAPK pathway (Schwartz & Davidson, 2004). The addition of bay to gefitinib did not prove superior in SCC25 over single agent treatment with gefitinib (Figure 22).

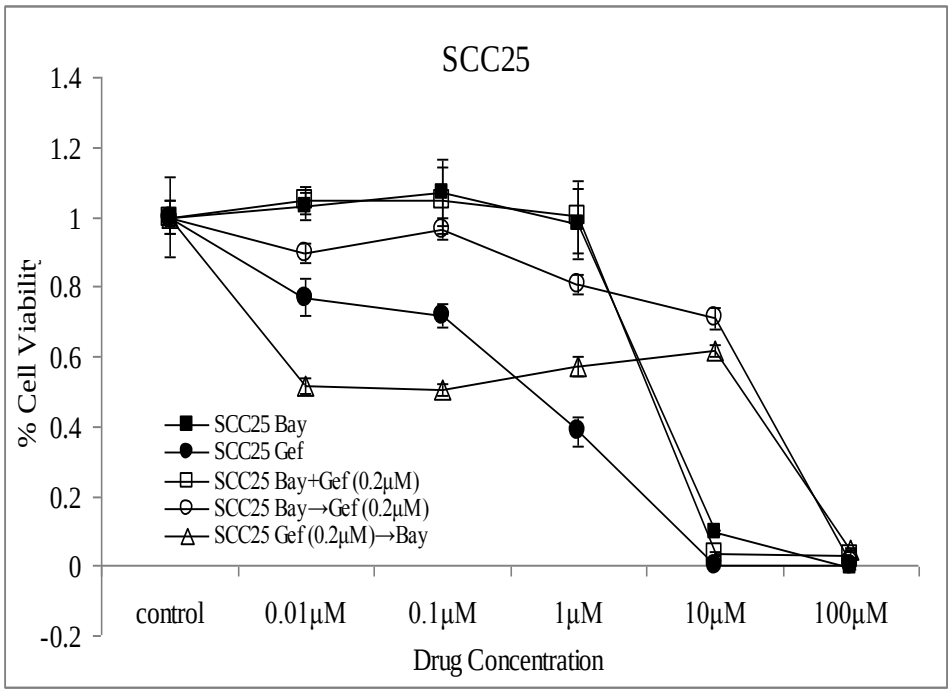

Figure 22. SCC25 Combination Experiments with Bay 11-7082 (Bay) and Gefitinib (Gef).

The combination of both inhibitors and pre-exposure with bortezomib demonstrated increased cytotoxicity compared to pre-exposure with gefitinib. Gefitinib as a monotherapy in SCC25 cells was comparable to combination treatments with bortezomib and gefitinib. Similar results were noted in SCC1 with combination treatments using bortezomib and gefitinib with the combination being equally effective as gefitinib alone (Figure 23). The addition of bay to gefitinib did not prove superior in

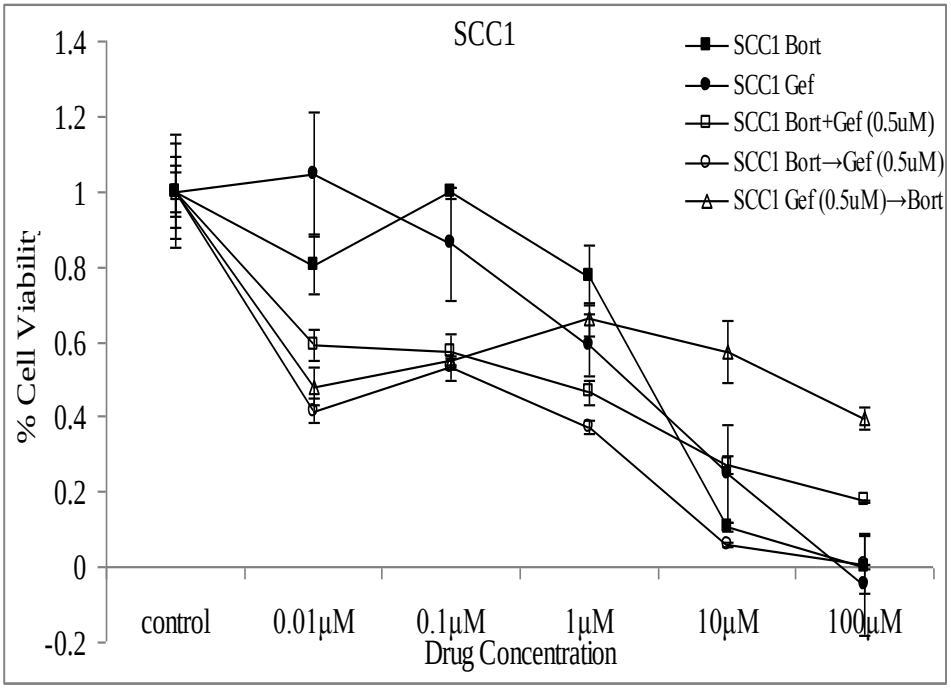

Figure 23. SCC1 Combination Experiments with Bortezomib (Bort) and Gefitinib (Gef).

SCC1 over single agent treatment with gefitinib (Figure 24). The significance of differences among drug combinations was assessed using ANOVA. When the data sets failed the normality test, the Kruskal-Willis one-way ANOVA was used. The null hypothesis was accepted if $P < 0.05$. The ANOVA and Kruskal-Willis tests revealed nonsignificant effects for the combinations of bortezomib and gefitinib or gefitinib and

bay 11-7082 in SQ20B, HN5, SCC25 or SCC1. Statistical results of drug combination regimens between the four cell lines are displayed below (Table 7).

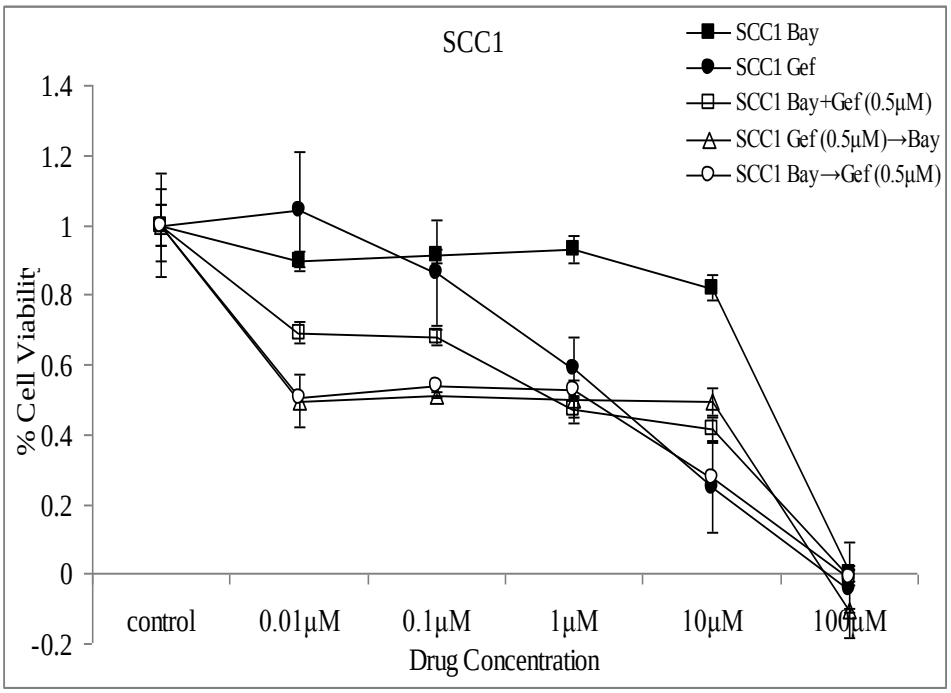

Figure 24. SCC1 Combination Experiments with Bay 11-7082 (Bay) and Gefitinib (Gef).

Table 7. ANOVA and Kruskal-Wallis† Results for Drug Combination Studies.

Cell Line	Drug combo	Df	F	P
SQ20B	Bort + Gef	14	1.215	0.331
	Bay + Gef	14	2.853	0.097
HN5	Bort + Gef	3	X=6.651†	0.084
	Bay + Gef	14	0.165	0.850
SCC25	Bort + Gef	14	1.682	0.227
	Bay + Gef	14	0.212	0.812
SCC1	Bort + Gef	3	X=3.380 †	0.185
	Bay + Gef	14	0.076	0.928

Summary

In the EGFR overexpressing cell lines, the combination of both inhibitors and the pre-exposure of bortezomib followed by gefinitib demonstrated increased sensitivity compared to gefitinib pre-exposure followed by bortezomib, although no combination demonstrated significantly increased sensitivity over bortezomib monotherapy. Bortezomib did demonstrate a sensitizing effect for gefitinib by decreasing cell viability at smaller drug concentrations for gefitinib. The sequential addition of bay 11-7082 followed by gefitinib demonstrated a trend towards sensitivity over other bay combinations in SQ20B although none of the bay 11-7082 inhibitor concentrations proved significantly superior in the four cell lines.

EGFR wild-type cell lines were sensitive to gefitinib alone but were insensitive to bortezomib after 48 hours of drug exposure. The combination of both inhibitors and pre-exposure of bortezomib before gefitinib demonstrated a trend towards increased sensitivity compared to gefitinib pre-exposure before bortezomib. Gefitinib as a monotherapy in SCC25 and SCC1 cells was comparable to combination treatments with bortezomib and gefitinib. The addition of bay 11-7082 to gefitinib did not prove superior in either EGFR wild-type cell line over gefitinib monotherapy.

Specific Aim 2

Western Blotting

The second specific aim of this study was to characterize gefitinib sensitivity in HNSCC's that is predictive of treatment response. It was hypothesized that the mechanisms of gefitinib response would be determined by expression of Akt, MAPK and

STAT3 of the EGFR pathway. It was hypothesized that increased activity of EGFR and its downstream pathways in EGFR amplified cell lines SQ20B and HN5 was responsible for gefitinib resistance. To examine this possibility, a primary ligand for the EGFR receptor TGFα was used to stimulate the EGFR pathway while examining the activation levels of the three major downstream pathways: STAT3, Akt and MAPK. Gefitinib was applied at a dose of 0.1μM for 24 hours to serum starved cells followed by post-treatment with TGFα stimulation. Serum starvation allowed for isolation of TGFα-stimulated effects without interference from additional activating factors present in serum. To measure activation of EGFR, an antibody targeting the tyrosine phosphorylation site Tyr1068 was chosen for analysis as studies indicate it mediates signaling to Akt and MAPK pathways (Pernas, et al., 2009). Gefitinib effectively downregulated phosphorylated (p) EGFR in all cell lines. Although EGFR was activated in the wild-type cell line SCC25, gefitinib suppressed activation of the receptor more effectively in comparison to the EGFR amplified cell lines SQ20B and HN5. Total EGFR levels were highly expressed in SQ20B and HN5 at baseline levels and after TGFα stimulation. Gefitinib did not suppress the activity of total EGFR protein expression (Figure 25A).

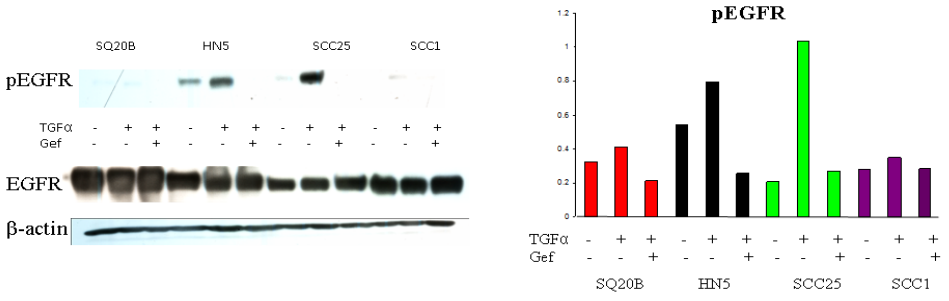

Figure 25A. Western Blot Assay of pEGFR Tyr 1068 in HNSCC Cell Lines.

Activated Akt was elevated at baseline levels for both EGFR amplified cell lines, SQ20B and HN5. Less dependence of this pathway was noted for the EGFR wild-type cell lines, SCC25 and SCC1. Gefitinib was able to suppress phosphorylated Akt activity in all four cell lines. Minimal differences were noted in total Akt levels between the four cell lines (Figure 25B).

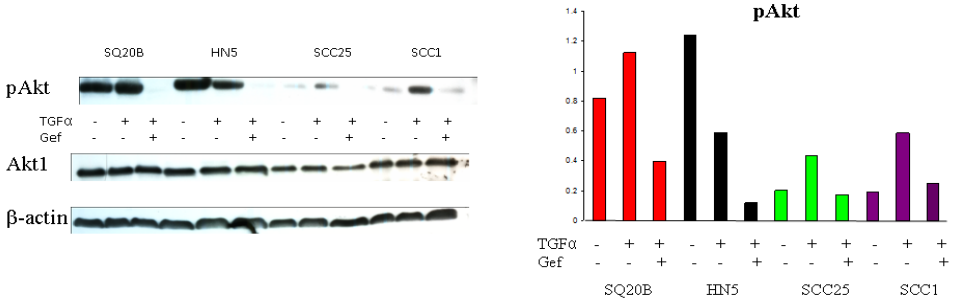

Figure 25B. Western Blot Assay of phosphorylated Akt in HNSCC Cell Lines.

SCC25 demonstrated the highest TGFα-stimulated expression of phosphorylated MAPK and interestingly an increase in this downstream marker after gefitinib dosing. The remaining cell lines demonstrated variable baseline levels of phosphorylated MAPK and increases in ligand-stimulated expression but were downregulated by gefitinib. Total MAPK levels were unaffected by gefitinib treatment (Figure 26A).

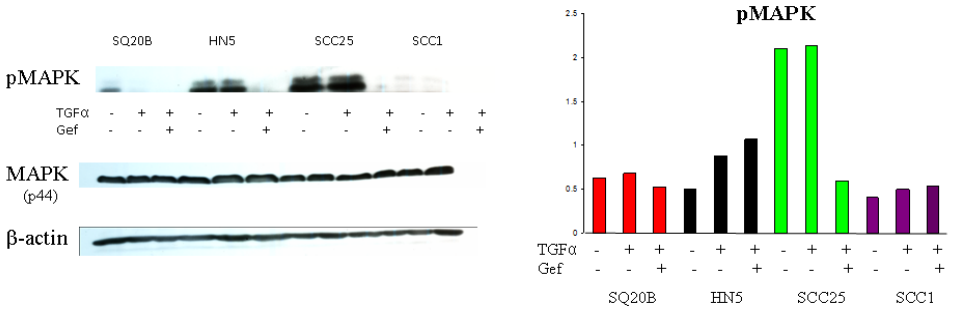

Figure 26A. Western Blot Assay of phosphorylated MAPK (p44/42).

Phosphorylated STAT3 was highly expressed in HN5 and SCC25 as a result of TGFα stimulation. Gefitinib effectively reduced phosphorylated STAT3 expression in the two cell lines, demonstrating increased ligand-stimulated expression, HN5 and SCC25. SCC1 demonstrated high levels of baseline phosphorylated STAT3 levels that remained unchanged after TGFα stimulation and increased after gefitinib administration indicating potential compensation of this cell line through other pathways unaffected by gefitinib. SQ20B did express basal protein expression levels of phosphorylated STAT3 protein, which remained unchanged by ligand stimulation or gefitinib inhibition (Figure 26B). STAT3 expression may be occurring through alternate pathways in this cell line.

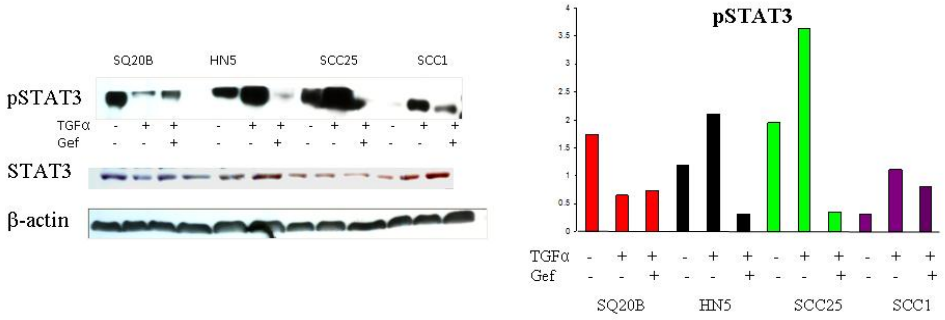

Figure 26B. Western Blot Assay of phosphorylated STAT3 in HNSCC Cell Lines.

Summary

While gefitinib does appear to be effective in downregulating activation of EGFR and its three main pathways, the degree of inhibition can vary between cell lines. The activated form of the receptor is completely inhibited in the cell lines SCC25 and SCC1, the two most responsive cell lines to lower doses of gefitinib. Although gefitinib is also able to downregulate the activation of EGFR in SQ20B and HN5, this effect is less inhibitory. Phosphorylated Akt is also effectively suppressed in all four cell lines by

gefitinib, although baseline levels and ligand-stimulated protein levels remain highest in the two more resistant cell lines SQ20B and HN5. Gefitinib was able to inhibit activated MAPK in all cell lines except SCC25 which increased after drug dosing. SCC1 responded similarly to phosphorylated STAT3 with increasing protein expression after gefitinib dosing.

Specific Aim 3

MTS Assay

The third specific aim of this study was to characterize bortezomib sensitivity and its dependence on the NFκB pathway. Head and neck cell lines SQ20B, HN5, SCC25, SCC1, and HSC-3 were previously established for bortezomib sensitivity by MTS Assay as demonstrated in Figures 11-16. Variable results to bortezomib were noted between EGFR amplified and wild-type cell lines. SQ20B and SCC25 proved to be significantly responsive to bortezomib while the remaining cell lines demonstrated variable but unsignificant sensitivity to the targeted agent. Hep-2, an EGFR wild-type cell line, was added as an additional cell line for analysis by DNA binding assay for measurement of NFκB nuclear binding activity after bortezomib dosing. Hep-2 cells (2×10^3 cells/well) were cultured in 96-well plates for 24 hr to allow 70-80% confluence then treated with varying concentrations (0.01μM, 0.1μM & 1μM) of bortezomib for 48 and 72 hours. The percent survival is plotted relative to control cells. Data points represent means of three independent experiments performed in triplicate. The bars indicate standard error of the mean (SEM). Hep-2 proved significantly sensitive to bortezomib by Student's t test with an IC_{50} of 0.096 μM at 72 hours (P=0.011) (Figure 27).

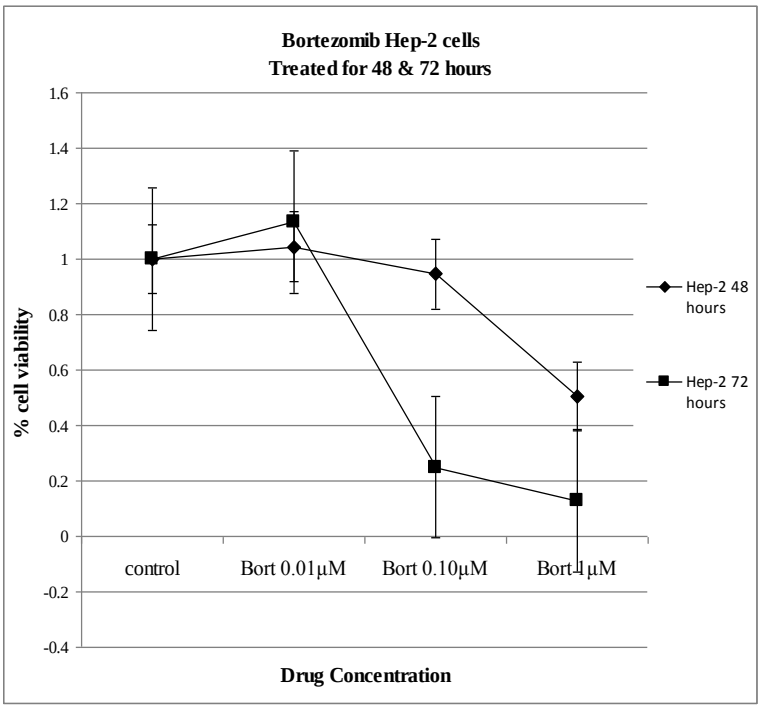

Figure 27. Bortezomib Treatment in Hep-2 Cell Line.

Nuclear Extraction and DNA Binding Assay

To test the hypothesis that bortezomib response in head and neck cell lines is dependent on the presence of NFκB activity through the canonical pathway, DNA binding assays were used to measure the nuclear protein expression levels of RelA in SQ20B, HN5, SCC25, SCC1, HSC-3, and Hep-2 after TNFα stimulation. TNFα is the primary ligand for the canonical pathway of NFκB activity. After stimulation of the canonical pathway, nuclear protein was isolated from each cell line and NFκB/RelA levels measured using the DNA binding assay before and after bortezomib dosing. SQ20B, Hep2 and SCC25 were shown to be significantly responsive to bortezomib by MTS assay and were expected to demonstrate increased signaling through the canonical pathway. HN5 was intermediate in response to bortezomib while SCC1 and HSC-3 were

the two most resistant cell lines as measured by MTS assay. In preparation for DNA binding assays three culture plates were established for each cell line and serum starved for 24 hours to isolate the effects of the ligand TNFα. The three culture plates consisted of: baseline nuclear protein levels without TNFα or drug stimulation, TNFα stimulation only, and 0.1μM bortezomib for 24 hours followed by TNFα stimulation for 30 minutes to measure the drug's ability to inhibit RelA upon ligand stimulation. The concentration of 0.1μM bortezomib for 24 hours was chosen based on previous studies by Allen et al. showing bortezomib was able to suppress TNFα-induced RelA in head and neck cell lines using the same concentration over 24 hours (Allen et al., 2009).

Nuclear binding activity was measured in cell lines after 24 hours of 0.1μM bortezomib treatment. SQ20B, Hep2, HSC-3 and SCC1 show significant inhibition of TNFα inducible DNA binding of RelA. HN5 and SCC25 demonstrated minimal increases of TNFα inducible DNA binding of RelA likely representing non-dependence on the NFκB pathway. * ($P<0.05$) denotes significant difference in NFκB DNA binding. Bortezomib was able to significantly decrease NFκB/RelA nuclear activity in SQ20B, Hep-2, HSC-3 and SCC1 by ANOVA (Figure 28). HN5 demonstrated increased binding activity whereas SCC25 demonstrated no change in NFκB/RelA binding after bortezomib dosing. Hep-2 and HSC-3 demonstrated the highest increases in NFκB/RelA binding in response to TNFα ligand stimulation as compared to the remaining cell lines. Hep-2 responded to bortezomib with a greater decrease in RelA binding as compared to resistant cell line HSC-3. The remaining bortezomib-sensitive cell lines, SQ20B and SCC25 demonstrated much lower levels of RelA binding in response to TNFα stimulation.

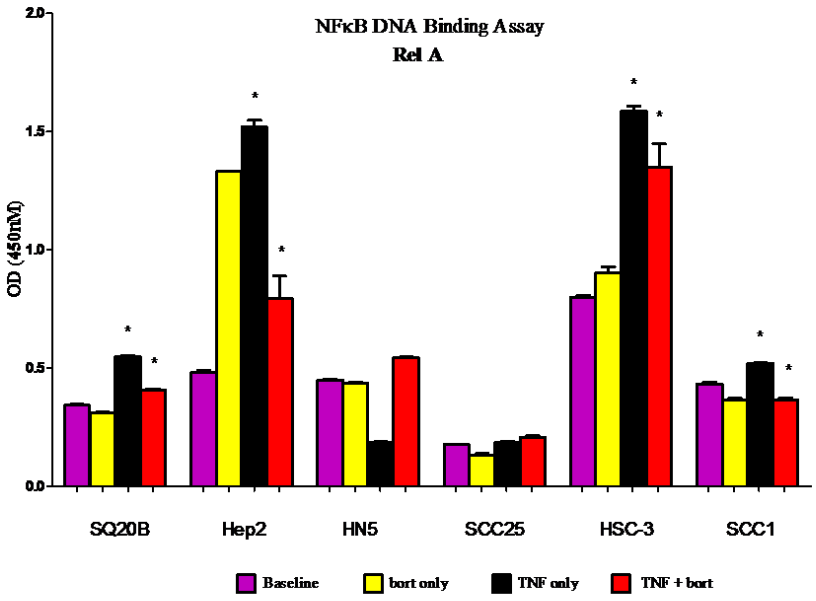

Figure 28. DNA Binding Activity of RelA in HNSCC Cell Lines.

Ingenuity Pathway Analysis

DNA binding results showed likely off-target effects (targets of cytotoxicity other than NFκB through the effects of non-specific proteasome inhibition) for bortezomib-sensitive cell lines SQ20B and SCC25 as a result of lower levels of response to TNFα stimulation. IPA was employed comparing the gene sets of the two most bortezomib sensitive cell lines SQ20B and Hep2 versus the two most resistant cell lines tested, HSC-3 and SCC1. This analysis determined which pathways were significantly linked to the microarray gene set previously compiled by the Chung laboratory (see Materials and Methods p. 70-71) and compared to the whole Ingenuity knowledge base. The analysis revealed p53 as the top significant pathway associated with the gene set. p53 is encoded by the TP53 gene (shown in red) determined to be significantly upregulated in

bortezomib-sensitive cells as compared to bortezomib-resistant shown below (Figure 29).

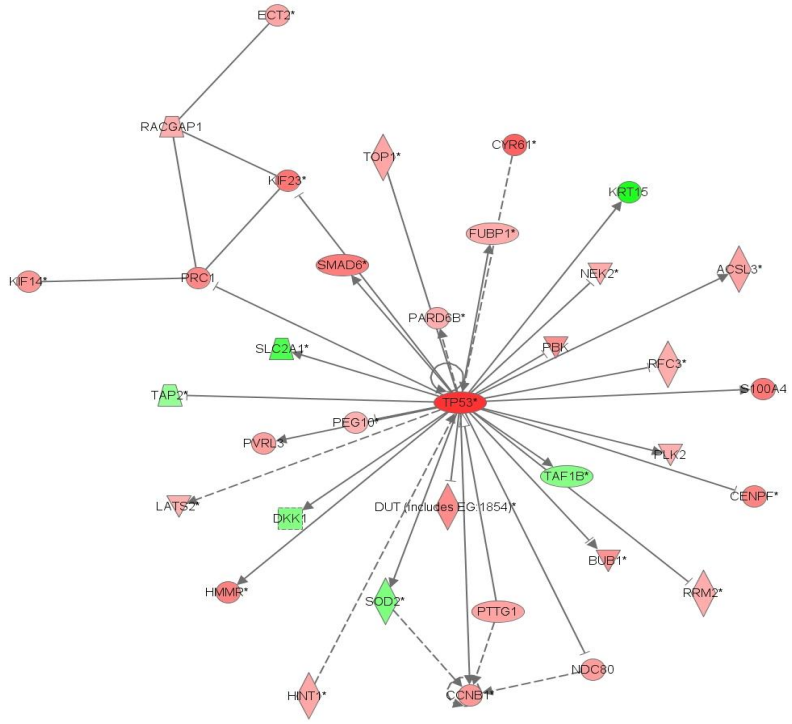

Figure 29. p53 Pathway Network Generated from Ingenuity Pathway Analysis.

Ingenuity Pathway Analysis was employed to identify biological networks that were affected by bortezomib sensitivity versus resistance between SQ20B and Hep 2 (two sensitive cell lines) versus HSC-3 and SCC1 (two resistant cell lines). Nodes represent genes/gene products identified by the network. Color intensity indicates significance of upregulated genes from most significant (dark red) to least significant (light pink). Green represents a decrease in gene expression. Shapes represent the functional class of the gene product: concentric circles equal a complex, down-pointing triangles equal kinases, diamonds equal enzymes, horizontal ovals equal transcription regulators, vertical ovals equal transmembrane receptors, vertical rectangles equal G-protein coupled receptors, horizontal rectangles equal ligand-dependent nuclear receptors

and circles represent other entities. Solid lines indicate direct interactions between nodes whereas dashed lines represent indirect interactions. Lines beginning and ending at a single node show self-regulation, while a line without an arrowhead represents binding.

Western Blot Analysis

Based on IPA analysis (see Figure 29), western blot analysis was employed to assess the p53 protein expression level differences in SQ20B, HN5, SCC25, SCC1, Hep2 and HSC-3 cell lines before and after bortezomib treatment (Figure 30). SQ20B demonstrated a small decrease in protein expression after 0.1μM bortezomib treatment after 24 hours. HN5 demonstrated an increase in p53 levels after 24 hours of treatment. Hep-2 cells demonstrated a low level of basal p53 protein level that decreased after bortezomib treatment. The remaining cell lines, SCC25, SCC1 and HSC-3 were negative for p53 protein at basal levels and after bortezomib treatment.

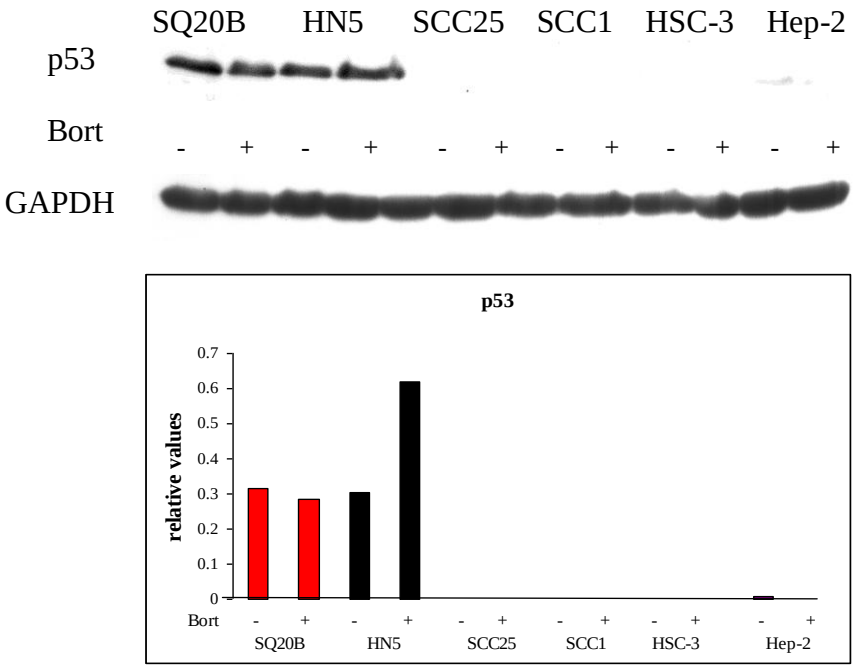

Figure 30. Western Blot Assay of p53 in HNSCC Cell Lines

Summary

The use of bortezomib as a monotherapy in solid tumors other than hematological carcinomas has so far yielded disappointing results. Bortezomib gained widespread attention for its ability to suppress NFκB which is constitutively active in many tumors as a result of radiation and cytotoxic therapies including head and neck cancer (McConkey & Zhu, 2008). Effective sequence administration of bortezomib may be important to its use in a responsive population. Because bortezomib's effects are targeted later in the cell cycle, the use of other agents may arrest the cell cycle before the point at which bortezomib is maximally effective. The data presented here in combination studies suggest similar kinetics with the use of gefitinib before bortezomib. In an attempt to further characterize bortezomib response, RelA activity was measured in four HNSCC cell lines by DNA binding assay. Activation levels varied between responsive and resistant cell lines, suggesting bortezomib's effectiveness is not limited to suppression of the NFκB pathway. Cancer cells have the ability to utilize a number of signaling pathways in order to avoid apoptosis and maintain cell survival. A detailed understanding of the complex signaling networks necessitates the optimal design of targeted therapies in head and neck cancers.

CHAPTER V: DISCUSSION

Specific Aim 1

Patient response to targeted agents such as gefitinib is suggested to depend mainly on the level of expression of the target in the tumor. So far, EGFR protein expression alone has not been a reliable marker for gefitinib response. A high copy number for the EGFR gene, on the other hand, may be a more effective molecular predictor of outcome. Clarification of the molecular mechanisms responsible for gefitinib's effects is needed to maximize the clinical benefits of targeted therapy with anti-tyrosine kinase inhibitors of EGFR. Bortezomib is one of the newest agents for targeted therapy, developed to specifically inhibit the proteasome, leading to increased apoptosis. Borteomib is currently being explored for clinical use in solid tumors. By targeting the proteasome, bortezomib affects numerous regulatory proteins necessary for malignant cells to proliferate, leading to apoptosis. The focus of this study was to analyze the relationship between EGFR gene amplification in HNSCC cell lines and their response to gefitinib and bortezomib as monotherapies and in combination. Combinations of these and other targeted agents may overcome the resistance that develops with single-agent therapy and could be incorporated either as part of initial therapy or later when disease resistance develops. Distinct differences were demonstrated within the context of EGFR expression status as indicated by measurable IC_{50} levels over 72 hours of exposure. EGFR amplified cell lines

to gefitinib. However, findings indicate significant bortezomib sensitivity is present in only two cell lines, SQ20B, an EGFR amplified cell line and SCC25, an EGFR wild-type were generally more responsive to bortezomib with the exception of HSC-3, but resistantcell line. DNA binding results indicate HSC-3 has increasingly high NFκB/RelA activity through the canonical pathway that may overwhelm bortezomib's ability to effectively suppress cellular proliferation. EGFR wild-type cells SCC1 and SCC25 demonstrated increased sensitivity to lower doses of gefitinib but generalized resistance to bortezomib with the exception of SCC25. Higher doses of gefitinib (>1μM) were required to achieve cytotoxicity in all four cell lines over 48 hours.

Clinical data on the predictive value of EGFR for gefitinib response in HNSCC are limited; however, in agreement with the *in vitro* data presented here, the gene expression levels of EGFR were not predictive of gefitinib response for HNSCC tumors at lower concentrations. This study noted higher concentrations of gefitinib were necessary to achieve IC_{50} levels by MTS Assay in EGFR gene amplified and EGFR over-expressing cell lines SQ20B and HN5. Simply assessing the quantity of EGFR in cell lines or tumors may not always give a reliable assessment of the EGFR-stimulated signaling activity or dependence of the tumor on downstream signaling. Consistent with the reports conducted by Pernas et al and Sebastian et al using EGFR–overexpressing head and neck cell lines, increased EGFR expression may not be definitive for gefitinib sensitivity (Sebastian et al., 2008; Pernas et al., 2009).

Previous studies suggest that heterodimerization of EGFR with other ErbBs is associated with resistance to EGFR inhibitors. This was in line with findings suggesting

higher concentrations of tyrosine kinase inhibitors like gefitinib are needed to suppressEGFR phosphorylation in cancer cells that also express high levels of ErbB2 when compared with cells expressing EGFR alone (Arteaga 2002).

Cellular cytotoxicity by bortezomib is most likely the result of several mechanisms of inhibition including the NFκB pathway. There remains controversy regarding if and how much of the cytotoxic effect of bortezomib is dependent on NFκB activation. Bortezomib was able to significantly block cell proliferation in SQ20B and SCC25, an EGFR amplified and EGFR wild-type cell line respectively. Variable results were noted in the remaining cell lines. Although IC_{50} levels were achieved at 72 hours with the remaining cell lines with the exception of HSC-3, these results did not prove significant. The present data is consistent with findings from previous studies noting the high prevalance of NFκB expression in head and neck tumors is an important but not the only determinant of bortezomib activity in HNSCCs (Allen et al, 2008, Kesselev & Goldberg, 2001, Williams & McConkey, 2003).

The rationale for combining bortezomib and gefitinib is based on their reported targeting of pathways contributing to treatment resistance. In this study, it was demonstrated that phenotypic differences in EGFR expression can account for certain differential drug sensitivities between bortezomib and gefitinib in HNSCC cell lines but was not definitive in determining drug response. Increased activation of the EGFR may overwhelm gefitinib's ability to inhibit downstream signaling, contributing to resistance in EGFR amplified cell lines. Bortezomib sensitivity and resistance profiles remain less delineated in the context of EGFR amplification. Although EGFR amplified cell lines

demonstrated a trend towards bortezomib sensitivity, significant IC_{50} levels were alsomeasured in the unamplified cell lines SCC25 and Hep2 after 72 hours. Further characterization of pathway dependence between each cell line is necessary while considering bortezomib's broad range of cytotoxic actions.

Since EGFR and NFκB inhibitors alone show limited effect in inhibiting growth of EGFR-expressing tumors, it is hypothesized that a combinatorial approach of bortezomib and gefitinib might be useful in augmenting growth suppression. This study also sought to further characterize and define the relevance of the NFκB pathway in HNSCCs through the use of a specific IKK inhibitor, bay 11-7082.

Overexpression of EGFR is associated with poor prognosis in HNSCC, and specific targets to the tyrosine kinase domain and proteasome have shown limited survival benefits in HNSCC patients as a monotherapy in solid tumors. However, very little is known about the mechanism of resistance, and currently there is no reliable biomarkers of gefitinib or bortezomib sensitivity in HNSCCs. The rationale for combining gefitinb and borezomib is based on their potential ability to block multiple downstream pathways that may contribute to treatment resistance. The present study shows increased cytotoxic activity using bortezomib as a monotherapy as well as a sensitizer for gefitinib in cell lines with EGFR amplification, although the present data does not support the use of combined inhibitors.

This study demonstrates that the nature of the interaction between bortezomib and gefitinib may be schedule-dependent. Three possible schedules were assessed: i.e., bortezomib (or bay 11-7082) plus gefitinib, bortezomib (or bay 11-7082) followed by

gefitinib, and gefitinib followed by bortezomib (or bay 11-7082), and found that increased cell cytotoxicity is possible in EGFR amplified cell lines with sequential dosing using bortezomib before gefitinib. These findings are consistent with the results of Wagenblast et al that noted synergistic effects using combination treatments with anti-EGFR inhibitors and bortezomib. Although Wagenblast used cetuximab, an extracellular EGFR inhibitor in combination with bortezomib, these findings support the rationale for combining anti-EGFR agents with proteasome inhibitors in HNSCC cell lines (Wagenblast, Hambeck, Baghi, & Knecht, 2008). Cascone et al suggested that synergism occurs when bortezomib is used prior to gefitinib, and may relate to the specific activation of the Akt pathway (Cascone et al, 2008). Piperdi et al also noted a cell cycle dependence effect related to bortezomib pre-exposure in non-small cell lung cancer cells. The use of the tyrosine kinase inhibitor erlotinib before the addition of bortezomib resulted in G1 cell cycle arrest, antagonizing the activity of bortezomib. Bortezomib works later in the cell cycle, causing G2/M cell cycle arrest. While pre-exposure with erlotinib was found to be antagonistic, preventing bortezomib from exerting its effects later in the cell cycle, dosing with bortezomib first or at the same time as erlotinib was more effective (Piperdi, Ling, & Perez-Soler, 2007). A similar antagonistic effect was apparent in all four cell lines studied here with gefitinib pre-exposure. EGFR wild-type cell lines SCC25 and SCC1 demonstrated sensitivity to gefitinib monotherapy but were less effectively inhibited by gefitinib pre-exposure which may be related to cell cycle kinetics. McConkey et al studied similar effects in pancreatic cell lines with the combination of bortezomib and the anti-mitotic chemotherapeutic agent docetaxel.

Usingflow cytometry and immunoprecipitation, bortezomib was found to block the apoptotic effects of docetaxel by acting earlier in the cell cycle (before M phase), inhibiting the activation of cyclin dependent kinase (cdk). Docetaxel initiates apoptosis by acting during the M phase causing apoptosis of rapidly dividing cells. Interestingly, the administration of bortezomib after docetaxel offset the cell cycle effects but did not increase the amount of cell death noted with the administration of docetaxel alone (Nawrocki, Sweeney-Gotsch, Takamori, & McConkey, 2004). Kassouf et al noted that the induction of G1 phase arrest before treatment renders human bladder carcinoma cells less sensitive to docetaxel. Because gefitinib induces G1 phase arrest, an apoptotic effect was enhanced only when gefitinib was administered after docetaxel (Kassouf, Luongo, Brown, Adam, & Dinney, 2006). Cell cycle kinetics play a prominent role in sensitivity to chemotherapeutic agents. It is expected that bortezomib, acting later in the cell cycle, may not be as effective in cells pretreated with gefitinib, an early inhibitor of the cell cycle. The use of gefitinib first may be abrogating the cytotoxic effects of bortezomib as the cell cycle is arrested before bortezomib can exert its drug killing effects.

The current study did not find the addition of an NFκB specific inhibitor, bay 11-7082, to be superior as a monotherapy or in combination with gefitinib in any of the cell lines tested. Although SCC25 was the most sensitive of the cell lines to bay 11-7082 at 3.9μM, this dose did not prove significantly different from control values. SCC25 was significantly inhibited by bortezomib after 72 hours which may indicate this cell line's dependence on other downstream markers or pathways as bortezomib is known to have

multi-dimensional effects. Previous studies have demonstrated the inability of bay 11-7082 to affect Akt activation and therefore noncanonical pathways of NFκB activation (Nakamura, Kawankami, Ida, Koji & Eguchi, 2007). Gasparian et al made a direct comparison of various proteasome inhibitors to IKK inhibitors including bay 11-7082 in prostate cancer cell lines and found NFκB to be more effectively suppressed through proteasome treatment (Gasparain et al, 2009). While it is generally accepted that bortezomib's primary mode of action is suppression of the NFκB signaling pathway, other important functions of proteasome inhibitors are implicated such as interruption of the cell cycle machinery and increased apoptosis through endoplasmic reticulum (ER) stress (McConkey & Zhu, 2008). The variable response of proteasome inhibitors in certain solid tumors is linked to incomplete inhibition of both canonical and noncanonical NFκB pathways (Allen et al., 2008).

Constitutive Akt activation can decrease bortezomib's effectiveness and may even be increased by bortezomib treatment (McConkey & Zhu, 2008). HN5 demonstrated a the highest baseline pAkt expression levels of the four cell lines but only stabilized levels of bortezomib inhibition over 48 and 72 hours. Akt may also be a central mediator in gefitinib resistance as well. Gefitinib has been postulated to have decreased efficiency in blocking downstream pathways of other tyrosine kinase receptors. Treatment with gefitinib has been shown to increase the activity of other ErbB family members such as ErbB2 and ErbB3. Akt is then upregulated through alternative receptor activation and downstream signaling (Cooper & Cohen, 2009). NFκB inhibitors such as bay 11-7082 have shown a limited ability to suppress growth and block DNA binding of additional

NFκB family members besides RelA (McConkey & Zhu, 2008; Allen et al., 2008). Bortezomib has also been reported to primarily block RelA through the canonical NFκB pathway but not IKKα-induced translocation of NFκB2/RelB through the noncanonical pathway, contributing to drug resistance (Allen et al., 2008).

These experiments were intended to characterize differential drug sensitivities in the context of EGFR expression status using MTS assays. EGFR gene and protein status of cell lines were confirmed by qPCR and western blot respectively. The sequential addition of bortezomib before gefitinib augmented the cytotoxic effects of gefitinib monotherapy in EGFR amplified cell lines SQ20B and HN5, yet the combination did not reveal significantly increased cytotoxicity over bortezomib alone. Gefitinib demonstrated an antagonistic effect when administered before bortezomib in all four cell lines. These results support single agent bortezomib as a viable treatment agent or as a sensitizer for gefitinib in effectively suppressing cellular proliferation in HNSCC cell lines. Support for combination treatment using gefitinib and bortezomib is cautious as the potential for increased toxicities using dual agents may not justify the minimal effects from combining these drugs. A specific NFκB inhibitor was not effective as a monotherapy or in combination with EGFR inhibition, justifying further characterization of the NFκB pathway in HNSCCs using additional experiments.

Specific Aim 2

The development of treatment resistance presents a significant obstacle toeffective tumor control in advanced stage head and neck patients. Mechanisms of EGFR inhibitor resistance were explored using western blots to monitor the activity of the three major

downstream pathways of EGFR. As previously described, EGFR amplification contributes to increased expression of the receptor on the cell surface. These results suggest that elevated total EGFR expression and activity of the receptor in gefitinib-resistant cells may be a contributor to decreased effectiveness of the drug. Drug resistance of SQ20B and HN5 could not be simply explained by the level of TGFα-induced EGFR phosphorylation in that gefitinib effectively inhibited activation of the receptor in all lines, although increased activation levels were noted in the EGFR amplified cell lines SQ20B and HN5. SCC25, an EGFR wild-type cell line also displayed increased activation of the receptor through the tyrosine phosphorylation site 1068 which was completely downregulated by gefitinib. SCC1 demonstrated low to absent levels of EGFR activation. SCC25 and SCC1 demonstrated decreased levels of basal pEGFR activation and although SCC25 responded to ligand stimulation, activation of the receptor was effectively inhibited in both cell lines. SQ20B and HN5 displayed a greater dependence on the EGFR pathway and predominantly the downstream marker Akt.

Variable activation levels of the three major pathways was noted in the four cell lines although it appears that pAkt may play a role in resistance as these results demonstrate high levels of baseline expression in the EGFR amplified cell lines. These findings suggest EGFR-dependent hyperphosphorylation of Akt may play an important role in gefitinib response. In support of these results, Sergina et al demonstrated that the activation of additional ErbB family members and Akt contribute to escape mechanisms from the inhibiting effects of gefitinib in both in vitro and in vivo models (Sergina, et al., 2007). MAPK and STAT3 activation appear to play less of a role in gefitinib resistance

with these cell lines. EGFR amplified cell lines did demonstrate basal and TGFα-stimulated expression of phosphorylated MAPK, although the expression levels were downregulated by gefitinib. Activated STAT3 was primarily noted in the cell lines HN5 and SCC25 upon TGFα stimulation which was suppressed by gefitinib. SCC1 demonstrated elevated levels of activated STAT3 which did not increase upon TGFα ligand stimulation or respond to gefitinib, suggesting alternative receptor activation of this downstream protein in this cell line. SQ20B did express basal levels of pSTAT3 but did not appear to signal through EGFR for this downstream protein as TGFα ligand stimulation did not result in increased activation levels.

Pernas et al studied the effects of gefitinib on EGFR overexpressing and wild-type HNSCC cell lines in vitro by MTT assay. Increased gefitinib doses were required to achieve IC_{50} levels with ranges of response measuring from 1.1μM to 2.5μM over a five day treatment period. Doses of 1μM were effective in suppressing levels of pAkt, pSTAT3 and pMAPK. Also in agreement with the data presented here, total EGFR levels were not affected by treatment. More responsive cell lines exhibited elevated basal levels of pAkt whereas the resistant cell line, SCC-11B demonstrated the highest pSTAT3 basal levels (Pernas et al., 2009). These results suggest a cell line dependence effect for gefitinib. Lower doses of gefitinib (<1μM) may not be sufficient for complete downregulation of amplified EGFR cell lines and resulting downstream pathways. The concentration of 0.1 μM used in this study is significantly below the mean plasma steady state concentration for gefitinib (0.4-1.4 μM) in patients (Mukohara, Engelman, Hanna, Yeap, Kobayashi, Lindeman, et al., 2005). Amplification and/or overexpression of EGFR

may contribute to disappointing responses noted with gefitinib in the clinical setting. Response to tyrosine kinase inhibitors such as gefitinib in HNSCCs may be due to deregulation of ErbB2 or ErbB3 rather than EGFR. Cooper et al showed treatment with gefitinib in resistant breast cancer cells leads to increased expression of ErbB3 to the plasma membrane. Treatment with gefitinib also increased ErbB3 trafficking to the plasma membrane, where dimerization with ErbB2 and activation occurred. ErbB3 then restores Akt signaling, since it is one of the primary activators of the PI3K/Akt pathway (Cooper & Cohen, 2009). Gefitinib resistance appears to be associated with EGFR and pAkt overexpression in this study, while sensitivity is associated with other factors. The aim was to find unifying characteristics to better define gefitinib response in advanced stage head and neck cancers, although these mechanisms of sensitivity appear to be diverse between cell lines.

Although poorer patient prognosis is known to be associated with EGFR gene amplification in HNSCC patients, what this means for optimal treatment regimens remains to be determined. The underlying molecular mechanisms contributing to the deregulation of EGFR require further investigation as targeted agents become increasingly used in clinical settings. This data is supportive of EGFR amplification and resulting pAkt overexpression as a contributing factor to gefitinib resistance, although further studies with additional cell lines are required to eliminate individual cell line variation. In addition, increased levels of basal pAkt may require higher dosages of gefitinib to effectively induce cellular cytotoxicity. Elevated expression of MAPK and STAT3 appear to be less relevant as markers of gefitinib sensitivity in these cell lines.

Specific Aim 3

The NFκB signaling pathway plays an important role in the development of tumor resistance to therapy and is known to be highly expressed in head and neck cancers. DNA binding assays were used to evaluate the ability of bortezomib to block TNFα-induced NFκB RelA activity. Bortezomib effectively interrupted TNFα-induced RelA activation in four of the six cell lines tested, a result that has been demonstrated in other HNSCC cell lines (Allen et al., 2008). The presence of EGFR amplification does not appear to play a role in determining bortezomib response as variable results were noted in these cell lines irrespective of receptor status. The three significantly sensitive cell lines included the EGFR overexpressing SQ20B and wild-type cell lines Hep2 and SCC25. Dependence on the NFκB pathway was also not conclusive for determining response to bortezomib as SCC25 and SQ20B express relatively lower levels of RelA activity yet significant response to the drug. Bortezomib may also downregulate other resistance pathways, including the p44/42 MAPK pathway. Commonly activated by other chemotherapeutic agents, proteasome inhibitors have been shown to block the activation of the p44/42 pathway leading to increased cell death (Schwartz & Davidson, 2004). This presents a potential pathway of inhibition for SCC25 by bortezomib, as previous western blot data demonstrated increased basal activation of MAPK in this cell line. The treatment of HNSCC cells with bortezomib has been reported to led to upregulation of activated STAT3, suggesting that the ability of bortezomib to kill HNSCC cells may be hindered due to increased activity of cellular STAT3 protein (Marmor et al., 2004). The bortezomib-resistant cell line SCC1 demonstrated increased basal levels of activated

STAT3 by western blot that was unresponsive to 0.1μM gefitinib over 24 hours. Single agent bortezomib may further elevate basal levels of this protein, preventing the drug from effectively suppressing cell survival.

Studies have suggested a number of cellular toxicity effects through the administration of bortezomib including stabilization of p53 and pro-apoptotic proteins, increased apoptosis through the unfolded protein or endoplasmic reticulum stress response and generation of oxygen species (McConkey & Zhu, 2008). Recent studies have shown increased activity of the proteasome is correlated with resistance. Chronic lymphocytic leukemia patients have increased proteasome activity and do not respond to bortezomib (Orlowski & Kuhn, 2008). Allen et al produced findings that incomplete inhibition of baseline RelA may contribute to the limited response to lower doses of bortezomib as illustrated with HSC-3 by DNA binding results in this study. Additionally IHC analysis of pre and post treatment biopsies by Allen et al revealed a lack of inhibition on other members of the NFκB family by bortezomib (Allen et al., 2008). Incomplete inhibition of RelB and c-Rel may contribute to survival and escape for resistant cell lines SCC1 and moderately sensitive cell line HN5.

Conclusions

EGFR is highly expressed in most human head and neck cancer tumors. Despite the prevalence of the receptor, EGFR-targeted agents as a monotherapy continue to demonstrate disappointing results in clinical trials. Studies have not been able to correlate EGFR protein expression status to anti-EGFR inhibitor sensitivity. Differences in downstream pathways exist between head and neck tumors, although the defining

phenotype that determines the optimal treatment regimen is not yet available. The current study noted high levels of phosphorylated EGFR and the downstream protein Akt in EGFR amplified cell lines, necessitating higher doses of gefitinib to achieve cytotoxicity. Downstream signal molecules may hold the key as cell lines that use Akt signaling have been shown to be gefitinib sensitive, although its overexpression, either by activation through receptor crosstalk, activating mutations in PI3K or deactivating mutations in PTEN may be an indicator of resistance. Combination therapies hold promise as the key to overcoming treatment resistance. Although the combination of gefitinib and the proteasome inhibitor, bortezomib did not prove superior in combination, cell cycle dependent effects were noted. The present study shows superior cytotoxic activity using bortezomib as a monotherapy as well as a sensitizer for EGFR amplified cell lines. The administration of gefitinib after bortezomib produced anatogonist effects.

Gene expression analysis has suggested patients with advanced stage head and neck cancer exhibit activation of NFκB signaling pathways. Bortezomib is a proteasome inhibitor approved by the FDA for hematological malignancies that is currently being investigated for effectiveness in solid tumors. As inhibition of NFκB is thought to be an important target of bortezomib activity, its effects were compared with that of the more specific NFκB inhibitor bay 11-7082, by inhibition of IKK. The cytotoxic effects of bortezomib were found not to be completely dependant on its ability to downregulate NFκB. Further characterization of these pathways is required to define those patients most likely to respond to targeted therapies.

Limitations

One potential limitation lies in the fact that only six head and neck cell lines wereinitially examined for bortezomib and gefitinib response and these may not be representative of all EGFR amplified and wild-type cell lines. Studies that examine the association between EGFR amplification in HNSCC and the efficiency of bortezomib with other EGFR inhibitors will help guide future targeted therapies to those patients most likely to benefit. Additional assays were employed in this study to support drug response results determined through MTS assays. Not all cell lines respond equally to NFκB activating ligands like TNFα, either because they lack the required receptor or because of missing downstream effectors (Pahl, 1999). Bortezomib has been reported to cause cell cycle arrest at the G_2-M phase in both sensitive and resistant cell lines. Although cell cycle arrest is induced, apoptosis is not necessarily the resulting end-point. MTS assays measure the number of proliferating cells but does not measure the level of apoptosis after treatment (Chen, Yeh, Yeh, Lu, & Huang, 2008). Bortezomib sensitive cell lines were determined by MTS assay in terms of cell proliferation, but DNA binding served to conclusively measure the amount of activity and inhibition of NFκB. Western blotting helped to further characterize cell line dependence on the EGFR pathway. DNA binding assays reflected NFκB activity and helped further delineate bortezomib's broad cytotoxic actions. IPA identified pathways of relevance to bortezomib resistance and sensitivity between the experimental set of head and neck cell lines.

Combination drug data was based on in vitro cytotoxicity profiles. The nature of in vitro systems allow for results which may be cell line dependent and not necessarily

based on phenotypic differences. These results did note a schedule-dependent result with bortezomib pre-exposure producing increased cytotoxicity when compared to simultaneous drug combinations or gefitinib pre-exposure in all four cell lines. These results were comparable to other published studies conducted by Piperdi et al (Piperdi et al., 2007). These authors, as in the current study, also examined a small number of cell lines, four non-small cell lung cancer lines. To further establish the cell cycle effects of bortezomib and tyrosine kinase inhibitors, a broader panel of cell lines requires examination. Variable results are also noted when comparing drug sensitivities in vitro versus in vivo. In this study, the combination of bortezomib and gefitinib in vitro was unremarkable in comparison to single agent drug treatment. Nawrocki et al was unable to demonstrate synergistic effects of bortezomib and docetaxel in vitro, although significant effects were noted in vivo with combination treatment as the result of bortezomib's ability to suppress angiogenesis (Nawrocki et al., 2004). Similar effects may be possible with the drug combination of bortezomib and gefitinib that would best be realized using in vivo systems.

Ligand binding with EGFR results in receptor homo- or heterodimerization at the cell surface, followed by internalization of the dimerized receptor. EGFR dimerization stimulates its intracellular protein-tyrosine kinase activity. As a result, autophosphorylation of several tyrosine (Tyr) residues in the C-terminal domain of EGFR occurs. Tyr1086, Tyr992, Tyr1068, Tyr1148 and Tyr1173. Tyr 1068, Tyr 1148, and Tyr1173, are the major sites of autophosphorylation, which occur as a result of EGF and TGFα binding. After dimerization and internalization, autophosphorylation of the

intracytoplasmic EGFR tyrosine kinase domains occur. Autophosphorylation induces downstream activation and signaling by several other proteins that associate with these phosphorylated tyrosines. The main EGFR signaling pathways, MAPK, Akt and STAT3 pathways are then initiated. It is theorized that different EGF-like growth factors may affect receptor conformations which will determine specific tyrosine phosphorylation site usage (Herbst 2004). This study evaluated the effects of pEGFR using an antibody targeted to Tyr1068, a primary site of activation for the Akt and MAPK pathways. Additional phosphorylated sites are capable of initiating Akt and MAPK pathways as well and this data may not present the complete activated status of the three downstream proteins. Pernas et al showed significant inhibition of three phosphorylated sites, Tyr845, Tyr1068 and Tyr1173 in HNSCC cell lines after gefitinib dosing, indicating gefitinib is effective at suppressing EGFR stimulated pathways at multiple sites of phosphorylation (Pernas et al., 2009).

Recommendations for Further Studies

Mechanisms of resistance appear to be diverse between and within head and neck cancer tissue types. Despite the development of new targeted anticancer therapies, mechanisms continue to evolve to protect cells against cytotoxic compounds and act as obstacles to successful treatment.

The choice of drug schedule administration may be important in terms of inhibiting cell cycle progression. Although the combination of bortezomib and gefitinib in vitro was less active than single agents in this study, the combined effect of these drugs in vivo may demonstrate additional effects on angiogensis and warrants further study.

Assays comparing the effects of bortezomib in pretreatment and post-treatment biopsies on NFκB activity could be useful to develop biomarkers for clinical trials in advanced stage head and neck cancers in which variable responses to bortezomib have been observed. These biomarkers could be useful in classifying patients into potentially responsive populations based on specific activation levels.

The selective inhibition of multiple signaling pathways in combination with current chemotherapeutic drugs may lead to an increased potency and efficacy of these agents. Additional studies are needed using gene array data to discern new potential therapeutic targets for advanced stage head and neck cancer patients.

REFERENCES

Adams, J., Palombella, V., Sausville, E., Johnson, J., Destree, A., Lazarus, D., Maas, J., Pien, C., Prakash, S., & Elliott, P. (1999). Proteasome inhibitors: a novel class of potent and effective antitumor agents. *Cancer Research, 59*, 2615-2622.

Aggarwal, B. (2004). Nuclear factor-kB. *Cancer Cell*, 6 (3), 203-208.

Agulnik, M., Santos, G., Hedley, D., Nicklee, T., dos Reis, P., et. al. (2007). Predictive and pharmacodynamic biomarker studies in tumor and skin tissue samples of patients with recurrent or metastatic squamous cell carcinoma of the head and neck treated with erlotinib, *Journal of Clinical Oncology, 25* (16), 2184-2190.

Ali, M., Gunduz, M., Gunduz, E., Tamamura, R., Beder, L., Katase, N., et al. (2009). Expression and mutation analysis of HER2 in head and neck squamous cell carcinoma. Cancer Investigation, Dec 16 Epub ahead of print.

Allen, C., Saigal, K., Nottingham, L., Arun, P., Chen, Z., & Van Waes, C. (2008). Bortezomib-induced apoptosis with limited clinical response is accompanied by inhibition of canonical but not alternative nuclear factor-KB subunits in head and neck cancer. *Clinical Cancer Research, 14*(13), 4175-4185.

Arteaga, C. (2002). Epidermal growth factor receptor dependence in human tumors: more than just expression? *The Oncologist, 7* (4), 31-39

Bancroft, C., Chen, Z., Yeh, J., Sunwoo, J., Yeh, N., Jackson, S., et al. (2002). Effects of pharmacologic antagonists of epidermal growth factor receptor, PI3K and MEK signal kinases on NF-kappaB and AP-1 activation and IL-8 and VEGF expression in human head and neck squamous cell carcinoma lines. *International Journal of Cancer, 99* (4), 538-548.

Bernier, J., & Bentzen SM.(2006). Radiotherapy for head and neck cancer: latest developments and future perspectives. *Current Opinion in Oncology, 18* (3), 240-2466.

Bernier, J., & Schneider, D. (2007). Cetuximab combined with radiotherapy: An alternative to chemoradiotherapy for patients with locally advanced squamous cell carcinomas of the head and neck? *European Journal of Cancer, 43* (1), 35-45.

Bianco, A. (2004). Targeting c-erbB2 and other receptors of the c-erbB family: rationale and clinical applications. *Journal of Chemotherapy, 16* (Suppl 4), 52-54.

Bonizzi, G., & Karin, M. (2005). The two NF-kappaB activation pathways and their role in innate and adaptive immunity. *Trends in Immunology, 25* (6), 280-288.

Braut, T., Krstulja, M., Kujundzic, M., Manestar, D., Hadzisejdic, I., Jonjic, N. et al. (2009). Epidermal growth factor receptor protein expression and gene amplification in normal, hyperplastic, and cancerous glottic tissue: Immunohistochemical and fluorescent in situ hybridization study on tissue microarrays. *Croatian Medical Journal, 50*, (4), 370-379.

Brownell, E., O'Brien, S., Nash, W., & Rice, N. (1985). Genetic characterization of human c-rel sequences. *Molecular and Cellular Biology 5* (10), 2826-2831.

Burguete, S., & McLachlan, G. (2009). Microarray data analysis for differential expression: a tutorial. *Puerto Rico Health Science Journal, 28* (2), 89-104.

Caroll, M. (2004). The complement system in regulation of adaptive immunity. *Nature Immunology, 5*, (10), 981-986.

Cascone T., Morelli, M., Morgillo, F., Kim, W., Rodolico, G., Pepe, S., et al. (2008). Synergistic anti-proliferative and pro-apoptotic activity of combined therapy with bortezomib, a proteasome inhibitor, with anti-epidermal growth factor receptor (EGFR) drugs in human cancer cells. *Journal of Cell Physiology, 216*, 698-707.

Chen, F., Castranova, V., Shi, X., & Demers, L. (1999). New insights into the role of nuclear factor-κB a ubiquitous transcription factor in the initiation of diseases. *Clinical Chemistry, 45* (1), 7-17.

Chen, K., Yeh, P., Yeh, K., Lu, S., Huang, S., & Cheng, A. (2008). Downregulation of phosphor-Akt is a major molecular determinant of bortezomib-induced apoptosis in hepatocellular carcinoma cells. *Cancer Research, 68* (16), 6698-6707.

Chin, D., Boyle, G., Porceddu, S., Theile, D., Parsons, P. & Coman, W. (2006). Head and neck cancer: past, present and future. *Expert Reviews Anticancer Therapy, 6*, 1111-1118.

Choong, N., & Vokes, E. (2008).Expanding role of the medical oncologist in the management of head and neck cancer. *CA: A Cancer Journal for Clinicians, 58* (1), 32-53.

Chung, C., Ely,, K., McGavran L., Varella-Garcia, M., Parker, J., Parker, N., et. al. (2006). Increased epidermal growth factor receptor gene copy number is associated with poor prognosis in head and neck squamous cell carcinomas. *Journal of Clinical Oncology, 24*, (25), 4170-6.

Chung, C., & Gillison, M. (2009). Human papillomavirus in head and neck cancer: its role in pathogenesis and clinical implications. *Clinical Cancer Research, 5*, (22), 6758-6762.

Chung, C., Levy, S. & Yarbrough, W. (2005). Clinical applications of genomics in head and neck cancer. *Head & Neck, 28*, 360-368.

Chung, C., Parker, J., Ely, K., Carter, J., Yi, Y., Murphy, B., et al. (2006). Gene expression profiles identify epithelia-to-mesenchymal transition and activation of nuclear factor-kB signaling as characteristics of a high-risk head and neck squamous cell carcinoma. *Cancer Research*, *66* (16), 8210-8218.

Chung, C., Parker, M., Levy, S., Slebos, R., Dicker, A., & Rodeck, U. (2007). *International Journal of Radiation Oncology, Biology & Physics, 69* (2), S102-S105.

Cohen, E. (2006). Role of epidermal growth factor receptor pathway-targeted therapy in patients with recurrent and/or metastatic squamous cell carcinoma of the head and neck. *Journal Clinical Oncology, 24* (17), 2659-2665.

Collins, K., Jacks, T., & Pavletich, N. (1997). The cell cycle and cancer. *Proceedings of the National Academy of Sciences, 94* (7), 2776-2778.

Combaret, V., Boyault, S., Iacono, I., Brejon, S., Rousseau, R., & Puisieux, A. (2008). Effect of bortezomib on human neuroblastoma: analysis of molecular mechanism involved in cytotoxicity. *Molecular Cancer, 7* (50).

Cooper, J., & Cohen, E. (2009). Mechanisms of resistance to EGFR inhibitors in head and neck cancer. *Head & Neck, 31* (8), 1086-1094.

Dassonville, O., Bozec, A., Fischel, J., & Milano, G. (2007). EGFR targeting therapies; Monoclonal antibodies versus tyrosine kinase inhibitors: Similarities and Differences. *Critical Reviews in Oncology and Hematology, 62* (1), 53-61.

Derveaux, S., Vandesompele, J., & Hellemans, J. (2010). How to do successful gene expression analysis using real-time PCR. *Methods, 50* (4), 227-30.

Dittman, K., Mayer, C., Fehrenbacher, B., Schualler, M., Raju, U., Milas, L. et al. (2005). Radiation-induced EGFR nuclear import is limited to activation of DNA dependent protein kinase. *Journal of Biological Chemistry, 280*, 31182-31189.

Eastmond, D., Schuler, M., & Rupa, D. (1995). Advantages and limitations of using fluorescence in situ hybridization for the detection of aneuploidy in interphase human cells. *Mutation Research Letters, 348,* (4), 153-162.

Eckberg, T., Nestor, M., Engstrom, M., Nordgren, H., Wester, K., Carlsson, J., et al. (2005). Expression of EGFR, Her2, Her3 and Her4 in metastatic squamous cell carcinoma of the oral cavity and base of tongue. *International Journal of Oncology, 26* (5), 11177-11185.

Erjala, K., Raitanen, M., Kulmala, J., & Grenman, R. (2007). Concurrent use of vinorelbine and gefitinib induces supra-additive effect in head and neck squamous cell carcinoma cell lines. *Journal of Cancer Research and Clinical Oncology, 133* (3), 169-176.

Franovic, A., Gunaratnam, L., Smith, K., Robert, I, Patten, D., Lee, S., et al. (2007). Translational up-regulation of the EGFR by tumor hypoxia provides a nonmutational explanation for its overexpression in human cancer. *Proceedings of the National Academy of Sciences, 104* (32), 13092-13097.

Gallagher, S., & Chakavarti, D. (2008). Immunoblot analysis. *Journal of Visualized Experiments, 20* (26), pii 759.

Gasparian, A., Guryanova O., Chebotaeve D., Shiskin A., Yemelyanov A., & Budunova I. (2009). Targeting transcription factor NFkB. *Cell Cycle, 8* (10), 1559-1566.

Graham, B., & Gibson, S. (2005). The two faces of NFkappaB in cell survival responses. *Cell Cycle, 4* (10), 1342-1345.

Gravetter, FJ & Wallnau, LB. (2006). *Statistics for the behavioral sciences* (7th ed). Florence, Kentucky: Wadsworth Publishing.

Hacker, H., & Karin, M. (2006). Regulation and function of IKK and IKK-related kinases. *Science Signaling*, 17, re13.

Hainsworth, J., Spigel, D., Burris, H., Markus, T., Shipley, D., Kuzur, M., et al. (2009). Neoadjuvant chemotherapy/gefitinib followed by concurrent chemotherapy/radiation therapy/gefitinib for patients with locally advanced squamous carcinoma of the head and neck. *Cancer, 115* (10), 2138-2146.

Huang, S., Armstrong, E., Benavente, S., Chinnaiyan, P., & Harari, P. (2004). Dual-agent molecular targeting of the epidermal growth factor receptor (EGFR): combining anti-EGFR antibody with tyrosine kinase inhibitor. *Cancer Research, 64*, 5355-5362.

Ingenuity.com. 1700 Seaport Blvd. Third Floor. Redwood City, CA.

Jackson-Bernitsas, D.,Ichikawa, H., Takada, Y., Myers, J., Lin X., Darnay, B., et al. (2006). Evidence that TNF-TNFR1-TRADD-TRAF2-RIP-TAK1-IKK pathway mediates constitutive NF-kappaB activation and proliferation in human head and neck squamous cell carcinoma. *Oncogene, 26* (10), 1385-1397.

Junttila, M., & Evan, G. (2009). p53-a Jack of all trades but master of none. *National Review of Cancer, 9* (11), 821-829.

Karin, M., Cao, Y., Greten, F., & Li, Z. (2002). NFκB in cancer: from innocent bystander to major culprit. *Nature reviews, 2*, 301-310.

Kassouf, W., Luongo, T., Brown, G., Adam, L., & Dimmey, C. (2006). Schedule dependent efficacy of gefitinib and docetaxel for bladder cancer. *The Journal of Urology, 176* (2), 787-792.

Keith, B. (2008). Systematic review of the clinical effect of glucocorticoids on nonhematologic malignancy. *Biomed Central Cancer*, *8***,** 84-102.

Kersting, C., Packeisen, J., Leidinger, B., Brandt, B., von Wasielewski, R., Winkelmann, W., et al. (2006). Pitfalls in immunohistochemical assessment of EGFR expression in soft tissue sarcomas. *Journal of Clinical Pathology, 59*, 585-590.

Killeen, A. (2003). *Principles of Molecular Pathology* (1st ed.) Totowa, New Jersey: Humana Press.

Kim, J., & Diehl, J. (2009). Nuclear cyclin D1: an oncogenic driver in human cancer. *Journal of Cell Physiology, 220* (2), 292-296.

Kisselev, A., & Goldberg, A. (2001). Proteasome inhibitors: from research tools to drug candidates. *Chemistry & Biology, 8*, 739-758.

Lalami, Y., de Castro, G., Bernard-Marty, C., & Awada, A. (2009). Management of head and neck cancer in elderly patients. *Drugs Aging, 26* (7), 571-583.

Levine, A. (1997). p53, the cellular gatekeeper for growth and division. *Cell, 88* (3), 323-331.

Lim, C., & Cao, X. (2006). Structure, function and regulation of STAT proteins. *Molecular biosystems, 2* (11), 536-550.

Livak, KJ & Schmittgen, TD. (2001). Analysis of Relative Gene Expression Data Using Real- time Quantitative PCR and the $2^{-\Delta\Delta CT}$ method. *Methods, 25*, 402-408.

Low, L., Ch'ng, S., Ng, D., Sullivan, M., Brasch, H., Davis, P., et al. (2009). Her2 polysomy in aggressive head and neck cutaneous squamous cell carcinoma. *Human Pathology*, 40 (6), 902-903.

Mandic, R., Rodgarkia-Dara, C., Zhu, L., Folz, B., Bette, M., Weihe, E., et. al. (2006). Treatment of HNSCC cell lines with the EGFR-specific inhibitor cetuximab (Erbitux) results in paradox phosphorylation of tyrosine 1173 in the receptor. *FEBS Letters, 580*, 4793-4800.

Marmor, M., Skaria, B. & Yarden, Y. (2004). Signal transduction and oncogenesis by ErbB/HER receptors. *International Journal of Radiation Oncology, 58* (3), 903-913.

Martin, V., Mazzucchelli, L., & Frattini, M. (2009). An overview of the EGFR FISH challenge in tumor pathology. *Journal of Clinical Pathology, 62*, 314-324.

Marur, S., & Forastiere, A. (2008). Head and neck cancer: changing epidemiology, diagnosisand treatment. *Mayo Clinic Proceedings, 83* (4), 489-501.

Matar, P., Rojo, F., Cassia, R., Moreno-Bueno, G., Di Cosimo, S., Tabernero, J., et. al. (2004). Combined epidermal growth factor receptor targeting with the tyrosine kinase inhibitor gefitinib (ZD1839) and the monoclonal antibody cetuximab (IMC-C225): superiority over single-agent receptor targeting. *Clinical Cancer Research, 10*, 6487-6501.

Mather, J., & Roberts, P. (1998). *Introduction to Cell and Tissue Culture Theory and Technique* (ed 1). New York, New York: Plenum Press.

McCarty, M., & Block, K. (2006). Preadministration of high dose salicylates, suppressors of NF-kB activation may increase the chemosensitivity of many cancers: an example of proapoptotic signal modulation therapy. *Integrative Cancer Therapies, 5* (3), 252-268.

McConkey, D., & Zhu, K. (2008). Mechanisms of proteasome inhibitor action and resistance in cancer. *Drug Resistance Updates, 11*, 164-179.

Modjtahedi, H., & S. Essapen. (2009). Epidermal growth factor receptor inhibitors in cancer treatment: advances, challenges and opportunities. *Anticancer Research, 20* (10), 851-855.

Montagut, C., Rovira, A., & Albanell, J. (2006). The proteasome: a novel target for anticancer therapy. *Clinical Translational Oncology*, *8* (5), 313-7.

Mukohara, T., Engelman, J., Hanna, N., Yeap, B., Kobayashi, S., Lindeman, N. et. al. (2005). Differential effects of gefitinib and cetuximab on non-small cell lung cancers bearing epidermal growth factor receptor mutations. *Journal National Cancer Institute, 97* (16), 1185-1194.

Nakamura, H, Kawakami A, Ida H, Koji T, & Eguchi, K. (2007). EGF activates PI3K-Akt and NFkB via distinct pathways in salivary epithelial cells in Sjogren's syndrome. *Rheumatology International, 28,* 127-136.

Nakano, H., Shindo, M., Sakon, S., Nishinaka, S., Mihara, M., Yagita, H., et al. (1998). Differential regulation of IkappaB kinase alpha and beta by two upstream kinases, NF-kappaB-inducing kinase and mitogen-activated protein kinase/ERK kinase kinase-1. *Proceedings of the National Academy of Sciences, 95* (7), 3537-3542.

Nakayama, H., Ikebe, T., Beppu, M., Shirasuna, K. (2001). High expression levels of nuclear factor kappaB, IkappaB kinase alpha and Akt kinase in squamous cell carcinoma of the oral cavity. *Cancer*, 92(12):3037-44.

Nawrocki, S., Sweeney-Gotsch, B., Takamori, R., & McConkey, D. (2004). The proteasome inhibitor bortezomib enhances the activity of docetaxel in orthotopic in human pancreatic tumor xenografts. *Molecular Cancer Therapeutics*, 3, 59-70.

Nencioni, A., Grunebach, F., Patrone, F., Ballestrero, A., & Brossart, P. (2007). Proteasome inhibitors: antitumor effects and beyond. *Leukemia, 21*, 30-36.

Olivier, S., Robe, P., & Bours, V. (2006). Can NF-kappaB be a target for novel and efficient anti-cancer agents? *Biochemistry and Pharmacology, 72* (9):1054-68.

Ooi, M., Hayden, P., Kotoula, V., McMillin, D., Charalambous, E., Daskalaki, E., et a. (2009). Interactions of the Hdm2/p53 and proteasome pathways may enhance the antitumor activity of bortezomib. *Clinical Cancer Research, 15* (23), 7153-7160.

Orlowski, R. & Kuhn, D. (2008). Proteasome inhibitors in cancer therapy: Lessons from the first decade. *Clinical Cancer Research, 14* (6), 1649-1657.

Pacifico, F., & Leonardi, A. (2006). NF-kappaB in solid tumors. *Biochemical Pharmacology, 72* (9), 1142-1152.

Pahl, H. (1999). Activators and target genes of Rel/NFkB transcription factors. *Oncogene, 18*, 6853-6866.

Papandreou, C., Daliani, D., Nix, D., Yang, H., Madden, T., Wang, X., et al. (2004). Phase I trial of the proteasome inhibitor bortezomib in patients with advanced solid tumors with observations in androgen-independent prostate cancer. *Journal of Clinical Oncology, 22* (11), 2108-2121.

Partridge, M., Costea, D., & Huang, X. (2007). The changing face of p53 in head and neck cancer. *International Journal of Oral Maxillofacial Surgery, 36* (12), 1123-1138.

Patel, V., Ramesh, A., Traicoff, J., Baibakov, G., Emmert-Buck, M., Gutkind, S., et al. (2005). Profiling EGFR activity in head and neck squamous cell carcinoma by using a novel layered membrane Western blot technology. *Oral Oncology, 41* (5), 503-508.

Pernas, F., Allen, C., Winters, M., Yan, B., Friedman, J. Dabir, B., et al. (2009), Proteomic signatures of epidermal growth factor receptor and survival signal pathways correspond to gefitinib sensitivity in head and neck cancer. *Clinical Cancer Research, 15* (7), 2361-2372.

Piperdi, B., Ling, Y., & Perez-Soler, R. (2007). Schedule-Dependent Interaction between the proteosome inhibitor bortezomib and the EGFR-TK inhibitor erlotinib in human non-small cell lung cancer cell lines. *Journal of Thoracic Oncology, 2 (8),* 715-721. Pop, C., & Salvesen, G. (2009). Human caspases: activation, specificity and regulation. *Journal of Biological Chemistry, 284* (33), 21777-21781.

Rasband, W. (1997-2009). ImageJ, U. S. National Institutes of Health, Bethesda, Maryland,USA, http://rsb.info.nih.gov/ij/.

Rocha-Lima, C., Soares, H., Raez, L., & Singal, R. (2007). EGFR targeting of solid tumors. *Cancer Control, 14* (3), 295-304.

Rogers, S., Box, C., Chambers, P., Barbachano, Y., Nutting, C., Rhys-Evans, P., et al. (2009). Determinants of response to epidermal growth factor receptor tyrosine kinase inhibition in squamous cell carcinoma of the head and neck. *Journal of Pathology, 218* (1), 122-130.

Sanderson, R., & Ironside, J. (2002). Squamous cell carcinomas of the head and neck. *British Medical Journal, 325,* 822-827.

Scaltriti, M., & Baselga, J. (2006). The epidermal growth factor receptor pathway: a model for targeted therapy. *Clinical Cancer Research, 12* (18), 5268-5272.

Schwartz, R., & Davidson, T. (2004). Pharmacology, pharmacokinetics and practical applications of bortezomib. *Oncology (Williston Park), 18* (14 Suppl 11), 14-21.

Sebastian, S, Azzariti, A, Accardi, R, Conti, D, Pilato, B, LaCalamita, R., et al. (2008). Validation of gefitinib effectiveness in a broad panel of head and neck squamous carcinoma cells. *International Journal of Molecular Medicine, 21* (6), 809-817.

Sergina, N., Rausch, M., Wang, D., Blair, J., Hann, B., Shokat, K., et al. (2007). Escape from HER-family tyrosine kinase inhibitor therapy by the kinase-inactive HER3. *Nature, 445,* 437-441.

Sharma S, Bell D, Settleman J, & Haber, D. (2007). Epidermal growth factor receptor mutations in lung cancer. *Nature Reviews in Cancer, 7,* 169-181

Shehata, M. (2005). Rel/nuclear factor kappa B apoptosis pathways in human cervical cancer cells. *Cancer Cell International, 5* (1), 10-23.

Sheu, J., Hua, C., Wan. L., Lin, Y., Lai, M., Tseng, H. et al. (2009). Functional genomic analysis identified epidermal growth factor receptor activation as the most common genetic event in oral squamous cell carcinoma. *Cancer Research, 69* (6), 2568-2576.

Sisti, D., Guescini, M., Rocchi, M., Tibollo, P., D'Atri, M., & Stocchi V. (2010). Shape based kinetic outlier detection in real-time PCR. *BMC Bioinformatics, 11* (1), 186.

Siu, L., Soulieres, D., Chen, E., Pond, G., Chin, S., Francis, P., et. al. (2007). Phase I/II trial of erlotinib and cisplatin in patients with recurrent or metastatic squamous cell carcinoma of the head and neck: a Princess Margaret hospital phase II consortium and National Cancer Institute of Canada clinical trials group study. *Journal of Clinical Oncology, 25* (16), 2178-2183.

Smyth, G. (2004). Linear models and empirical Bayes methods for assessing differential expression in microarray experiments. *Statistical Applications in Genetics and Molecular Biology*, 3, (1), 1-25.

Song G, Ouyang G., & Bao, S. (2005). The activation of Akt/PKB signaling pathway and cell survival. *Journal of Cell and Molecular Medicine, 9* (1), 59-71.

Spencer, K., Ferguson, J., & Wiesenfeld, D. (2002). Current concepts in the management of oral squamous cell carcinoma. *Australian Dental Journal, 47* (4), 284-289.

Squarize, C., Castilho, R., Sriuranpong, V., Pinto, D., & Gutkind, J. (2006). Molecular cross-talk between the NFkappaB and STAT3 signaling pathways in head and neck squamous cell carcinoma. *Neoplasma, 8* (9), 733-746.

Staal, S. (1987). Molecular cloning of the Akt oncogene and its human homologues AKT1 and AKT2: amplification of AKT1 in a primary human gastric adenocarcinoma. *Proceedings of the National Academy of Sciences, 84* (14), 5034-5037.

Sun, Z. & Andersson, R. (2002). NF-kB activation and inhibition: a review. *Shock, 18* (2), 99-106.

Sun, S., & Ley, S. (2008). New insights into NF-kappaB regulation and function. *Trends in Immunology, 29* (10), 469-478. Temam, S., Kawaguchi, H., El-Naggar, A., Jelinek, J., Tang, H., Liu, D., et. al. (2007). Epidermal growth factor receptor copy number alterations correlate with poor clinical outcome in patients with head and neck squamous cancer. *Journal of Clinical Oncology, 25,* (16), 2164-2170.

Tergaonkar, V. (2006). NFkB pathway: A good signaling paradigm and therapeutic target. *The International Journal of Biochemistry & Cell Biology, 38*, 1647-1653.

Theoret, M., Cohen, C., Nahvi, A., Ngo, L., Suri, K., Powell, D., et al. (2008). Relationship of p53 overexpression on cancers and recognition by anti-p53 T cell receptor-transduced T cells. *Human Gene Therapy, 19* (11), 1219-1232.

Tse, G., Yu, K., Chan, A., King, A., Chen, G., Wong, K., et al. (2009). Her2 expression predicts improved survival in patients with cervical node positive head and neck squamous cell carcinoma. *Otolaryngology-Head and Neck Surgery,* 141 (4), 467-473.

Varella-Garcia, M. (2006). Stratification of non-small cell lung cancer patients for therapy with epidermal growth factor receptor inhibitors: the EGFR fluorescence in situ hybridization assay. *Diagnostic Pathology, 1*, 19-29.

von Biberstein, S., Spiro, J., Lindquist, R., & Kreutzer, D. (1995). Enhanced tumor cell expression of tumor necrosis factor receptors in head and neck squamous cell carcinoma. *American Journal of Surgery*, 170 (5), 416-422.

Wagenblast J, Hambeck M, Baghi M, & Knecht R. (2008). Effect of bortezomib on EGFR expression in head and neck squamous cell carcinoma cell lines. *Anticancer Research, 28*(2A), 687-692.

Wang, C., Mayo, M., & Baldwin, A. (1996). TNF- and cancer therapy-induced apoptosis: potentiation by inhibition of NF-kappaB. *Science, 274* (5288), 784-787.

Weber, C., Cerniglia, G., Maity, A., & Gupta, A. (2007). Bortezomib sensitizes human head and neck carcinoma cells SQ20B to radiation. *Cancer Biology & Therapy, 6* (2), e1-e4.

Wells, D. (2007). Use of real-time polymerase chain reaction to measure gene expression in single cells. *Methods in Molecular Medicine, 132*, 125-133.

Wheeler, D., Huang, S., Kruser, T., Nechrebecki, M., Armstrong, E., Benavente, S., et al. (2008). Mechanisms of acquired resistance to cetuximab: role of HER (ErbB) family members. *Oncogene, 27* (28), 3944-3956.

Williams, S. & McConkey, D. (2003). The proteasome inhibitor bortezomib stabilizes a novel active form of p53 in human LNCaP-Pro5 prostate cancer cells. *Cancer Research, 63*, 7338-7344.

Yarbrough, W., Slebos, R., & Liebler, D. (2006). Proteomics: clinical applications for head and neck squamous cell carcinoma. *Head & Nec*k, 28 (6), 549-555.

VITA

Pamela Susan Wirth was born on January 5, 1973 in Portsmouth, VA and is an American citizen. She graduated from Churchland High School in Portsmouth, VA in 1990. She received her Bachelor of Science in Biology in 1995 from Virginia Polytechnic and State University. She later received a Master of Science in Biology in 1999 from Northeastern Illinois University in Chicago, IL. She is currently employed at Vanderbilt University.